



**University of
Zurich**^{UZH}

Landslide reconstruction and monitoring in Brienz based on dendrogeomorphology

GEO 511 Master's Thesis

Author

Andrea Lina Bringolf
16-710-220

Supervised by

Dr. Holger Gärtner (holger.gaertner@wsl.ch)
Prof. Dr. Markus Egli

Faculty representative

Prof. Dr. Markus Egli

29.01.2023

Department of Geography, University of Zurich

Landslide reconstruction and monitoring in Brienz based on dendrogeomorphology

GEO 511 Master's Thesis



Author:

Andrea Lina Bringolf

16-710-220

andrealina.bringolf@uzh.ch

Supervisor:

Dr. Holger Gärtner, WSL

holger.gaertner@wsl.ch

Supervisor & Faculty Representative:

Prof. Dr. Markus Egli, UZH

markus.egli@geo.uzh.ch

Abstract

Mass movements such as landslides and rockfalls are driving forces in mountainous regions and pose a major threat to its people and infrastructure. The alpine village of Brienz in Switzerland is threatened by both an ongoing landslide and the danger of a major rockslide. Regular rockfalls also threaten the village. The entire area is therefore strictly monitored. The additional creation of a drainage system is intended to slow down or stop the landslide by reducing the water pressure in the mountain. While these approaches enable authorities to gain knowledge about the present state of the landscape and to plan on the future course of action, they do not give any information about the past development of the landslide. Dendrogeomorphology offers the possibility to reconstruct the time before the start of monitoring, by analysing the annual formed tree rings.

In this Master's thesis different methods are applied to gather information about past movement in a subarea of the Brienz landslide. In addition, the approaches used, and the obtained results are compared to each other to assess their reliability. Furthermore, location and visual inclination of individual trees are discussed as indicator of the extent of disturbance to be expected. First, a visual inspection of all chronologies was used to get a basic impression of possible activity phases. Second, the chronologies of each tree were examined individually, and years of disturbance were noted manually. Third, using the eccentricity index with different thresholds (based on the average, median, and artificially set), the years of disturbance of each tree were also calculated. Fourth, an attempt was made to confirm identified event years by making thin sections and search for reaction wood. However, this was not successful, probably due to a too small sample size or errors in setting the cores.

The results of tree-ring analyses showed that as far back as the tree rings went (~1820), the area was in motion and still is today. The sites experienced periods of activity, that were separated by resting phases in 1850-1875, 1945-1955, and 1975-1985. The comparison of the different methods has also shown that it is important to interpret the results with caution, as manual assessment and eccentricity index calculations sometimes identified different activity phases. One advantage of the eccentricity approach is that it is sensitive enough to notice the landslide increase, while the manual approach failed to do so. But this sensitivity is also a disadvantage. If the arbitrary threshold is set low, "false" events (noise) are detected, if it is set too high, events are ignored. The manual approach on the other hand is not dependent on a general threshold but on the estimation of each individual event by itself. Lastly, high numbers of disturbances in individual trees could often be associated with cracks in the soil in close proximity. On the other hand, both inclined trees and vertical trees show equally often high numbers of disturbances. Consequently, based on the results of this work, location appears to be a better disturbance indicator than visible damage on the tree.

Tree ring analyses not only allow to record the history of a landslide dating back for several centuries, which is a great advantage compared to other monitoring methods, but also to monitor dynamics within a sliding area based on analysis of individual trees and their locations. Some predictions for the future might also be possible for example an acceleration of the slide if the tree ring analysis indicates an increase in event number per year. For all these reasons, the inclusion of dendrogeomorphology in the comprehensive monitoring of landslides should be considered.

Contents

Abstract	ii
List of Figures.....	v
List of Tables	vii
1. Introduction.....	1
1.1 Study Objects.....	3
2. State of the Art	4
3. Study Site	6
3.1 Location	6
3.2 Geology.....	8
3.3 The landslide of Brienz	9
3.3.1 Landslide Village	9
3.3.2 Landslide Mountain	10
3.4 Climate.....	11
3.5 Tree species	11
4. Theory.....	13
4.1 Dendrochronology.....	13
4.2 Tree growth	13
4.3 Dendrogeomorphology	14
4.4 Reaction wood.....	16
4.5 Eccentricity	17
5. Material & Methods	19
5.1 Sampling	19
5.2 Sample preparation	20
5.2.1 Core preparation.....	20
5.2.2 Micro sections.....	20
5.3. Measurements.....	21
5.3.1 Skippy.....	21
5.3.2 CooRecorder	22
5.4 Cross-dating.....	22
5.5 Determination of event years.....	23
5.5.1 Manual comparison of year ring chronologies.....	24
5.5.2 Eccentricity calculations	25

6. Results	27
6.1 Visual overview of chronologies.....	27
6.1.1 Site 1	28
6.1.2 Site 2	29
6.1.3 Site 3	30
6.2 Total event count based on the manual approach	31
6.3 Total event count based on eccentricity index	34
6.4 Reaction wood in thin sections	36
6.5 Comparison of event phases identified by different approaches	37
6.6 Disturbance count in individual trees.....	38
6.7 Comparison of precipitation data with the number of events	41
6.8 Measured soil movement near the investigated sites	42
7. Discussion	43
7.1. Strengths and limitations of the different methods used in this study	43
7.2. Determination of major event phases based on activity at three different sites	44
7.3 Disturbance of individual trees in relation to their location	46
7.3.1 Influence of the location on the number of disturbances.....	46
7.3.2 Conclusion drawn from analysing the disturbance number of individual trees	47
7.4 Climatic influence on the study site	48
7.5 Movement data in comparison to the number of events.....	48
8. Conclusion	50
8.1 Outlook.....	51
9. Bibliography.....	52
10. Appendix.....	58
11. Acknowledgements	67
12. Personal Declaration	68

List of Figures

Figure 1:	Geographic overview of the study area location in Brienz GR.	6
Figure 2:	Detailed map of the study area with all three sites.	7
Figure 3:	Geologic composition of the Brienz landslide.	8
Figure 4:	Visual overview of the subzones of the Brienz landslide.	9
Figure 5:	The four most likely scenarios for landslide mountain processes.	11
Figure 6:	Distribution of <i>Pinus sylvestris</i> in Switzerland.	11
Figure 7:	Distribution of <i>Picea abies</i> in Switzerland.	12
Figure 8:	<i>Pinus sylvestris</i> strongly inclined to the edge.	12
Figure 9:	<i>Picea abies</i> torn apart due to crack opening.	12
Figure 10:	<i>Picea abies</i> lifted out of the soil due to ground movements.	12
Figure 11:	Thin section showing the cambium in between the phloem and xylem.	14
Figure 12:	Example of compression wood cells in <i>L. decidua</i> .	16
Figure 13:	Examples for different forms of eccentricity due to geomorphic processes.	17
Figure 14:	Sample prepared for cutting on core microtome.	20
Figure 15:	Workplace set up.	20
Figure 16:	Lab-microtome for cutting micro sections.	20
Figure 17:	Set up for dyeing the thin sections.	21
Figure 18:	Skippy set up at WSL.	21
Figure 19:	The panoramas of the samples in the CooRecorder program.	22
Figure 20:	Schematic example of cross-dating.	23
Figure 21:	Example of the two chronologies in TSAP-Win showing <i>Gegenläufigkeit</i> .	24
Figure 22:	Example of the two chronologies in TSAP-Win showing <i>Gleichläufigkeit</i> .	24
Figure 23:	Example for genral strong increase and a drop in the chronologies of site 3.	25
Figure 24:	Overview of all taken chronologies at the three sites.	27
Figure 25:	Overview of all chronologies taken from site 1.	28
Figure 26:	Overview of all chronologies taken from site 2.	29
Figure 27:	Overview of all chronologies taken from site 3.	30
Figure 28:	Total event count (254) at all three sites based on the manual approach.	31

Figure 29:	Event count for site 1 based on the manual approach.	32
Figure 30:	Event count for site 2 based on the manual approach.	32
Figure 31:	Event count for site 3 based on the manual approach.	33
Figure 32:	Total event count based on the eccentricity index calculations (average).	34
Figure 33:	Total event count based on the artificially adjusted threshold.	35
Figure 34:	Thin sections of spruce B03Fi08d at site 3.	36
Figure 35:	Visual comparison of all event phases based on different approaches.	37
Figure 36:	Visual comparison of activity phases for all sites and all approaches.	38
Figure 37:	Location and event count of individual trees at site 1.	39
Figure 38:	Location and event count of individual trees at site 2.	39
Figure 39:	Location and event count of individual trees at site 3.	40
Figure 40:	Precipitation data from compared to the number of events.	41
Figure 41:	Motion data from four measurement points near the study sites.	42
Figure 42:	Detailed geological profile with different components of the landslide.	58
Figure 43:	Geomorphic sketch of site 1.	59
Figure 44:	Geomorphic sketch of site 2.	59
Figure 45:	Geomorphic sketch of site 3.	60
Figure 46:	Total event count of events based on the eccentricity index (median).	60
Figure 47:	GPS Measurements of all Points in the Caltegras area.	61

List of Tables

Table 1:	Event-related disturbances in tree phenology.	15
Table 2:	Sample trees chosen in the field and actually sampled trees.	19
Table 3:	Resulting thresholds depending on calculation approach.	26
Table 4:	Overview of the number of sampled trees and detected events per site.	33
Table 5:	Overview of the detected phases based on the different approaches.	59
Table 6:	Distance of the four measuring points to the study areas.	61
Table 7:	Complete Excel File that shows all results based on the manual approach.	62

1. Introduction

Landslides belong to the driving natural forces in mountainous regions. In affected areas they cannot only cause considerable financial damage to infrastructure but also pose a danger to human lives, making them a challenging task of hazard mitigation in mountainous regions (Lopez Saez et al. 2012; Lopez Saez et al. 2013; Shi et al. 2022; Šilhán et al. 2019; Stoffel & Bollschweiler 2009; Wistuba et al. 2019). Additionally, the damage potential of landslides has risen over the past years (Alexander 2008, IPCC 2022).

One reason for this is global climate change. Rising temperatures have a profound impact on global and local ecosystems and mountainous regions are particularly affected. The European Alps, for example, are part of a complex climatic balance. From the south comes the warm Mediterranean air, from the north cold polar air. From the west, moist air masses from the Atlantic reach the Alps, and from the east, the drier continental climate (Wanner et al. 2021). This balance is now disturbed by climate change. To date, the Alps, like other mountain ranges have already been affected by a strong warming and a change in precipitation. In addition to rising temperatures and changing seasonal weather, the mountains have already seen less snowfall and a shorter duration of snow cover, glacier melt, increased permafrost thaw, and an increase in the number and size of glacial lakes (IPCC 2022). Since landslides and other mass movements occur mainly in mountainous regions, they are also influenced by climate change (Chiarle et al. 2021, IPCC 2022).

Although many of the factors (e.g., geology, topography, or seismic activity) that influence the probability of landslides are invariable, others are sensitive to climate change. Climate change can affect slope stability directly. For example, landslides, debris flow and rockfall are triggered by intense precipitation. Deep-seated landslides are often triggered by a high groundwater pressure due to long above average rain or snowmelt. However, climate change can also affect slope stability indirectly. Higher temperature, for example, can lead to different vegetation, different land use or the retreat of a glacier. All these climate change induced reactions in turn can lead to slope instabilities. Both the direct and indirect influence of climate change promote landslides in areas that were not previously subject to such risk (Chiarle et al. 2021). However, the higher risk of landslides is not only due to an increased probability of occurrence. Often, landslides only classify as hazardous if they threaten human life or manmade objects (Alexander 2008). With growing population numbers living in mountainous regions, the potential damage from landslide and other mass movements grows as well (IPCC 2022, Petrascheck & Kienholz 2003). While there is a global increase in fatality numbers due to landslides over the past 20 years, at the same time fatalities in Europe and North America are declining due to a decrease in vulnerability (IPCC 2022).

For the reasons presented above landslide areas in Switzerland are closely monitored by collecting and analysing meteorological, hydrological, and terrain movement data (BAFU 2023). In addition to landslides, other geomorphological processes such as rockfall are also monitored. It is the task of the cantons to prepare hazard maps for rockfall and landslide areas and to assess the event risk. If necessary, protection goals and measures are developed and implemented. In Switzerland, 6-8% of the country is affected by past or active mass movements (BAFU 2016). One of these active landslide regions is the village Brienz and surroundings in the canton of Grisons. Both the village

and the hillside above it are continuously moving down towards the valley and the river Albula. Though the area is known to be in motion since the 19th century, the speed of the landslide has increased strongly in recent years. As of now the mountain flank above the village is moving with several meters per year (Huwiler & Larigiader 2021, Gischig et al. 2021, Sartorius et al. 2022). If this slope movement continues to accelerate, the entire village must be relocated. Apart from the landslide already taking place, there is the possibility of a sudden extreme event. Depending on the magnitude of such an event, other villages like Vazerol, Surava and Tiefencastel, the river Albula and the main infrastructure in the Albula valley (trainway and road) could also be affected (Gischig et al. 2021, Schneider 2022). Since a hazardous event of a certain magnitude cannot be ruled out, the region is very closely monitored by the authorities. In addition, great efforts are being made to prevent such a catastrophic event from occurring. To achieve this, surface water drainage systems have already been installed and a large-scale drainage tunnel is currently being built under the mountain. Both are intended to remove as much water as possible from the endangered area and thus reduce the pressure on the system (Ernst 2022). In the case of a major event, constant monitoring and a permanent evacuation plan will enable the safe evacuation of all people from the area (Gemeinde Albula 2019).

It is fundamental to understand the movement mechanisms of the landslide in detail. This can only be achieved by gaining detailed knowledge of the past and present landslide dynamics. For this purpose, geological surveys are prepared, and the movements of the mountain are monitored closely with tachymetry, photogrammetry, georadar, GNSS and regular GPS measurements (Sartorius et al. 2022). What these methods cannot provide, however, is an overview of past motion data prior to the start of monitoring. A long-term recording is not only needed in the case of Brienz but also for other landslide areas. This presents a challenge: only for the last few decades landslides were closely monitored and recordings of past events are often incomplete. Either the spatial, the temporal resolution or both of landslide monitoring are insufficient. In contrast to other methods dendrogeomorphology can offer both a high temporal and spatial resolution for dating mass movement (Bodoque et al. 2005; Corona et al. 2010; Corominas & Moya 2010; Lopez Saez et al. 2012; Perret et al. 2006; Šilhán et al. 2012; Stefanini 2004; Wistuba et al. 2019). Trees form annual rings, which in turn reflect the conditions and disturbances of that year. Hence, dendrogeomorphology allows the calculation of mass movement frequencies using the year of disturbance in trees (Corominas & Moya 2010; Stoffel 2010). Consequently, trees in a landslide area act as a natural archive of past landslide movements.

1.1 Study Objects

A better understanding of the causes of natural hazards, such as rockfalls or landslides, enables a better risk management (Corominas & Moya 2010; Lopez Saez et al. 2012; Šilhán & Stoffel 2022; Stefanini et al. 2004; Wistuba et al. 2019). The current activities at Brienz result in a wide range of disturbances to the regional forest. Since the entire area is very large and also not accessible everywhere without safety risks, the focus of this Master's thesis lies on a sub-area. The overall aim of this Master's thesis is to gain knowledge about the development and frequency of the landslide in this area.

This will be done by using tilted conifers for assessing the movements over time based on (1) growth behaviour, (2) their eccentric growth and (3) their reaction wood. This approach will allow (1) to learn about the development of the subzone of this landslide and (2) evaluate possibilities and limitations of dendrochronological analysis of such areas.

The following are the Research Questions and associated hypotheses for this work:

1. Can tree ring data be used to gain knowledge about past activity phases of the Brienz landslide?
 - Hypothesis: *By analysing the annual rings, it is possible to date past landslide movements.*

2. Can using different approaches to answer the same questions a) provide more reliable results and b) provide insight into the reliability of the method itself?
 - Hypothesis a): *Consistent results using different approaches allow for a more reliable statement.*
 - Hypothesis b): *The direct comparison of different methods allows a realistic assessment of their advantages, their limitations and thus their reliability.*

3. Is the location of the tree or visual damage to the tree, or both a good indication of expected disturbance?
 - Hypothesis: *Location and visual assessment of sampled trees are a good indicator of disturbed trees.*

2. State of the Art

Dendrochronology first became a scientific field when A. Douglass (1935) developed the method of cross-dating. Following this development many subareas such as dendroecology, dendrochemistry, dendrogeomorphology, and dendroclimatology were developed by different authors (Bovi et al. 2022).

Alestalo (1971) was the first to use dendrochronology to date geomorphic processes and coined the term dendrogeomorphology. His work was later taken up and refined by Shroder (1980). Since these beginnings many authors have contributed to the field of dendrogeomorphology. Bovi et al. (2022) have collected 286 articles on dendrogeomorphology and elaborated the central topics of investigation in the current literature. They concluded that there are six main areas of interest: (i) soil erosion, (ii) debris flow, (iii) landslide, (iv) flood/flash flood, (v) snow avalanche, (vi) rockfall activity.

Depending on the approach, dendrogeomorphology can answer very different questions related to landslides. Kashiwaya et al. (1989) were the first to use dendrogeomorphic methods to study landslides. They studied landslides in Japan by comparing precipitation characteristics and tree ring width. Chelli & Stefanini (1999), Corona et al. (2010) and Wistuba et al. (2013) all used dendrogeomorphology to determine the correct chronology of landslides. In addition to the temporal distribution, many authors have also studied the spatio-temporal distribution of events (Lopez Saez et al. 2012; Lopez Saez et al. 2013, Šilhán et al., 2013, Stefanini 2004). Corominas and Moya (2010) and Stoffel (2010) had a look on the relationship of magnitude and frequency of mass movements in mountainous regions. Přecechtělová & Šilhán (2019) have dealt with the dating of cracks triggered by landslide block displacement.

Apart from the spatial and temporal dating of events, the literature also deals with the different approaches to detect disturbances in trees. Carrara & O'Neill (2003), Corominas & Moya (1999) and Šilhán et al. (2013) use reaction wood to date landslides. The occurrence of scars can be used to draw conclusions about the disturbance year and disturbance type (Bégin 2001; Hebertson & Jenkins 2003; Perret et al. 2006; Stefanini 2004; Stoffel et al. 2005; Stoffel & Perret 2006). Several authors additionally use callus tissues for dating past geomorphic processes (Bollschweiler et al. 2007; Corona et al. 2010; Lopez Saez et al. 2021; Schneuwly et al. 2009). Growth patterns can also provide information about disturbances in the past. By looking at eccentric growth Braam et al. (1987), Wistuba et al. (2013) and Šilhán et al. (2015) have each developed an approach to detect landslide signal. Wistuba et al. (2019) point out that studying tree ring eccentricity could be also a possible method to detect slopes that are at a high risk for landslides. Šilhán & Stoffel 2022 investigated if a landslide also affects the cell-anatomy of a tree and if it could be used to date small-landslides. They found that decreased tracheid lumen areas (TLA) and traumatic resin ducts (TRD) could help dating landslides if no macro-reactions could be found.

However, not only tree trunks but also the roots of the tree can give information about past geomorphological processes. The anatomical changes in the structure of roots that take place when they are exposed due to erosion or landslides also allow an exact event dating. Gärtner (2007) uses this approach to reconstruct and quantify soil erosion and Přecechtělová & Šilhán

(2019) use it to assess the block displacement of landslides. Although dendrogeomorphology covers a wide range of questions and methods there are still some knowledge gaps. For example, Stoffel & Bollschweiler (2009) and Bovi et al. (2022) point out that dendrogeomorphic studies mostly focus on temperate and boreal regions and that there is a need to increase research in the tropics. Šilhán & Stoffel (2015) argue that more attention should be paid to the age mix of sampled trees because trees can respond differently to inclination depending on their age.

The upper section clearly shows that by using dendrogeomorphological methods much knowledge can be gained about the temporal and spatial factors of a past, present, or even future landslide. However, in the case of the landslide of Brienz currently the existing knowledge is based mainly on geological surveys (Breitenmoser 2022) and the data obtained by means of active monitoring in recent years (Sartorius & Schneider 2021; Sartorius et al. 2022). This knowledge is therefore limited to a basic geological understanding and data from the beginning of the measurement. With the help of a dendrogeomorphological survey, it is possible to obtain information about the activities in the area over the years before the start of the measurement. Additionally, some authors rely on only one specific method to date or reconstruct events (Malik & Wistuba 2012; Přecechtělová & Šilhán 2019; Šilhán & Stoffel 2022; Wistuba; Malik & Badura 2019). The use of several methods for the same purpose allows a more differentiated result and at the same time the comparison of different methods and thus an assessment of the reliability of the methods (Šilhán 2019).

3. Study Site



Figure 1: Geographic overview of the study area location in Brienz, the canton of Grisons (map.geo.admin.ch 2022).

3.1 Location

The investigated area is located above the village of Brienz in the canton of Grisons, Switzerland (see Figure 1). To reach the area one can turn onto a forest road just before Brienz and drive up the mountain slope to the Maiensäss Propissi Sot. From there it is a short walk into the study area.

The study area is situated on the lower south-eastern flank of Piz Linard (2768 m.a.s.l.) and part of a large landslide, known as the “Brienzer Rutsch”. The landslide is a long-lasting phenomenon that has been regularly documented since the late 19th century but is also presumed to have begun as far back as the retreat of the glacier after the last glacial maximum (Häusler et al. 2021). This is also strongly reflected in the landscape itself. The part of the mountain flank that has already slid down consists of gravel, large boulders, fallen trees and other vegetational remains. In the forest above the main edge, the ground is characterized by cracks with a diameter of only a few centimetres to several meters. The strong inclination of several trees also reflects the regular movements of the ongoing landslide.

Since the affected area is quite extensive, three smaller sites were chosen for the investigation. The sites are at a height between 1750 and 1800 m.a.s.l. A complete overview of the area and the sample locations can be seen in Figure 2. Site 1 and 3 are close to the active breakaway edge (Figure 2; yellow line), while site 2 is farther away in the forest, close to the area of subsidence formed between the landslide affected ground and the stable rocks (Figure 2; orange line).

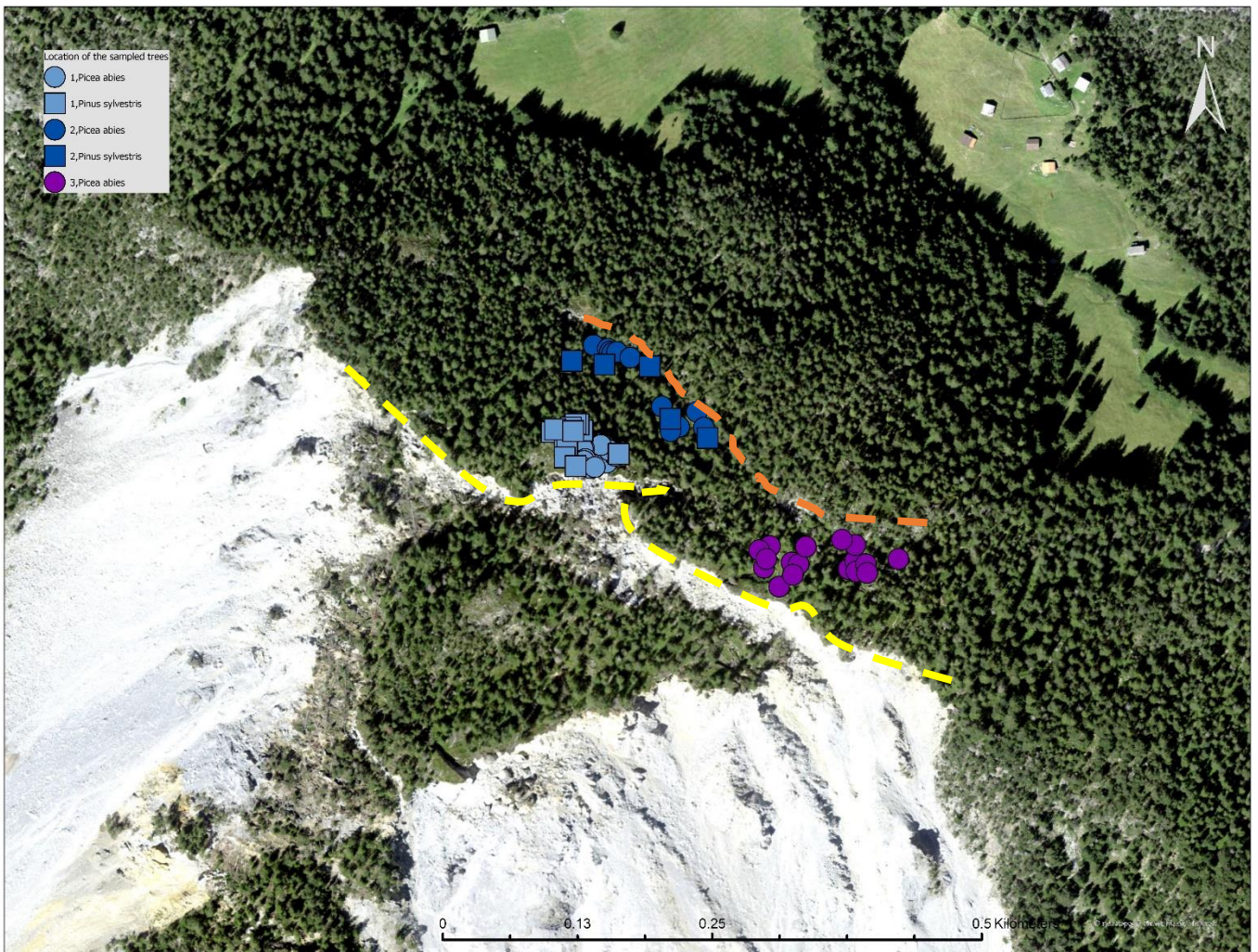


Figure 2: Detailed map (©swisstopo) of the study area with all three sites. The upper map shows the general location of all sampled trees, the lower maps show the distribution of the sampled trees at their respective site. The dashed lines mark two incipient edges that represent natural boundaries to the field work area. The orange line represents the transition to stable bedrock and the yellow line represents a second breakaway edge, after which the terrain is mostly loose scree. The fieldwork area is located in between, in moving but still forested terrain.

3.2 Geology

The geological composition of the southern flank of Piz Linard is characterized by several overlapping geologic formations and therefore a variety of rock types. In total, there are four main geologic groups (see Figure 3): At the top lies the *Vallatscha* formation consisting of water permeable limestones and dolomites. Below lies the *Raibler* formation also consisting of water permeable rocks such as *Rauwacken*, gypsum and dolomite. The other two formations are less water permeable. First is the *Allgäu* formation with its sandy-calcareous clay slates and at the bottom lies a *Flysch* layer. The structure of the upper layers causes precipitation to seep through and accordingly, there are few upper-ridged watercourses. At the same time, the water is dammed up in the mountain by the non-permeable layers. This provides an additional sliding cushion for the rock masses. This results in pressure currently being exerted on the slide horizon from both above (from the slide mass) and below (solid rock). Consequently, higher water input adds further pressure on the system. Events such as snow melting in spring or heavy rainstorms are reflected in faster movements. (Breitenmoser et al. 2021, Breitenmoser 2022). A more detailed geologic profile can be found in the appendix, Figure 42.

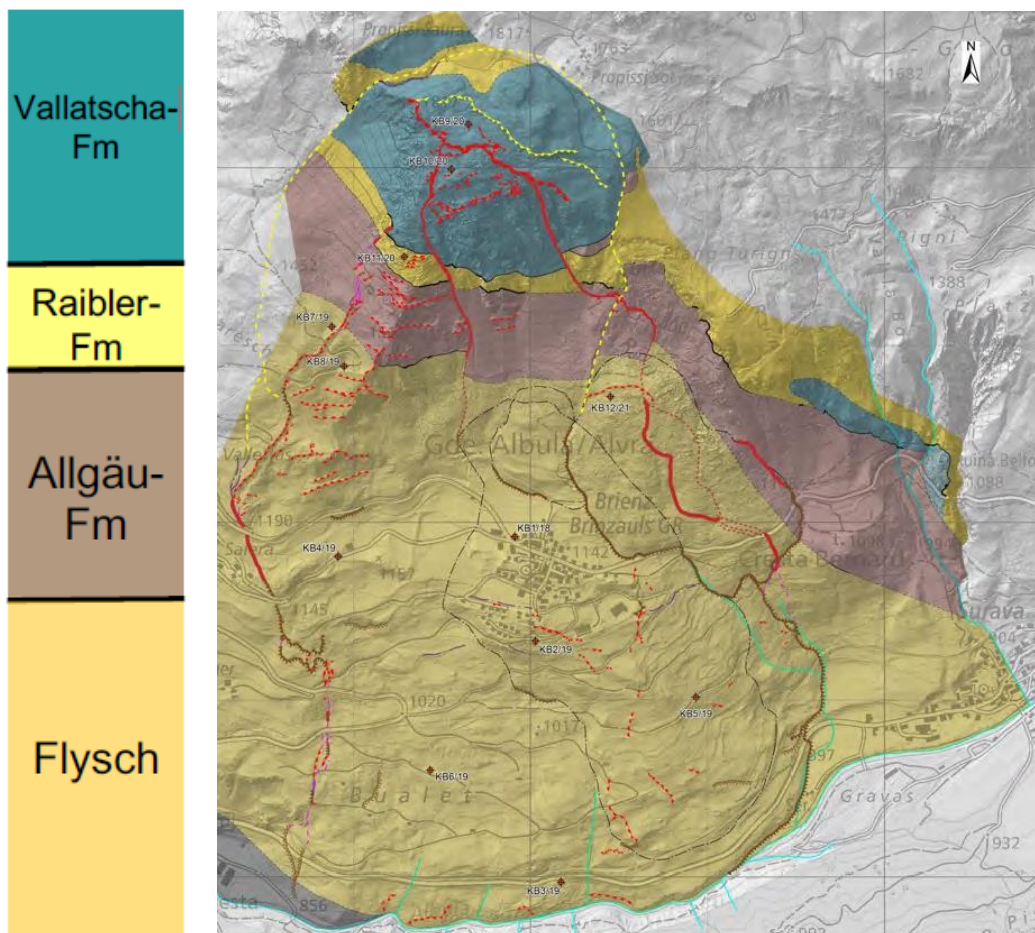


Figure 3: Geologic composition of the Brienz landslide. It should be noted that this figure only shows the existing geological structure, and not the current displacement of rock masses due to the landslide. (Breitenmoser 2022, p.17).

3.3 The landslide of Brienz

The landslide can be divided into two main zones: The village of Brienz and its surrounding area, and the mountain side above it. The zones are named landslide village (*Rutschung Dorf*) and landslide mountain (*Rutschung Berg*) by local authorities (see Figure 4). The structures of the two landslides can be roughly divided into the same three categories: a firm ground, a basal sliding horizon and on top the mass of the actual landslide (Breitenmoser et al. 2021). Although both landslides are connected to each other, as far as is known today, there is no uniform landslide surface from the Albula to the incipient edge on the mountain. While the *Vallatascha*, *Raibler* and *Flysch* formations show gliding surfaces, the *Allgäu* formation is characterized by tilting (Breitenmoser 2022).

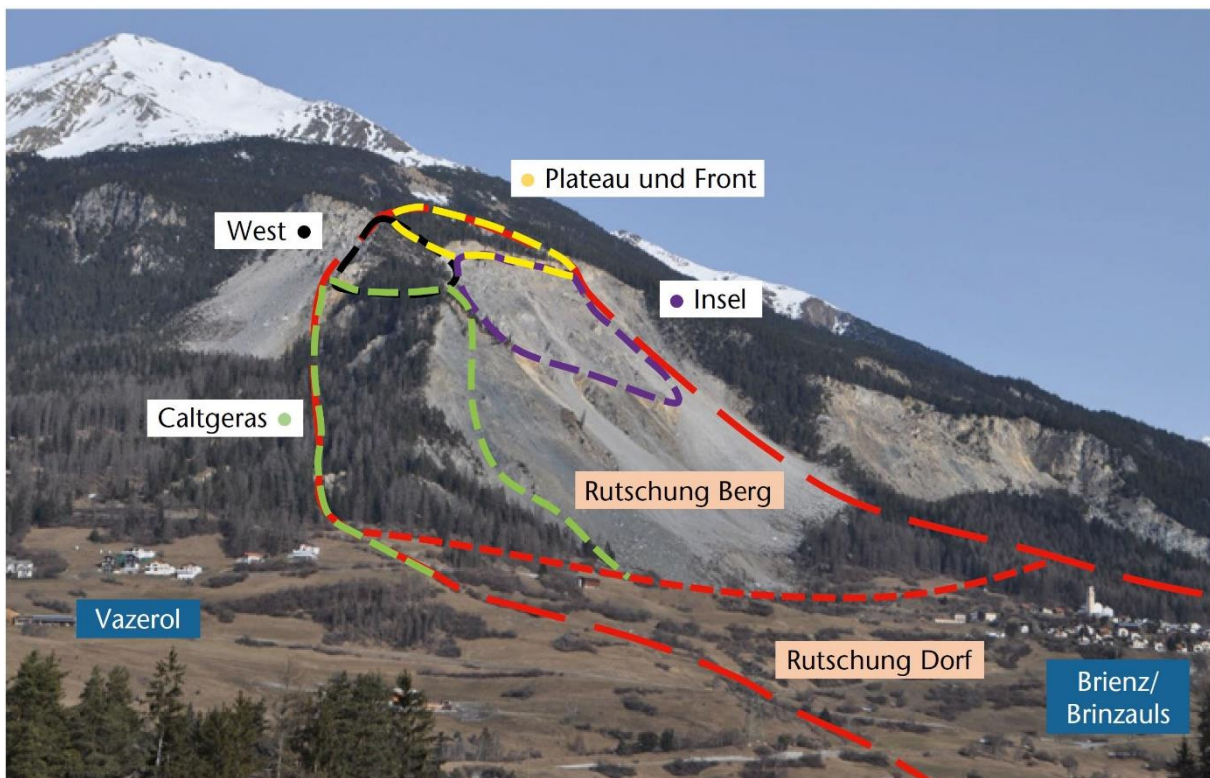


Figure 4: Visual overview of the Brienz landslide area. In red the total area and the distinction into two landslides mountain (Berg) and village (Dorf) and in different colours the various subzones of the landslide mountain (Sartorius 2022, p.144).

3.3.1 Landslide Village

That Brienz moves was already known in the 19th century. For a long time, however, the mountain moved only a few centimetres per year. Between 2000 and 2010 the speed increased sharply and a rockfall above the village in 2008 also indicated a slope instability further up the mountain. The situation was considered threatening for Brienz and from 2011 onwards the entire area was monitored from the village (Gischig et al. 2021). The village of Brienz and its surrounding area are currently gliding with more than 1 m per year towards the Albula. The consequences of this movement are strongly affecting the village. Many house walls have cracks, streets must be mended frequently, and water pipes burst (Gartmann 2021). If the speed of the landslide increases to 2 m a year, the village will have to be abandoned permanently (SRF Einstein 2019).

The landslide mass is thickest at the village with 150 m, towards the river Albula the mass decreases to 30 m. The basal sliding zone beneath the landslide is 10 m thick and consist of silt and clay. Underneath lies, apart from the valley floor where river sediments have accumulated, solid rock. It is also noteworthy that the eastern edge area was overlaid by another event called the *Igl-Rutsch* which took place in 1877 and had a thickness of about 20 m (Breitenmoser et al. 2021).

3.3.2 Landslide Mountain

The landslide mountain can be divided into several subzones with differing sliding velocities (see Figure 4): *Caltgeras*, the *western slope (West)*, the *plateau and front* and the *island (Insel)*. The last two are also referred to as *Creplas*.

All subzones are moving with a speed of several meters per year. In the past two years, *Caltgeras* has moved the slowest at 2 to 3 m per year. The *island* reached peak velocities of more than 10 m per year, making it the fastest subzone. All chosen sampling sites for this Master's thesis lie in the subzone *plateau and front*. The basal landslide horizon at the incipient edge lies at a depth of 50 m and drops to 183 m in the *Caltgeras* subzone (Breitenmoser et al. 2021).

Possible processes that can be expected in future development are landslide, 1, debris stream and rockfall. Heavy rockfalls are characterized by high velocity and very large mass movements (up to several million m³). One order of magnitude smaller rockfalls could take place. They cause somewhat smaller masses to break off (still up to several 100'000 m³), but the rock masses normally remain at the foot of the slope. Events of this magnitude already took place in Brienz in 2011 and 2015. Debris streams on the other hand are not characterized by falling and/or rolling boulders but result in the mixture of the moving mass with water and are thus flowing dynamically. The speed of a debris stream can reach several meters per day. One such event was the *Igl-Rutsch* mentioned in the previous subchapter. Another process to be expected are singular rockfalls, which collapse into the valley as single blocks (max 150'000m³) (Schneider 2022). Consequently, the area is affected by both rockfall and (rock)sliding. Depending on which process(es) occurs in which zone of the area, the potential extent of damage can vary. Meaning not only the village of Brienz could be affected, but also the villages of Vazerol and Tiefencastel (Gischig et al. 2021, Schneider 2022). The villagers of Brienz and the surrounding villages are kept informed about the investigations and developments in regular population information events. The most recent one took place on April 4th, 2022, where the four most probable scenarios were presented, which can be seen in Figure 5 (Schneider 2022). At the same time, attempts continue to be made to prevent these scenarios. For this purpose, drainage tunnels are currently planned in the mountain to achieve deep drainage. In the first step the stable rock will be drained and in the second step the gliding horizon will be drilled through, and drainage tunnel will be built directly into the active landslide mass. This method seems to be successful for the time being, as the movement speeds

of the village have decreased. (SRF Einstein 2023). Construction work on the drainage system began in May 2021 and is at this time still in process (Kurath 2021, Ernst 2022).

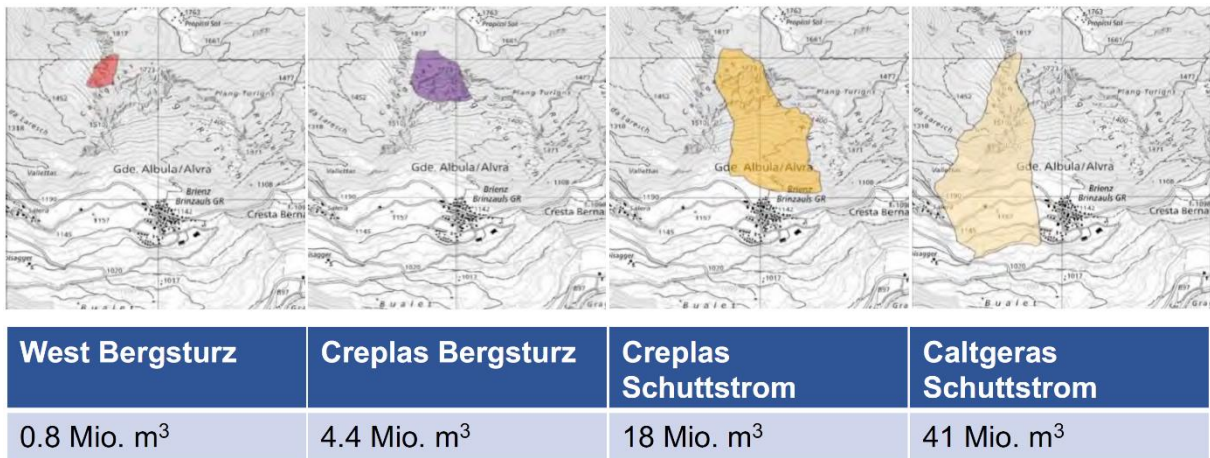


Figure 5: The four most likely scenarios for Landslide Mountain processes. The subzone, event type (Bergsturz meaning Rockfall, Schuttstrom meaning debris steams) and expected rock volume are indicated (Schneider 2022, p. 56).

3.4 Climate

The yearly precipitation in Brienz is variable and ranges in the last years between 780 and 1200 mm, which is slightly lower than the Swiss average, but not unexpected for the area.

The closest meteorological station to the study area that measures temperature is located at Valbella (approx. 10 km to the north and about 200 m below the study site). The mean annual temperature of the last decade in Valbella is 4.8°C. Consequently, the average temperature at Brienz can be expected to be somewhat lower. This is below the average temperature of Switzerland, which is 5.8 degrees (Meteo Schweiz 2022).

3.5 Tree species

The forests above Brienz GR consist mainly of *Pinus sylvestris* L. (pine) and *Picea abies* (L.) H. Karst. (spruce) and occasional *Larix decidua* Mill. (larch) which were not sampled.

Pines are a common species in Switzerland. They are also native throughout Europe as well as in the northern half of Asia. Figure 6 shows the distribution of this species in Switzerland. The map also shows that although *Pinus sylvestris* grows in alpine cantons such as the Valais and Grisons, it is not a high alpine species. While Pines grow often as pioneer species on lean soils, they are also common in forests. In the field they are easily recognizable by the reddish colouring of the bark and needles growing in pairs. The species can reach a height of up to 35 m and an age of 500 years (Häne 2007; info flora 2022).

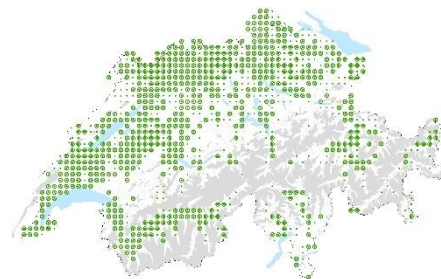


Figure 6: Distribution of *Pinus sylvestris* in Switzerland (info flora 2022).

With a share of 37%, spruce is the most common tree species in Switzerland. It grows both subalpine and montane in forests over acidic soil. Although spruces did not originally occur on the Central Plateau, they are now widespread there (see Figure 7). This is due to strong forestry support in the 17th and 18th century after large parts of the forests in the Central Plateau were cut down. In order to reforest the bare areas, the fast-growing spruces were widely planted. Globally, they are common in Central and Northern Europe. *Picea abies* can reach up to 50 m in height. The tree species is recognizable by its needle growth. The needles are relatively short and pointed. They grow singly around the branch (Häne 2017; info flora 2022).

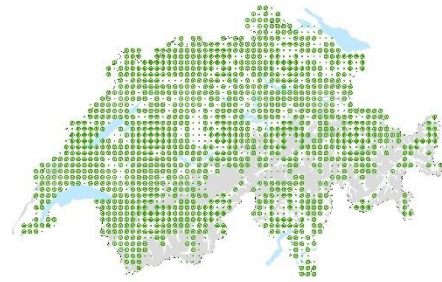


Figure 7: Distribution of *Picea abies* in Switzerland (info flora 2022).

Both tree species accumulated a high number of disturbed individuals in the selected study area. Numerous trees were either tilted towards or away from cracks of various sizes (see Figure 8). A few others stood exactly on a gap opening (see Figure 9). These trees were torn in two by the opening of the ground – an excellent example of the forces at work in the area. Another spruce that grew close to the tear edge was extracted in large parts from the ground due to the movements in the ground (see Figure 10).



Figure 8: *Pinus sylvestris* strongly inclined to the edge.



Figure 9: *Picea abies* torn apart due to crack opening.



Figure 10: *Picea abies* lifted out of the soil due to ground movements.

4. Theory

4.1 Dendrochronology

Dendrochronology can be defined as the science of answering environmental and historical questions by means of studying the structure of dated tree rings (Kaennel & Schweingruber 1995). This definition is also represented in the name itself. The term *dendrochronology* is composed of three ancient Greek words: *dendro* (tree), *chronos* (time) and *logos* (study) (Worbes 2004).

First mentions of the study of tree rings date back to Leonardo da Vinci, who suggested the relation of tree ring size to weather conditions. Since then, the discipline has been further developed by countless scientists (Speer 2010). Especially noteworthy is Andrew Ellicott Douglass, who first developed the method of matching the ring patterns of different trees in 1935, in order to date the ruins of a Native American village (Pueblo Bonito). This technique is now known as cross-dating (Douglass 1935). Today, dendrochronology is one of the most prominent and reliable ways to provide accurate and detailed recordings of past times (Šilhán 2019; Speer 2010; Stoffel 2010).

A great advantage of this discipline is that dendrochronology is very versatile. It allows not only the reconstruction of environmental processes and events such as changes in the climate or debris flows, but also man-made influences like pollution or contamination. Still, there are also a few challenges. For example, only trees that are subject to a regular growth period followed by a dormant period can build reliable annual tree rings (Speer 2010; Zink-Sharp 2004). However, there are trees that build their rings according to dry seasons or periods of heavy rainfall (Rathgeber et al. 2016; Smith 2008). And even if conditions for a regular formation of annual rings are met, an extreme year can lead to omission or forming of an additional annual ring (Smith & Lewis 2007). Another limitation can be found in the age of the trees in the investigated area. It may be that the age of the trees does not go back far enough to cover a searched event. Or on a greater scale compared to other methods e.g., radiocarbon dating, dendrochronological data does not reach very far into the past (Speer 2010).

4.2 Tree growth

From the previous subchapter it is clear that dendrochronology is based on the analysis of regular tree ring formation (Ferguson 1970; Speer 2010). Therefore, it is important to understand how they are formed. Accordingly, the following subchapter discusses the biology and growth of trees in more detail.

As other green-leaved plants perform photosynthesis trees do so as well. The sugar obtained this way is then used for various functions such as maintenance, reproduction, protection, and growth. Tree growth can be divided into two groups. Primary growth is responsible for the extension of shoots and roots. This furthers the trees' ability to intercept solar energy, water, and mineral elements. And secondary growth that allows a tree to grow upward and outward. This allows a tree to outgrow its competition (Smith 2008). The secondary growth is responsible for building the annual rings (Schweingruber 2007).

Secondary growth takes place annually in the growth period, which is in temperate zones usually a period of 10-12 weeks. The formation of wood takes place in the vascular cambium, where new cells are produced through cell division. The living cells of the cambium, which lie in between the

lignified cells of the xylem and the phloem (see Figure 11), undergo a complex process of division and differentiation, such as cell enlargement, cell wall thickening and lignification. This results in different woody tissues with specific purposes (Gärtner & Heinrich 2013; Funada et al. 2016; Rathgeber et al. 2016; Zink-Sharp 2004). For example, new built cell layers that are facing outwards become phloem (inner bark) whose task is to transport carbohydrate and other biomolecules. The cells that are built inwards become new xylem (wood) which have the task of conducting water and mineral elements (Smith 2008; Zink-Sharp 2004). In addition, a different xylem structure is formed depending on whether it is the early or late growth phase. Early wood cells are formed in spring. Their focus lies on rapid and quantitative growth, often resulting in thin-walled cells with a large diameter. Late wood is formed late in the growth season. These rings are generally smaller and thicker walled resulting in visually darker cells. While early wood is mainly responsible for the nutrient and water transport, late wood contributes with its thicker cell walls to the stability of the tree. Both early and late wood together form an annual ring (Gärtner & Heinrich 2013; Rathgeber et al. 2016; Smith 2008; Zink-Sharp 2004). This applies to both deciduous and coniferous trees. Nevertheless, there are differences in the cell structure of coniferous and deciduous trees. For example, the cells of deciduous trees are often characterized by large vessels for water transport (Gärtner & Heinrich 2013).

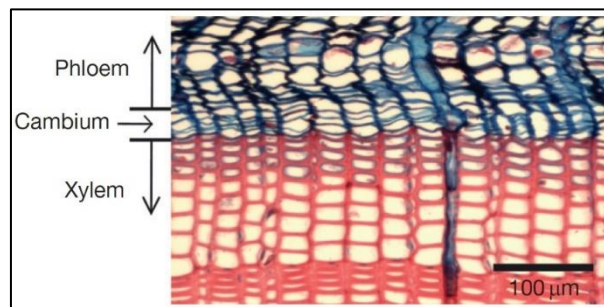


Figure 11: Thin section showing the cambium in between the phloem and xylem (Gärtner et al. 2013, p.92).

4.3 Dendrogeomorphology

Since dendrochronology can be used for such a wide array of possibilities, subcategories have developed over time. One of these subcategories is called dendrogeomorphology. The term was coined by J. Alestalo (1971), who was the first to use it. Dendrogeomorphology combines dendrochronology with geomorphology. Geomorphology is the study of land surfaces and of the aeolian, fluvial, gravitational, or tectonic processes behind it (Gärtner 2007). The combination of these two terms is accordingly the approach to explain landscape forms with the help of dendrochronology.

The approach is based on analysing the response of tree growth to different external environmental events in order to date geomorphologic processes (Bodoque et al. 2005; Bovi et al. 2022; Speer 2010; Stoffel & Bollschweiler 2009). Dendrogeomorphology therefore starts where normal tree growth is disturbed by external forces. Shroder (1980) summarized these

considerations in a *process-event-response-system*, meaning that geomorphic processes causing events, which lead to measurable changes in the growth of affected trees. He has stated seven events that influence tree growth: inclination, shear of rootwood or stemwood, corrosion, burial of stemwood, exposure of rootwood, inundation and denudation; and seven possible reactions to them: reaction wood, growth suppression, growth release, ring termination and new callous growth, sprouting, succession and miscellaneous structural or morphological changes in external or internal wood character.

Table 1: Event-related disturbances in tree phenology or the tree's direct environment and related growth response according to Gärtner & Heinrich (2013, p.94).

<i>Disturbance</i>	<i>Visible effect</i>	<i>Growth response</i>
Directed pressure	Tilting, bend of stem	Eccentricity (compression/tension wood)
Destabilizing ground	Tilting, bend of stem	Eccentricity (compression/tension wood), growth suppression, traumatic resin ducts
Nudation	Not visible (possibly remnants of trees in direct environment)	Growth release
Punctual impact	Scars (sometimes overgrown and for this not visible)	Callous tissue, growth suppression, traumatic resin ducts
Burial	Root collar not visible ^a	Growth suppression/ growth release ^b adventitious roots
Erosion (A)	Roots partly exposed, living	Anatomical changes in annual rings of roots
Erosion (B)	Root tips exposed and mostly dead tilting of the stem, frequent	Growth suppression in stem (compare: pressure)
Water-table changes	Not visible	Growth release/ suppression die-off

^aThe development of an adventitious root system may give the impression of an undisturbed root collar. In case of any doubts, the situation has to be checked by digging.

^bDepending on the material deposited around the stem.

Table 1 also shows a summary of various disturbances, their visual effect and possible resulting growth reaction of the tree. However, these processes do not always have to lead to a visible effect. For example, the nudation of a tree is primarily the result of the removal of other trees by a natural or manmade process; this does not affect the remaining tree visually at first. However, this tree now has access to more light and nutrients because the competition was removed. This leads to a growth release in the next years. It has also to be noted that one single process can lead, depending on how the tree was affected, to several different growth responses (Gärtner & Heinrich 2013).

4.4 Reaction wood

As it was stated in Table 1, geomorphic processes such as landslides, avalanches, erosion or rockfall can lead to direct pressure on a tree, which in turn may result in the tilting of said tree. The presence of inclined trees, therefore, may indicate a geomorphologically active area. Yet, trees are also characterized by the fact that they want to grow vertically. Consequently, if a tree is tilted by such an event, it will try to regain its former vertical position (Fabiánová et al. 2021; Šilhán 2019; Stoffel & Bollschweiler 2008).

For broadleaved trees this leads to the formation of tension wood on the upper side of the inclined tree. Tension wood is easy to miss, because it does not have a reliable and clear visual impact on the wood. Indicators for tension wood are according to Gärtner & Heinrich (2013, p.97): a silvery sheen macroscopically visible on trunk cross sections, a gelatinous layer (G-layer) or structural modifications of the secondary wall of the fibres. The detection difficulties result in less frequent use of deciduous trees to determine dendrogeomorphological events using reaction wood (Heinrich et al. 2007; Gärtner & Heinrich 2013).

Inclined conifers build compression wood on the underside of the tilted trunk to regain their vertical position. Unlike tension wood, compression wood is clearly recognisable due to the formation of round and thick-walled tracheid cells. Additionally, the intercellular spaces take the form of a triangle (see Figure 12). However, depending on the species, affected tree part, physiological status, and stage of cell maturation, characteristics of the compression wood can still differ. In Figure 12 an example for the visual difference of round compression wood cells and regular cells can be seen. This example shows the reaction of a *Larix decidua* to trunk tilting outside the growth phase. Therefore, directly at the beginning of the growth phase compression wood cells were built (Gärtner & Heinrich 2013). The formation of compression wood cells also leads to visible darker and larger annual rings (Fabiánová et al. 2021; Gärtner & Heinrich 2013; Stoffel & Bollschweiler 2008; Malik & Wistuba 2012). This and the fact that conifers are widespread in the alpine region makes them very suitable for dating disturbances. However, there are also limitations present. For example, disturbances often lead to the formation of reaction wood, not only in the disturbance year, but also in the following years. Furthermore, it is not possible to distinguish between one big or several individual disturbances in one year based on the concentration of reaction wood (Stoffel et al. 2008).

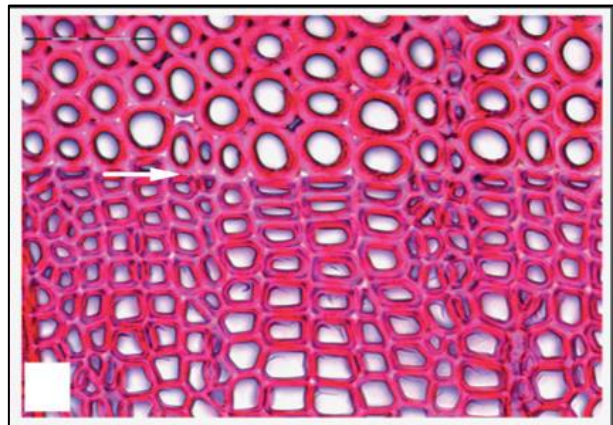


Figure 12: Example of compression wood cells in *L. decidua*. The white arrow shows where the late wood cells of the previous year (below) and the compression wood cells (above) of the following year meet (Gärtner 2013, p.96).

4.5 Eccentricity

As stated before, an undisturbed tree grows vertically. This leads to a concentric growth of annual rings where the pith of the tree is located at the geometric centre of the tree. But when a disturbance results in the tilting of the tree, the ring formation no longer takes place evenly. When a tree starts to grow narrower rings on only one side of the trunk, it is called eccentric growth. This growth can be divided in downslope and upslope eccentricities. Figure 13 shows an example of how geomorphic forces lead to different forms of eccentricity (Wistuba et al. 2013)

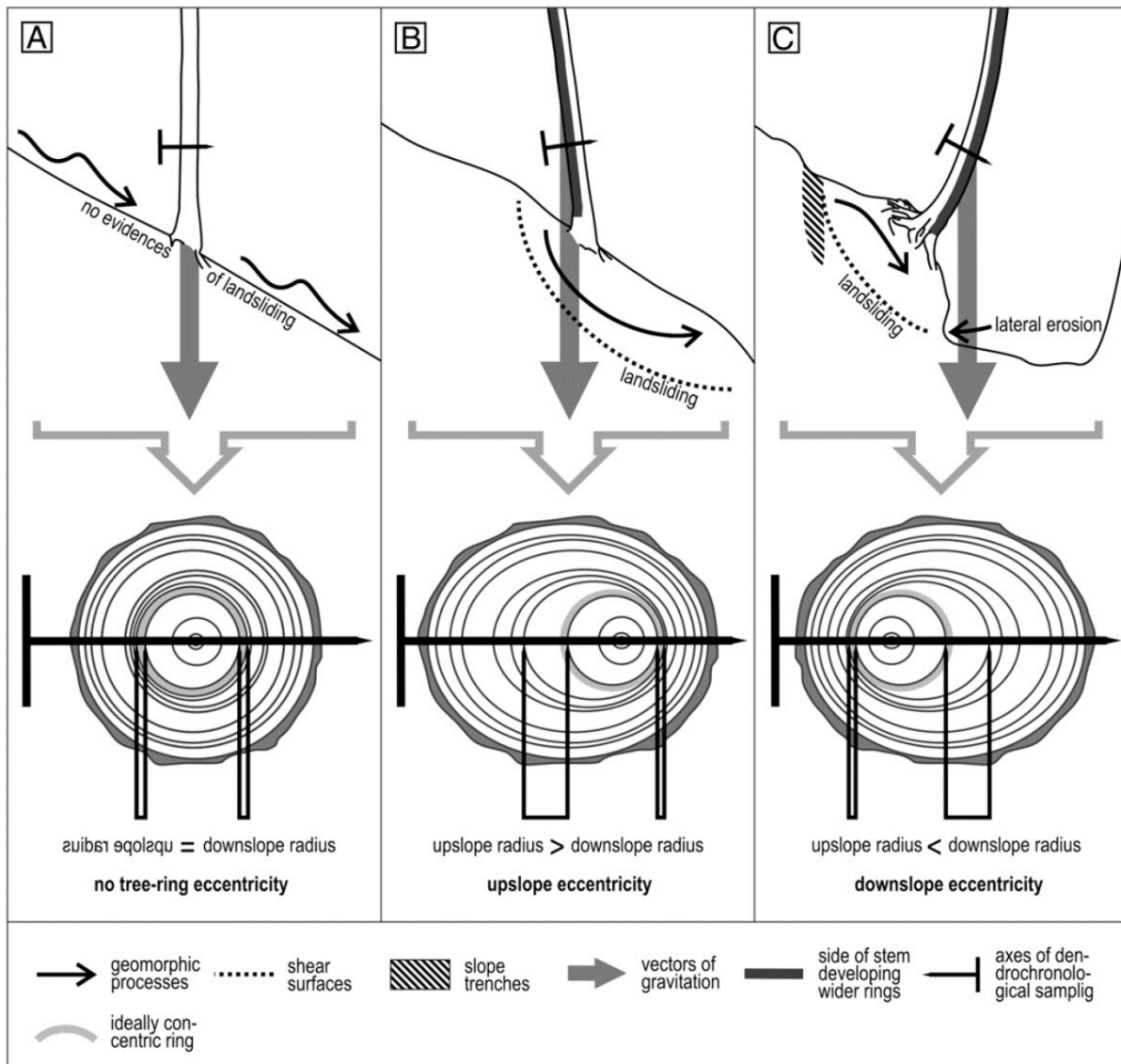


Figure 13: Examples for different forms of eccentricity due to geomorphic processes. In [A] no eccentric growth and [B] upslope eccentric growth due to inclination uphill and [C] downslope eccentric growth due to inclination downhill (Wistuba et al., 2013, p. 47).

The calculation of eccentricity indices and the choice of an appropriate threshold can also help dating events. For this Master's thesis the formula of Malik & Wistuba. (2012) was directly adopted. The used values of the formula are the annual ring widths on the downslope side D (mm) and the upslope side U (mm), the eccentricity value E (mm) calculated from them and the eccentricity index Ei (%). In the following section the formulas will be presented in detail:

$$Ex (mm) = Ux - Dx$$

The x represents the annual tree ring. For each year, the downslope ring widths are subtracted from the upslope widths. This results in Ex. The value of Ex indicates the type of eccentricity and thus decides the next calculation step. If $Ex > 0$ upslope eccentricity is assumed and if $Ex < 0$ downslope eccentricity is assumed. If both sides have the same width ($Ex = 0$) there is no tree ring eccentricity. In case of upslope eccentricity, Ex is divided by the ring width of the downslope side (Dx) and for downslope eccentricity Ex is divided by the ring width of the upslope side (Ux). The results are then multiplied by a factor of 100 to get a percentage change (Eix).

$$Eix (%) = (Ex / Dx) \times 100\% \quad > 0$$

$$Eix (%) = (Ex / Ux) \times 100\% \quad < 0$$

$$Eix (%) = Ex (mm) \quad = 0$$

The resulting Eix values can be used as indicators for tree responses to disturbances. For example, several years in a row with decreasing positive values may indicate the recovery of a tree (= the achievement of no eccentricity) (Malik & Wistuba 2012). However, for dating a landslide, the relative variation from year to year, vEix (%) is needed:

$$vEix (%) = Eix - Eix-1$$

By holding the vEix values against an appropriate threshold (see chapter 5.5.2 Eccentricity calculations), the most probable years for landslides can be dated (Malik & Wistuba 2012)

5. Material & Methods

5.1 Sampling

The actual sampling was carried out in seven days. Frequent thunderstorms in the late afternoons made for very irregularly distributed field days. Therefore, the sampling took place over several weeks ranging from late May to early July. Samples were taken within a less active part of the subzone *plateau and front*, as it was safe to access without greater risk. All samples were taken from either pine or spruce, whereas the pre-existing reference chronology is based on spruce only. The chosen reference chronology is based on spruces taken the previous year in the immediate vicinity, but outside the active area. Hence, it was decided to not create an additional reference, but rather to invest more time in taking more samples from disturbed trees. Until further preparation, all samples were stored in paper straws to prevent rotting.

All sampled trees were chosen either based on their position (close to a rift or the tear-off edge) or their inclination. The location of the sampled trees was recorded with the help of GPS and in the geomorphological sketch of the area. In the sketch were also the breakaway edges and the main cracks recorded. The combination of the map and the GPS data was later used to discuss the results in relation to the location of individual trees. The geomorphologic map sketch for each site can be seen in the appendix Figure 43, Figure 44 and Figure 45.

A few of the chosen trees could not be used for any further analysis since they proved to be rotten on the inside. In total 41 spruces and 17 pines were successfully sampled. According to Corona et al. (2014) a sample size of 50 to 100 trees is sufficient to base reasonable conclusions on it. In Table 2 a short overview of all sampled trees can be seen.

Table 2: Sample trees chosen in the field and actually sampled trees.

Site	Tree species	Selected trees	Sampled trees
1	Spruce	14	13
	Scots Pine	13	12
2	Spruce	11	11
	Scots Pine	5	5
3	Spruce	18	17

Per disturbed tree, four cores were extracted with a 5 mm increment corer. In order to be able to detect a tilting event, a core was taken each from the upslope side and the downslope side. However, the ground was often disturbed to such an extent, that it was not possible to determine the exact direction of the inclination. Some trees appeared also to be tilted in several different directions. In addition, some trees were growing very close to the edge, making it too dangerous to sample the downslope side. For the listed reasons, two additional cores were taken from the two sides parallel to the slope. The samples were extracted roughly at breast height (1.3 m).

5.2 Sample preparation

5.2.1 Core preparation

In a first step all core-surfaces were prepared with a core-microtome (see Figure 14). A core-microtome is a device that allows to cut the surface of the cores rather than sanding them. This has the advantage of preserving the thin cell walls, which tend to break when sanded. The core-microtome consists of two main components (1) the core holder, which is affixed to the positioning table and (2) a knife holder on a sledge, which allows a steady movement of the blade. Angle and orientation of the blade can be adjusted freely to improve the quality of the cut (Gärtner & Nievergelt 2009).



Figure 14: Sample prepared for cutting on core microtome.

In preparation for the cutting and therefore achieving a smooth core surface, all samples were soaked in water for a few minutes. After that, the cores were put in the holder (see Figure 14). For this step it was important to check the fibre direction. The cut must be made perpendicular to the direction of the fibre. Since a cross section rather than a longitudinal section through the cells is needed for the planned analysis. The cutting itself did not pose any challenges but a few of the core samples were partially broken into pieces. Putting them together in the right order and cutting such small pieces proved to be quite difficult at times.

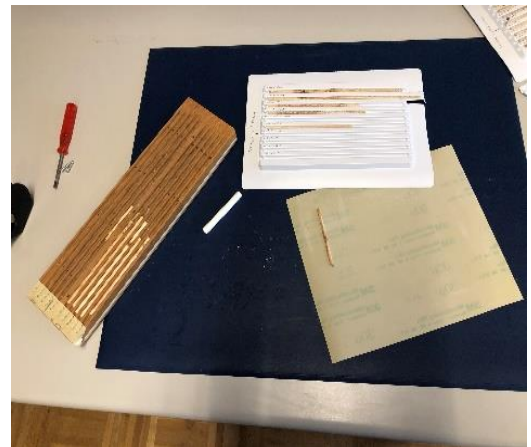


Figure 15: Workplace set up.

To prevent any distortions due to drying, all samples were stored in a wooden box with narrow sub compartments which do not leave enough space for any distortions. Once the cut cores were dry, they were stored in white standard plastic holders (see Figure 15).

5.2.2 Micro sections

The cell structure and therefore reaction wood can be seen best in thin sections of the sample. For this, the already cut samples were cut again. This second time, the goal was not a smooth surface but the preservation of the cut away material in one piece, which is called a thin section. Since 20 μm thin cuts are needed, a lab-microtome rather than a core-microtome is used. This microtome can make particularly small adjustments to the blade position (see Figure 16). To prevent the sample from tearing, water was constantly applied with a brush while cutting. This caused the micro section to slide onto the blade on a water



Figure 16: Lab-microtome for cutting micro sections.

cushion. The section was subsequently placed on a microscope slide using the brush. Glycerine was added to keep the micro sections from drying out.



Figure 17: Set up for dying. From left to right Canada balsam, bleach dye, ethanol solutions, xylol and water.

To enhance the visibility of the cell structure, the micro sections were dyed. The complete set up for this process can be seen in Figure 17. First, the glycerine had to be washed away with tap water. The next step was to add the dye and let it soak in for a few minutes. The dye consists of Safranin, which colours the lignified cell walls (lignin) and Astrablue, which colours unligified cell walls (cellulose). After dyeing, the excess colour was washed out with three ethanol solutions of strengths 75%, 96% and dehydrated ethanol. The remaining ethanol was then removed with xylol. To protect the finished micro section, a cover glass was placed on the microscope slide, and both were and glued together with Canada balsam (Gärtner & Schweingruber 2013).

5.3. Measurements

5.3.1 Skippy

After the cutting of the cores, all samples were digitized using Skippy. Skippy is the name of a device and its corresponding computer program which allow taking precise pictures of the cores in a regular interval. It was developed by Loïc Schneider and Holger Gärtner at the WSL in Birmensdorf (WSL 2022). As visible in Figure 18, the camera (a Canon SRL) is fixed in a frame above a movable platform. The sample is placed in a holder on said platform that moves in predefined steps (here 5 mm) past the camera. For each step the camera takes a picture. Depending on the quality of the sample (preparation, narrowness of the year rings, etc.) the settings like height of camera, picture interval, etc. can be adjusted. This process results in multiple



Figure 18: Skippy set up at WSL.

high-resolution pictures that only show a part of the complete sample. These can subsequently be stitched together into a single panorama with another computer program called PTGui.

5.3.2 CooRecorder

The rings were then measured and counted using the program CooRecorder (see Figure 19) (Cybis Elektronik & Data AB). For this purpose, the previously created panoramas were loaded into the program where each annual ring was marked manually. By assigning the outermost complete annual ring a year, CooRecorder assigns all other rings the corresponding year too. Since the samples for this Master's thesis were taken in early June of this year and most of the samples showed incomplete new annual rings, the first complete ring was dated to the year 2021.

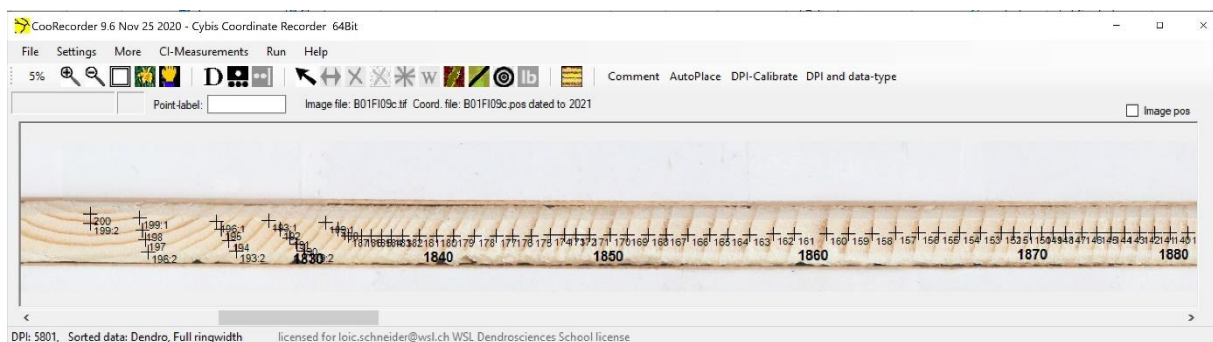


Figure 19: The panoramas of the samples in the CooRecorder program, where each annual ring is counted.

Since the program calculates the distances between every marked ring, it is important to set the points perpendicular to each other, respectively to each ring. Otherwise, the width of individual annual rings is overestimated. The counted annual rings are saved as .pos file. However, for further use an .fh file is needed. The CDendro program (Cybis Elektronik & Data AB) was used to transform the data into .fh formatting.

5.4 Cross-dating

At first glance the principle of dendrochronology is simple: Count the annual rings in order to date past events. However, by counting the tree rings, one learns the approximate age span of the sample but cannot necessarily place the data in time. This is particularly true for samples of dead trees but even for live trees, the year of the outermost ring may not reflect the sampling year.

Cross-dating different chronologies against each other helps to overcome such uncertainties. It is the principle of comparing annual ring patterns of different samples against each other to identify the exact year when the ring was built (Kaennel & Schweingruber 1995). The individual annual patterns that are analysed arise due to changes in the environmental parameters surrounding the tree, thus influencing the annual width of the ring (Cherubini et al. 2004). Figure 20 demonstrates how comparing these ring patterns against each other allows to connect the data to one chronology.

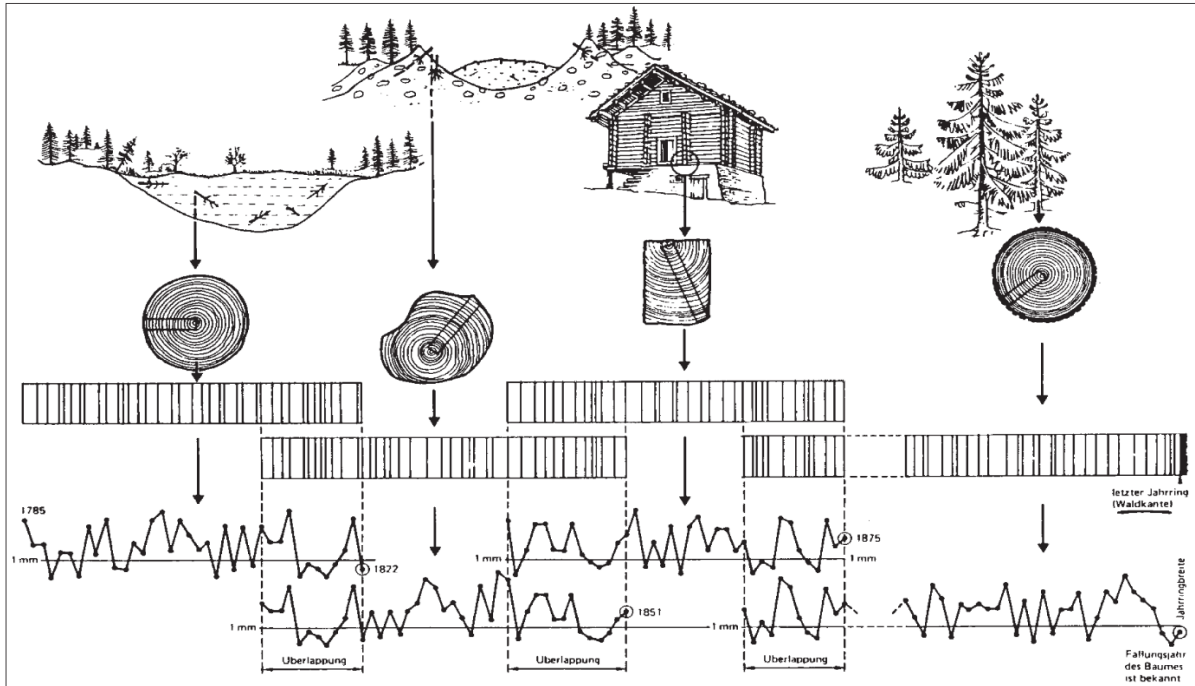


Figure 20: Schematic example of cross-dating. Matching chronology sections allows to bridge data holes and create a coherent chronology (Cherubini et al. 2004, p.163)

The program TSAP-Win (©Rinntech) was used to analysis the annual ring widths. This program allows the visual comparison of two or more samples for their *Gleichläufigkeit*. Although the year of sample extraction is known, since all cores for this thesis were taken in the summer of 2022, the samples were still cross-dated. Cross-dating does not only allow the dating of samples of unknown age. By cross-dating samples against each other, possible errors in counting rings can be identified and corrected. Additionally missing rings can be detected.

First, the uphill and downhill samples from the same tree were examined for their *Gleichläufigkeit* with each other. Afterwards, pairs that fit well together were compared with other pairs with a good fit. A mean curve was created from 3-5 pairs with reasonable uniformity. These mean curves were used to cross-date the less unambiguous samples. If the cross-dating revealed a missing annual ring, the concerned sample was checked again in CooRecorder and if necessary, again under the microscope. Only if no ring could be found, a missing ring was inserted in CooRecorder, with the width 0. Lastly, after cross-dating all samples against each other, all samples were checked against the reference chronology.

It is to note again that the reference chronology consisted only of spruce. However, the sampled pines aligned well with the reference chronology and the spruce. Certain anchor years could be found regularly in the spruce samples, the pine samples, and the spruce chronology. For this reason, the pine samples were deemed appropriate to include in the further analysis.

5.5 Determination of event years

Two different methods were used to determine the event count in the study sites. The first, referred to below as the manual approach is based on the individual analysis of each sampled tree. The second, hereafter called the eccentricity approach, is based on the calculation of the change

in annual eccentricities of the sampled trees. Both approaches are defined in more detail in the following subsections.

5.5.1 Manual comparison of year ring chronologies

This approach is based on manual interpretation of the annual ring pattern. The downhill and uphill cores for each tree were compared to each other. Events are likely to be reflected in years where a gap between the lines opened. This could be due to a) *Gegenläufigkeit* of the lines, meaning an increased width of the annual ring on one side, but decreased width on the other as seen in Figure 21.

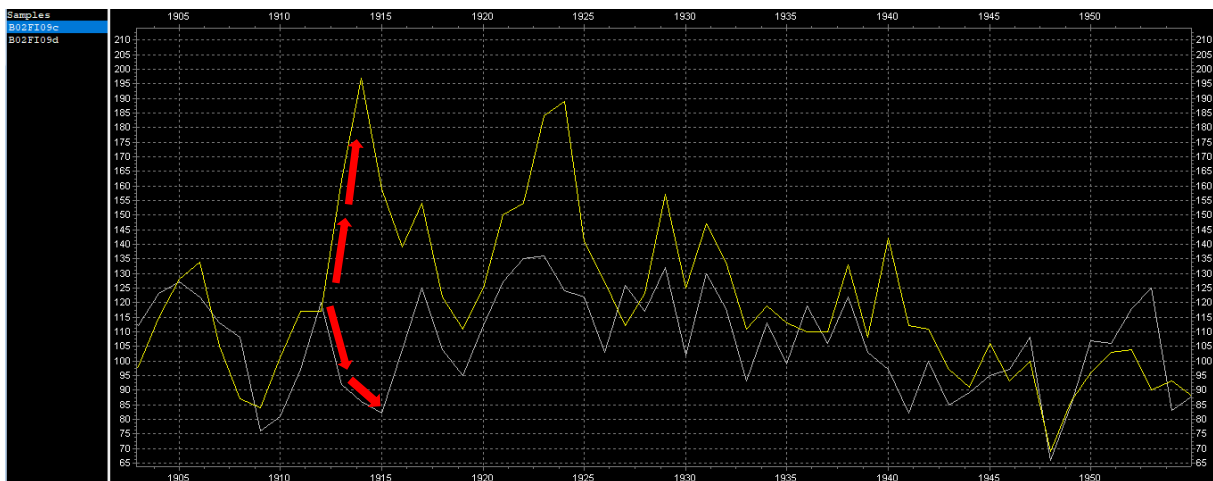


Figure 21: Example of the two chronologies from Spruce 9 at site 2 displayed in TSAP-Win. This tree did not show a strong inclination but grows very close to a gap in the ground. The yellow line shows the drill core taken from the upper side of the inclined tree; the white side shows the sample from the lower side. The red arrows mark an example for *Gegenläufigkeit*.

A gap opens as well if b) both lines show *Gleichläufigkeit*, but one side of the tree grows a much wider ring. This can be seen nicely in Figure 22.

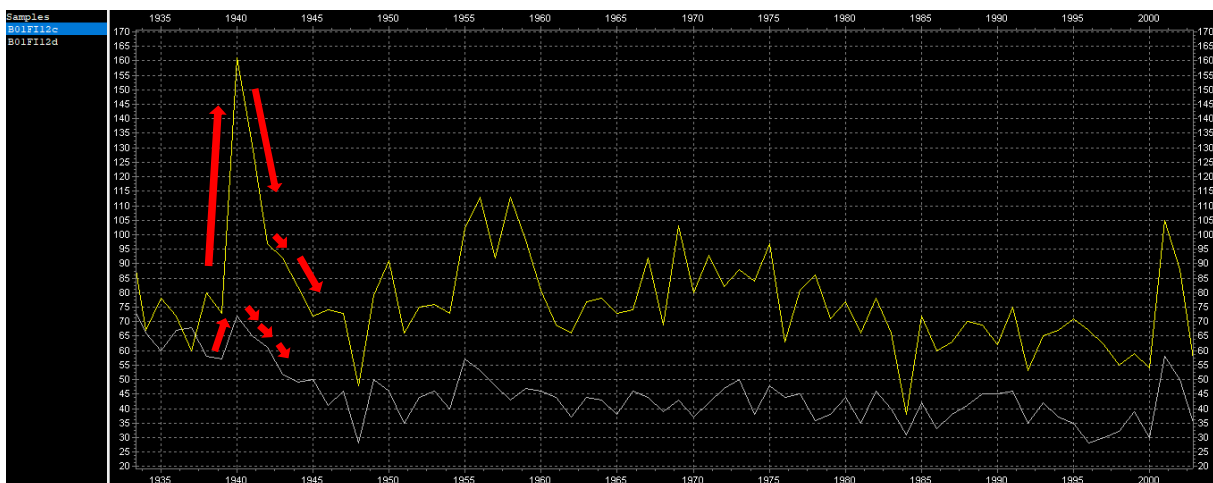


Figure 22: Example of the two chronologies from Spruce 12 of site 1 displayed in TSAP-Win. This spruce stands on a small gap opening and has a slight inclination to the breakaway edge. The yellow line shows the drill core taken from the upper side of the inclined tree; the white side shows the sample from the lower side. The red arrows show 4 years of *Gleichläufigkeit* in the samples.

Depending on the size of the gap between the lines and the number of years that contributed to the gap, possible events were divided into three categories. When to chronologies displayed several years of *Gegenläufigkeit* and a clear gap opening between them they were labelled as (1) *certain*. If the chronologies showed several years of *Gegenläufigkeit* but without a clear divergence of the chronologies an event was noted down as (2) *probable*. Lastly all instances with only one or two years of *Gegenläufigkeit* and no divergence were labelled as (3) *uncertain*. *Gleichläufigkeit* with clear (2) to very clear (1) scissor opening of chronologies were also counted as events and assigned a category. Figure 21 and Figure 22 both show examples for the *certain* category. However, the *uncertain* category was not used further, since according to its name, these events were not reliable enough.

Additionally, all samples per site were displayed in TSAP-Win simultaneously to detect bigger shifts in year ring widths. Striking years, (strong) peaks and lows in several trees, were also marked. In Figure 23 examples for an overall low in (a) 1870 and a strong change in the ring widths in (b) 1947 are shown. The cause of such peaks and drops are various, it could be changes in climate, the landslide or human intervention by analysing the data with the reference chronology and/or comparing it to other data sets (e.g., precipitation data), conclusions can be made.

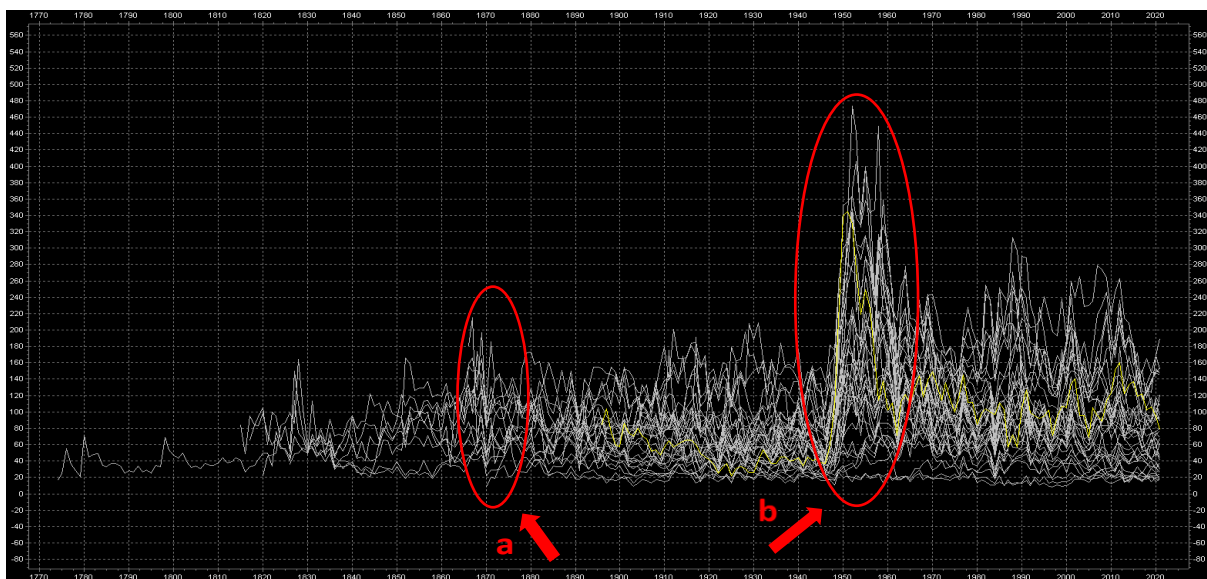


Figure 23: All chronologies of site 3 displayed together show in (a) a strong drop in 1870 for most spruces and in (b) an extreme increase in 1947.

All above observed events, peaks and lows were noted down in an excel file. The complete file can be seen in the appendix, Table 7.

5.5.2 Eccentricity calculations

The second approach to determine event years is based on eccentricity calculations. Here, the annual changes in tree ring widths (νE_{ix}) are held against a set threshold. If a year exceeds this threshold, it counts as an event year. In total, three different approaches to the threshold calculations were used. In addition, each calculation approach results in two thresholds: one for the positive and one for the negative eccentricity values. For all threshold calculations νE_{ix} values of the reference chronology were used. The values of the reference chronologies were used since

they represent the undisturbed trees under the same climatic and geographic conditions. The first threshold was calculated based on the arithmetic mean and the standard deviation of the vEix values according to Wistuba et al. (2019).

$$T = A + \sigma$$

where T = threshold, A = arithmetic mean and σ = standard deviation. Depending on whether the positive or the negative threshold was calculated, A and σ were either calculated from the positive or negative vEix values.

The second threshold was calculated with the same formula, but instead of the arithmetic mean (A) the median (M) was used.

$$T = M + \sigma$$

The third threshold was not calculated based on literature. It was set in such a way that the sensitivity was as similar as possible to that of the manual approach. Meaning, it was set to closely resemble the event count of the manual approach in number per year and overall number. The threshold was artificially increased until this target was reached. Table 3 shows an overview of the different thresholds.

Table 3: Resulting thresholds based on the vEix values of the reference chronology dependent on different approaches for the calculation.

Number	Positive [%]	Negative [%]	Calculation Type
Threshold 1	37.1434	-35.9013	Average
Threshold 2	32.4329	-31.1587	Median
Threshold 3	100	-100	Artificial

6. Results

6.1 Visual overview of chronologies

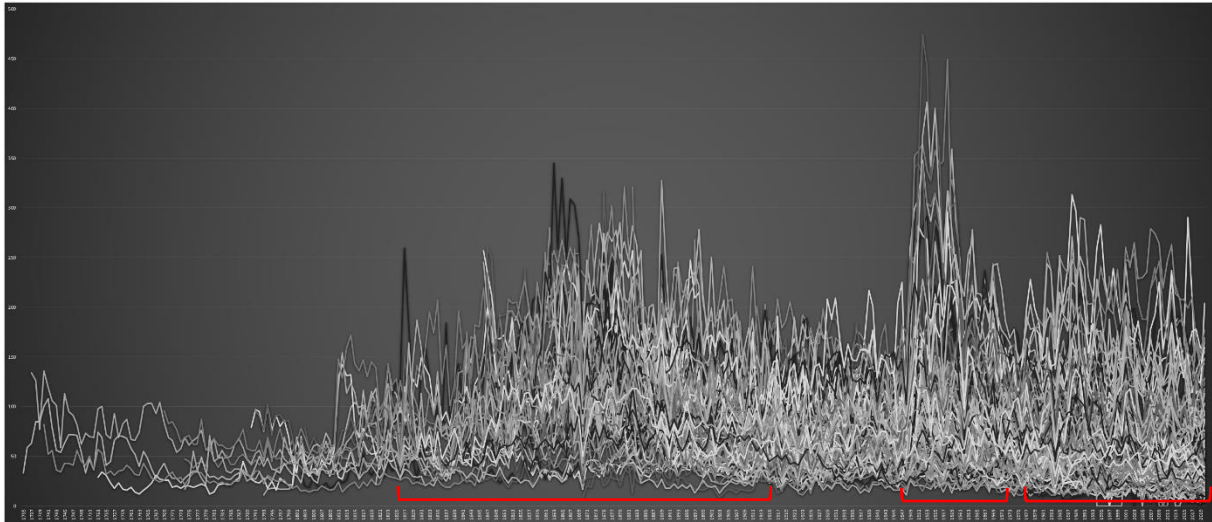


Figure 24: Overview of all taken chronologies at the three sites. Marked in red are the three possible event phases. The unit of tree ring width is in 10^{-2} mm.

Figure 24 shows an overview of all sampled trees and their respective annual chronology. The oldest sample dates back to the year 1735 (B02FI01c) and the youngest to the year 1932 (B03FI10d). As discussed earlier in the Methods, diverging chronologies indicate a disruptive event while reapproximating chronologies indicate overcoming the disruption. This approach cannot only be used for the comparison of two core samples from the same tree, but also on a larger scale. By looking at all chronologies at once, larger trends can be detected. In Figure 24 three possible event phases can be identified. Beginning roughly in the year 1828 the dispersion between the individual chronologies becomes larger. After 1877, the lines begin to converge again and remain at about the same dispersion level from 1915 onwards. The second phase starts abruptly in 1947 with a sharp increase in growth of some chronologies which lasts only a short time. Only 30 years later the third dispersion can be seen in the chronologies. Based on this visual interpretation of the data, a first assumption can be drawn: The disturbed trees did record an accumulation of events roughly in the years 1828-1915, 1947-1970 and 1977-today.

To get a more detailed overview of the data, the different chronologies are going to be studied individually per site in the following subchapters.

6.1.1 Site 1

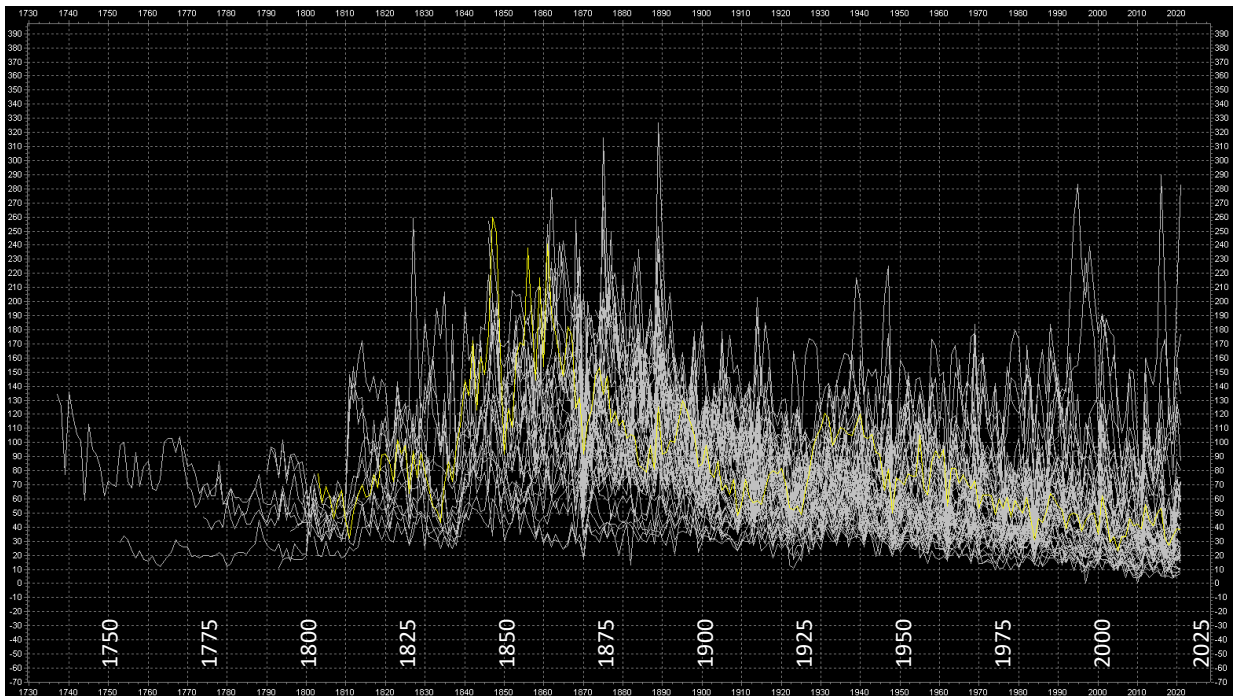


Figure 25: Overview of all chronologies taken from site 1, the yellow line is an example for a single chronology. The unit of tree ring width is in 10^{-2} mm.

Figure 25 shows all chronologies taken from the first site. In accordance with the phases in Figure 24, the chronologies from site 1 also begin to diverge in 1810. It should be noted that there are only a few cores at site 1 that date back to this time. However, the increasing number in the following years does not lead to an approximation of chronologies but emphasizes the dispersion. It is striking that in 1870 there was a very uniform drop, even though the years before and after are very scattered. In the early 1900 the gap between the chronologies shrinks, before opening again in 1990.

6.1.2 Site 2

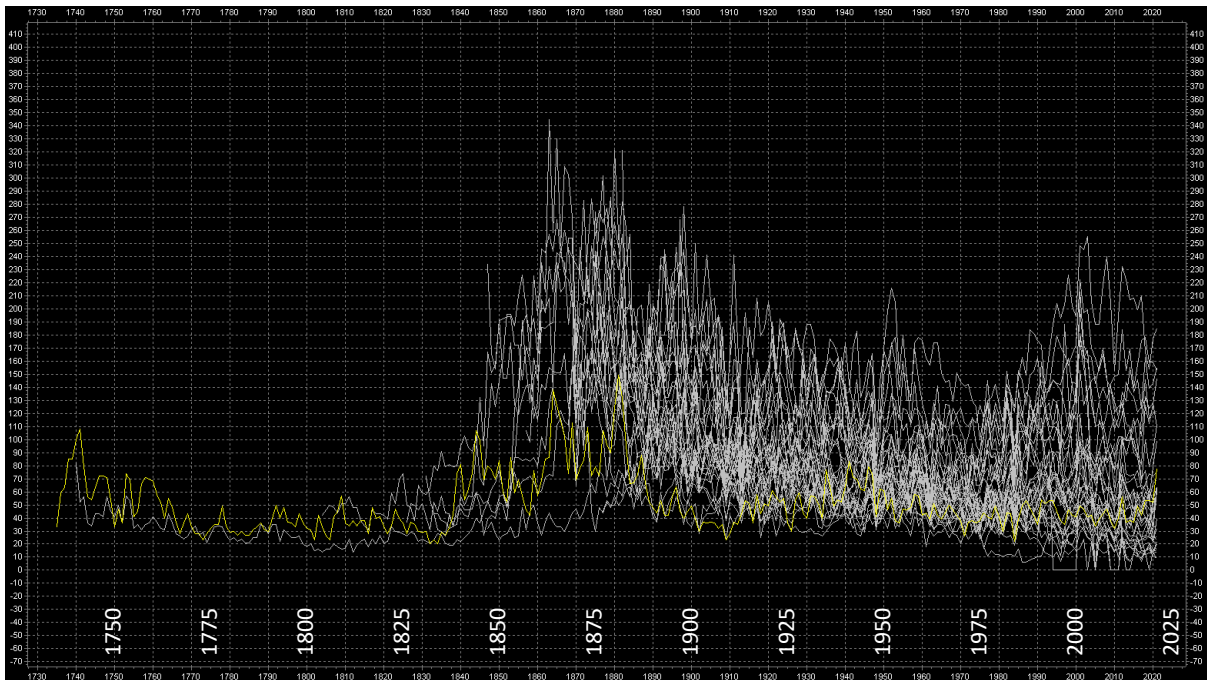


Figure 26: Overview of all chronologies taken from site 2, the yellow line is an example for a single chronology. The unit of tree ring width is in 10^{-2} mm.

Site 2 (see Figure 26) also shows a strong dispersion of the chronologies in 1870 and subsequent years. The beginning of this phase appears to be around the year 1840, however only five samples date back to this time, which might not be enough to draw any conclusions. In 1975 the gap opens again and does not close anymore until 2021. Between 1994 and 2011 several pine chronologies show years with 0 ring growth. These are dated as missing rings.

6.1.3 Site 3

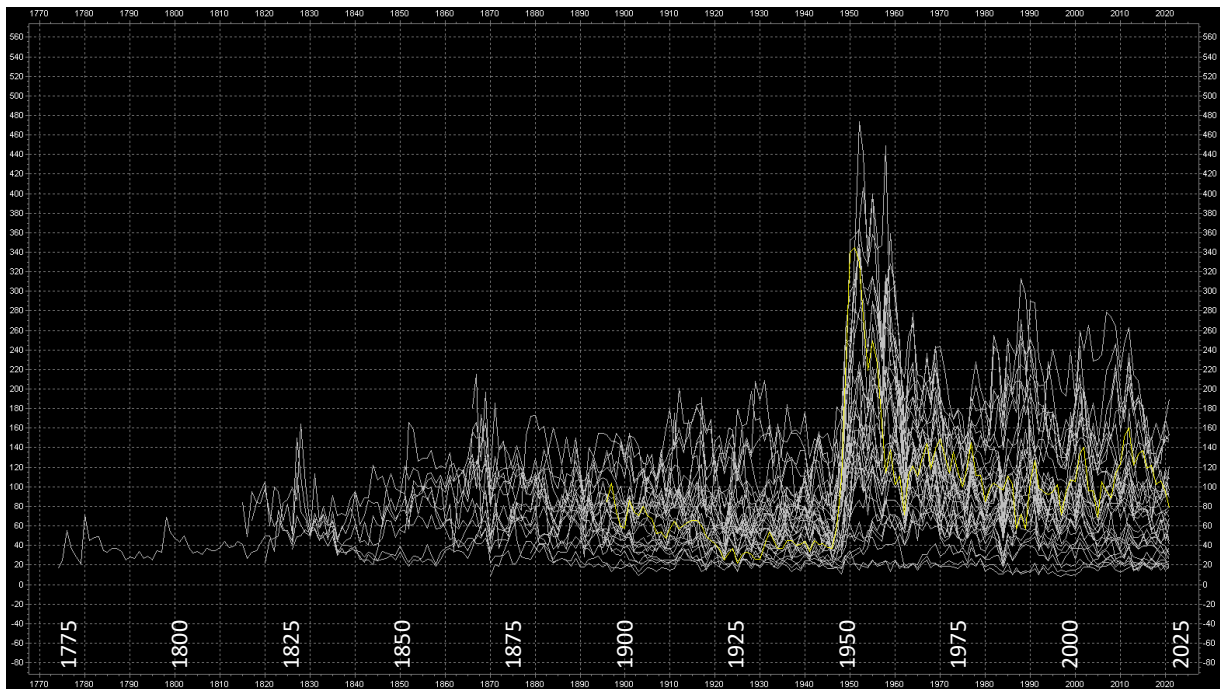


Figure 27: Overview of all chronologies taken from site 3, the yellow line is an example for a single chronology. The unit of tree ring width is in 10^{-2}mm .

Figure 27 shows the growth curves of site 3. Many of the chronologies between 1910 and 1940 are close to each other with some exceptions which are keeping the gap wide open. However, when looking at Figure 27 the extreme increase in growth in the years 1947/49 is most striking. Although the annual ring widths of the chronologies are dropping anew after this extreme peak, they remain on an averagely higher level afterwards. Shortly before 1980, the gap between most chronologies closes, only to spread again sharply after 1980. The chronologies are closing the gap towards the end of the data set, but this could be misleading since it is not yet known how the data for the following years looks.

6.2 Total event count based on the manual approach

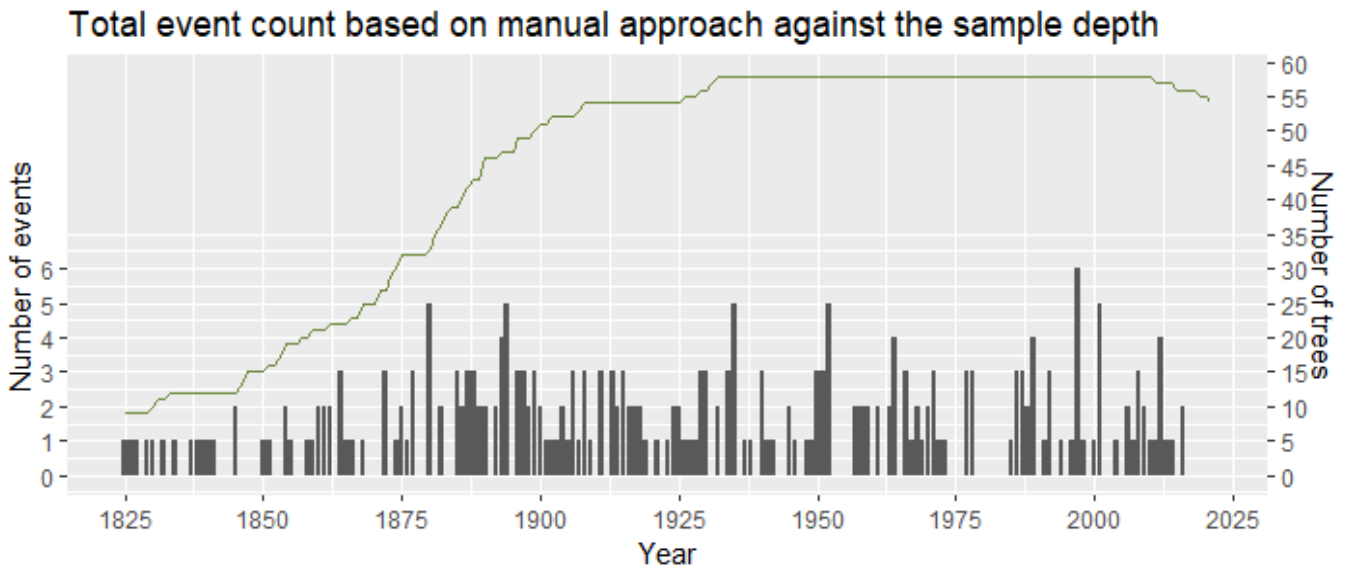


Figure 28: Total event count (254) at all three sites based on the manual approach. The sample depth is 58 trees. In green the number of tree samples for each year.

Figure 28 shows the number of all detected events based on the manual approach. As described in the methods the two samples that were taken on the inclined side and its opposite were compared for each individual tree. If they showed *Gegenläufigkeit* (see Figure 21), meaning one side of the tree showing an increase in growth and the opposite side a decrease they were marked as events. Years that showed much wider rings on one side while the other stayed at the same level (see Figure 22) were also noted down as events. This approach leads to a total of 254 events distributed over all three sites. In six years, a particularly large number of events was registered: 1880 (5), 1895 (5), 1935 (5), 1952 (5), 1997 (6) and 2001 (5). Only a handful of years do not show at least one disturbance. Still there are a few consecutive years without disturbances, which in turn help distinguish possible phases of activity. Such potential event phases are: (1) 1825-1841, (2) 1850-1882, (3) 1885-1952, (4) 1957-1973 and (5) 1985-2016. The distinction between phase 2 and 3 is made even though there is only a very short event-free period in between. However, beginning with the year 1885 the event frequency regarding the events per year and successiveness in years appears to be higher.

The following figures show all detected events broken down to their respective site. The maximum of events for each site per year is three. No distinction was made between the tree species.

Total event count for site 1 against the sample depth

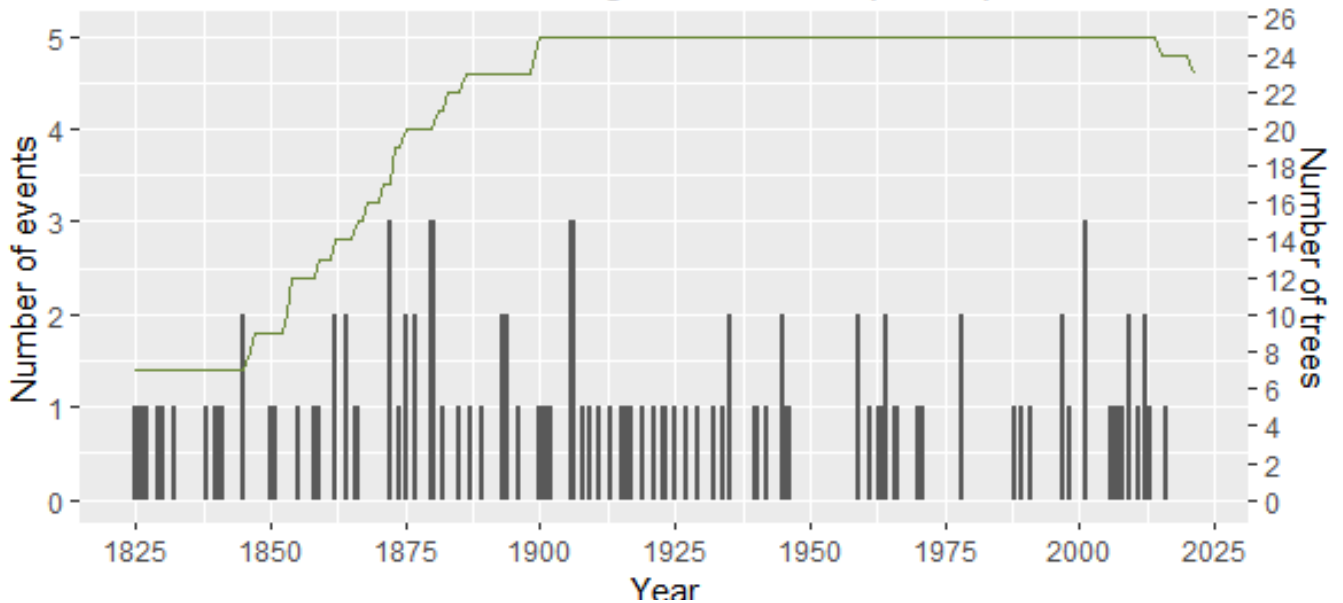


Figure 29: Event count for site 1 based on the manual approach. In black are the number of events and in green the number of tree samples for each year.

The total event count for site 1, which can be seen in Figure 29, shows quite consistently one or more events until 1946. The time periods from 1947-1958 and 1972-1987 (with an exception in 1978) do not show any disturbances. Thereafter however, events were again regularly dated with a peak around the year 2000. The last event at this site was noted in 2016. In contrast to site 1, hardly any events were recorded at sites 2 (Figure 30) and 3 (Figure 31) before 1850. However, at Site 1 there were seven trees going back to 1850. Contrary to that, the other two sites cover the 1850s with only three (B02) and four (B03) trees.

Total event count for site 2 against the sample depth

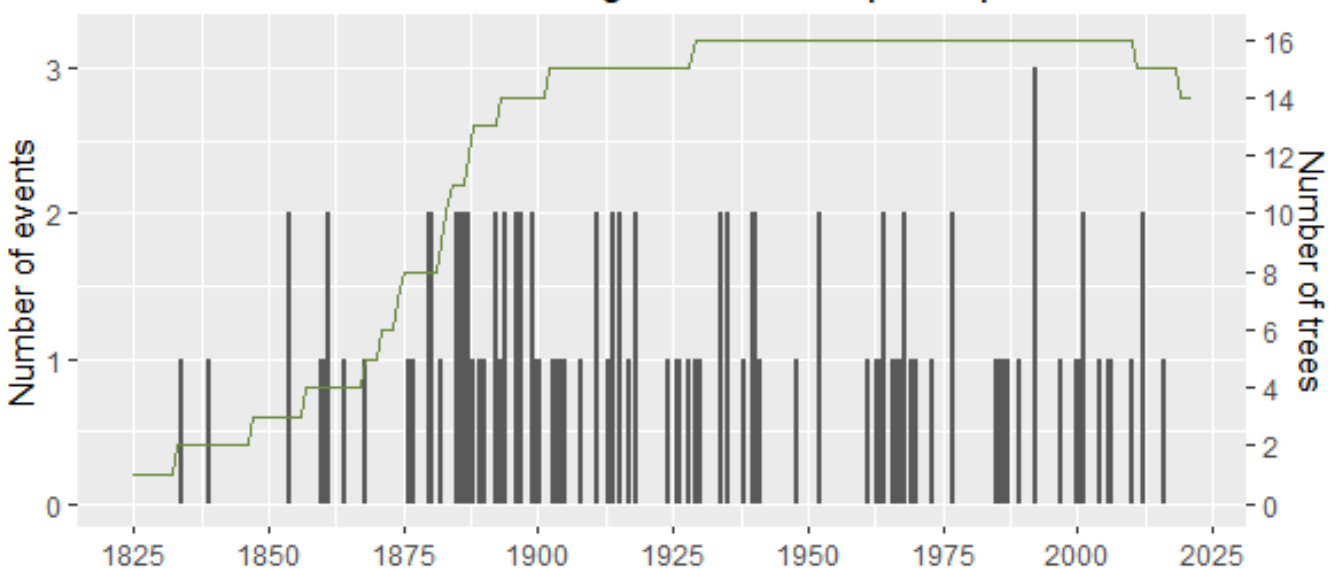


Figure 30: Event count for site 2 based on the manual approach. In black are the number of events and in green the number of tree samples for each year.

Beginning with the year 1876 regular events were also noted at the second site (see Figure 30). The year 1992 with 3 events is conspicuous, but also the time periods 1885-1894 and 1966-1970 where in every single year at least one event was identified. At this site the last event was detected in 2016.

Total event count for site 3 against the sample depth

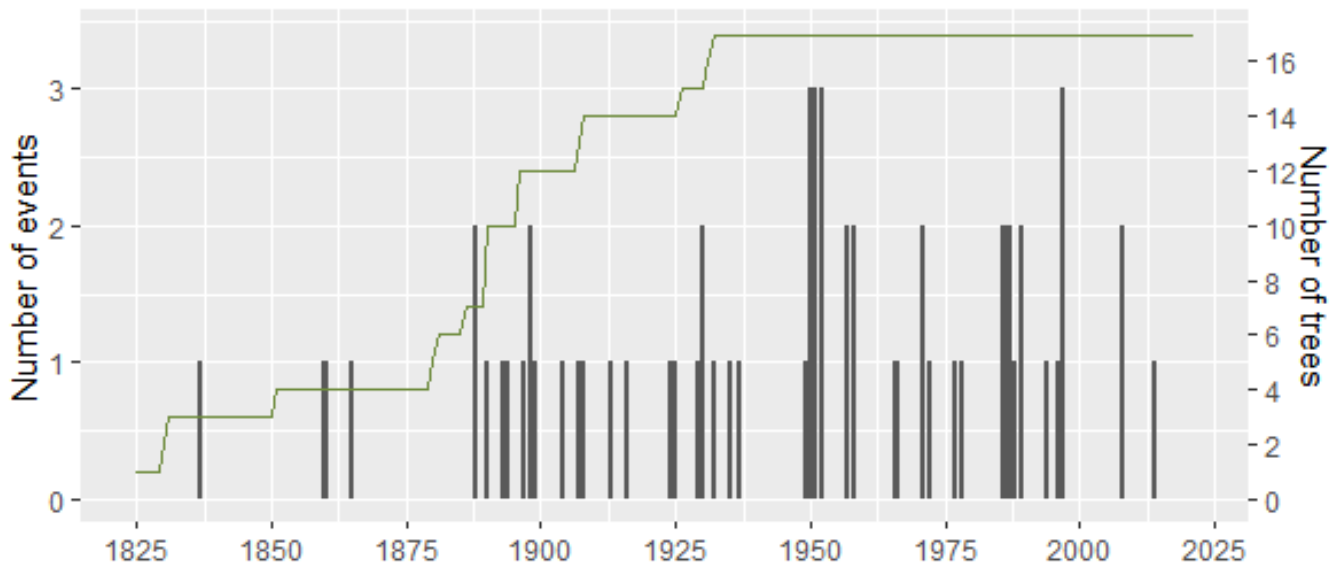


Figure 31: Event count for site 3 based on the manual approach. In black are the number of events and in green the number of tree samples for each year.

Figure 31 shows the recorded events for site 3: Before 1888 only three events were recorded. However, beginning with the year 1888 until 1937 a more active phase took place. Then another resting phase a series of several events per year took place from 1949-1952. After these years another quite active phase took place from 1986-1997. Apart from that, there are mainly single event years to be found after 1950. The last disturbance for site 3 was noted in 2014.

It must also be considered that there is much less data for the first phase for all sites, as only a few cores have been dated back that far. Therefore, fewer years with a high number of events do not have to indicate less strongly disturbed years than the following phases. In addition, not an equal number of trees was sampled at all sites. An overview of the number of sampled trees and the number of detected events can be seen in Table 4. It is interesting that even though almost the same number of trees were sampled at sites 2 and 3, but one and a half times more disturbances were found at site 2.

Table 4: Overview of the number of sampled trees and detected events per site.

Site	Sample Depth	Event count
1	25	99
2	16	95
3	17	60

6.3 Total event count based on eccentricity index

While the results from chapter 6.2 are based on a manual approach, eccentricity was also calculated for event detection as a contrast to visually detecting event years. Detecting event years based on eccentricity is highly dependent on the chosen threshold. The first chosen threshold is based on the average and the standard deviation (see methods). The threshold for the positive eccentricity was set to 37.14 and for the negative to -35.90, respectively. This threshold is subsequently called threshold 1.

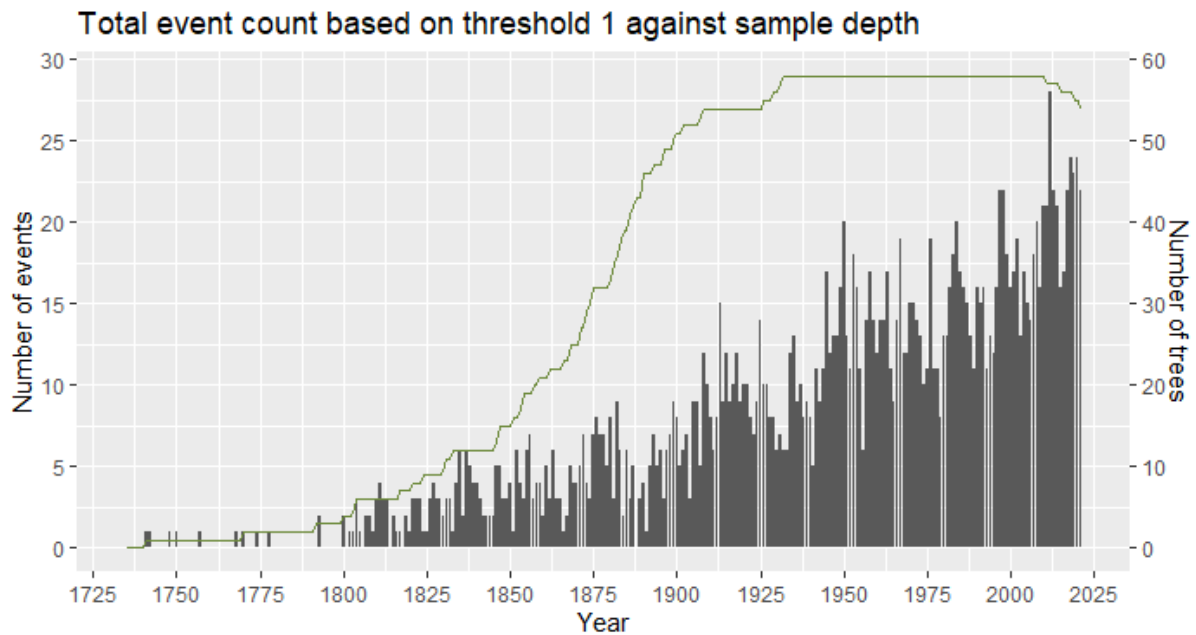


Figure 32: Total event count of detected events based on the eccentricity index calculations compared to the sample depth. The threshold of the index is based on the average ring width variations of the reference chronology and set to -35.90 and 37.14. In green the number of tree samples for each year.

It is evident that this approach results in a much higher event count (see Figure 32). With this threshold the highest event count per year is 28 in 2012 and the total event count is 1973. Likewise, one can see a strong event increase over time. Before further interpretation the increase in available tree data must also be considered. Interestingly the number of events continues to increase from 2011 onwards, despite the decreasing number of trees. Additionally, the event-free years registered from 2016 onwards in the manual approach are not reflected here. Due to the high number of events, it is also not possible to detect individual phases. Apart from the year 1888, starting from 1818 there is no year without disturbances.

This event count is extremely high, which could indicate that the chosen threshold is overly sensitive to changes in ring widths over the years. The second threshold (2) calculated from the median shows very similar results and thus the same limitations (see in appendix, Figure 46). The results of threshold 2 will not be shown or discussed, since they are the same as for threshold 1.

A third threshold was chosen to approximate the maximum event number per year and the total number of events of the manual approach as closely as possible. The threshold was set artificially to 100. Which means an eccentric growth had to be almost three times as strong to be detected. With this approach the highest event count per year can be found at 10 (see Figure 33), which is still higher than in the manual approach (see Figure 28). On the other hand, the total event count is with 238 slightly lower. This threshold is referred to as threshold 3.

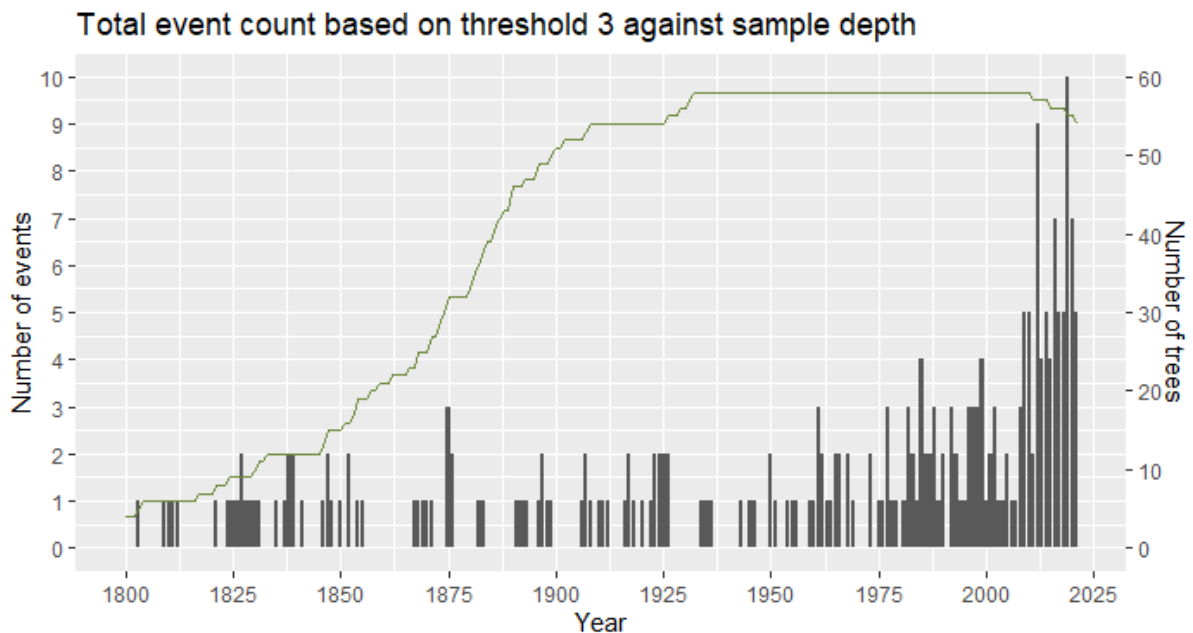


Figure 33: Total event count based on the artificially adjusted threshold, which is set to -100 and 100. In green the number of tree samples for each year.

Figure 33 shows the result of this less sensitive threshold. Since the number of events is strongly cut down, individual motion phases could be defined again. Mainly there appears to be an active phase between 1821-1855, followed by 11 years without any disturbance. After those three shorter periods from 1867-1883, 1891-1899 and 1906-1926 follow. The years from 1927-1942 again were, apart from a short intermezzo from 1933-1935, quite undisturbed. This was followed by a hardly interrupted active phase with the highest event numbers per year, which continues to this day. A possible distinction of this last period into two different phases could be the quieter years between 1970 and 1974. Another distinction could be the year 2009 where the event count reaches five for the first time. From this year until the end of the data series, the average number of events is significantly higher than before. Looking at the overall picture, a division into three main phases would also be possible: 1800-1855, 1867-1926, 1942-2021.

6.4 Reaction wood in thin sections

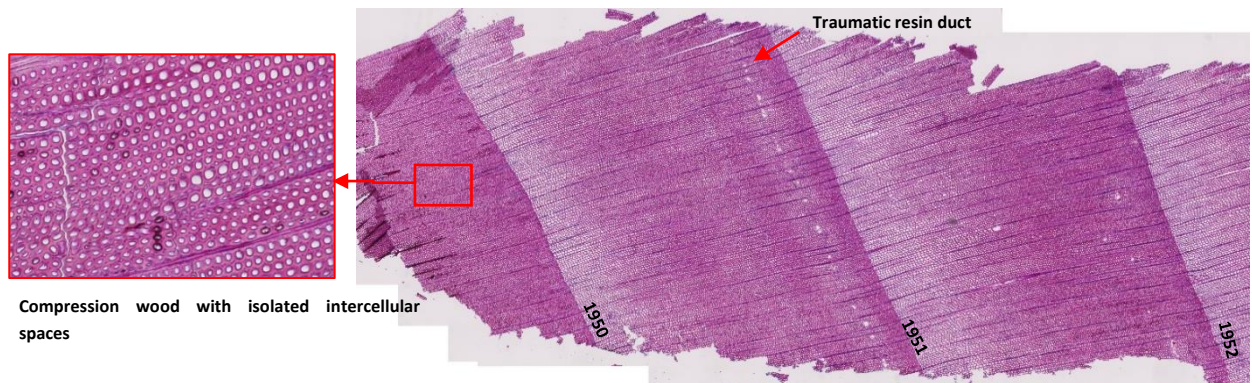


Figure 34: Thin sections of spruce at site 3 (B03Fi08d). The sample shows in all three years compression wood, but only in 1950 intercellular spaces (see red box). In 1951 a traumatic resin duct can be seen.

The thin sections were made where an event was already dated using the manual approach. The idea was to confirm with a small number of samples, certain event classifications (three samples) and to gain more information in case of uncertain classifications (three samples). Unfortunately, the expected compression wood was only found in one sample. The sample was of a spruce tree at site 3 (see Figure 34). Based on the divergence of the chronologies a *certain* event was dated for the year 1950. Accordingly, a thin cut of this year ring and the following rings was made. Figure 34 shows the results of this thin section. Additionally, to the clear compression wood in 1950 and the two consecutive years, also a traumatic resin duct can be seen in the sample. Although the traumatic resin duct was found in the 1951 tree ring, it could still have been caused by the same disturbance that caused the formation of the compression wood. The reason is that traumatic resin ducts do not necessarily form in the same year that their cause occurs (Bollschweiler et al. 2008, Gärtner & Heinrich 2013). The presence of these two growth responses clearly indicates that, as expected, a disturbance of the tree has occurred during this time period.

Some of the other samples show arguable hints of compression wood but certainly not enough to base a valid argument on it. Therefore, the thin sections cannot be used to support the other results, which were presented in the previous subchapters.

6.5 Comparison of event phases identified by different approaches

All these different approaches lead to partly consistent and partly divergent results. Figure 35 shows the summary of the results. The defined activity phases are based on the data of all three sites combined. The exact years of the phases by approach can be seen in the appendix, Table 5. It is noticeable that depending on the method, quite different disturbance-free phases were assigned.

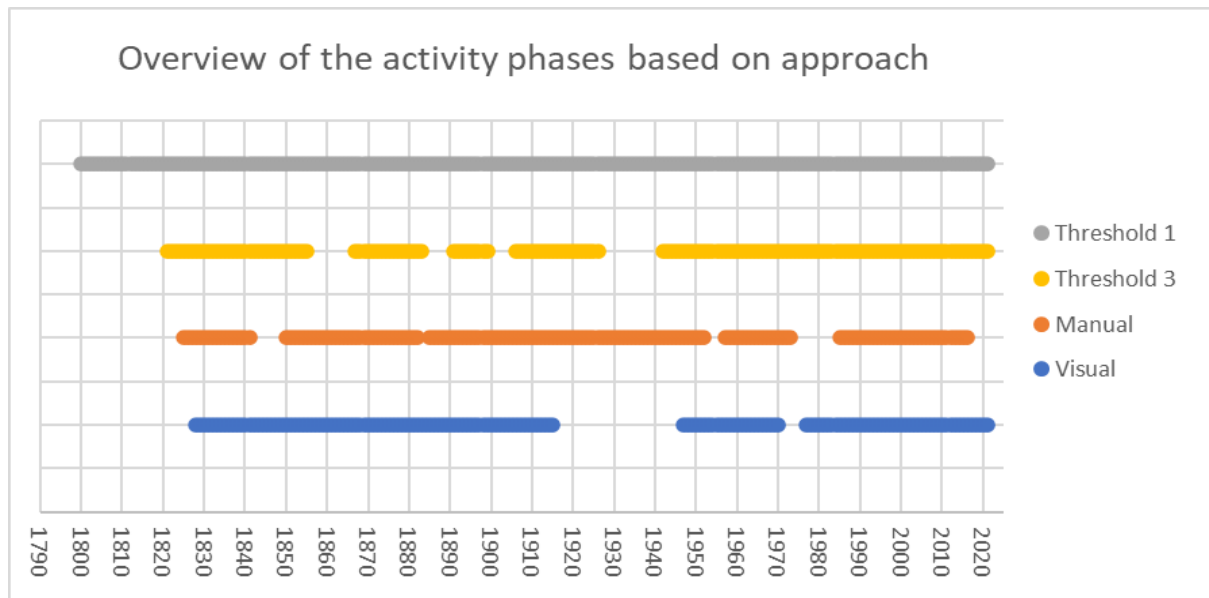


Figure 35: Visual comparison of all event phases based on different approaches. Threshold 2 is not shown since the result is the same as threshold 1. All events are looked at tighter without a distinction for site or species.

The results of the phasing for the whole area show that activity phases could always be detected in all approaches. The results of the eccentricity approaches establish the activity phases earlier than the visual interpretation or the manual approach. Threshold 1 results in a continuous activity phase due to the very deep-set threshold. Therefore, threshold 1 is not specifically mentioned in the following description of the results. In the 1930s, the visual classification and the eccentricity approach with threshold 3 coincide but not the manual approach. In the time period between 1970 and 1985, the results from the artificial threshold (3), the manual approach, and the visual classification all show a break in activity. These do not cover the exact same time period but are within a ten year span of each other.

In Figure 35, the activity phases were shown for the area as a whole. However, the individual sites also often have only partially overlapped phases. If all sites are collectively looked at, the phases complement each other to form one big continuous phase (compare Figure 35 to Figure 36). Hence, it is reasonable to look at the results of the sites individually rather than as a whole in the following section.

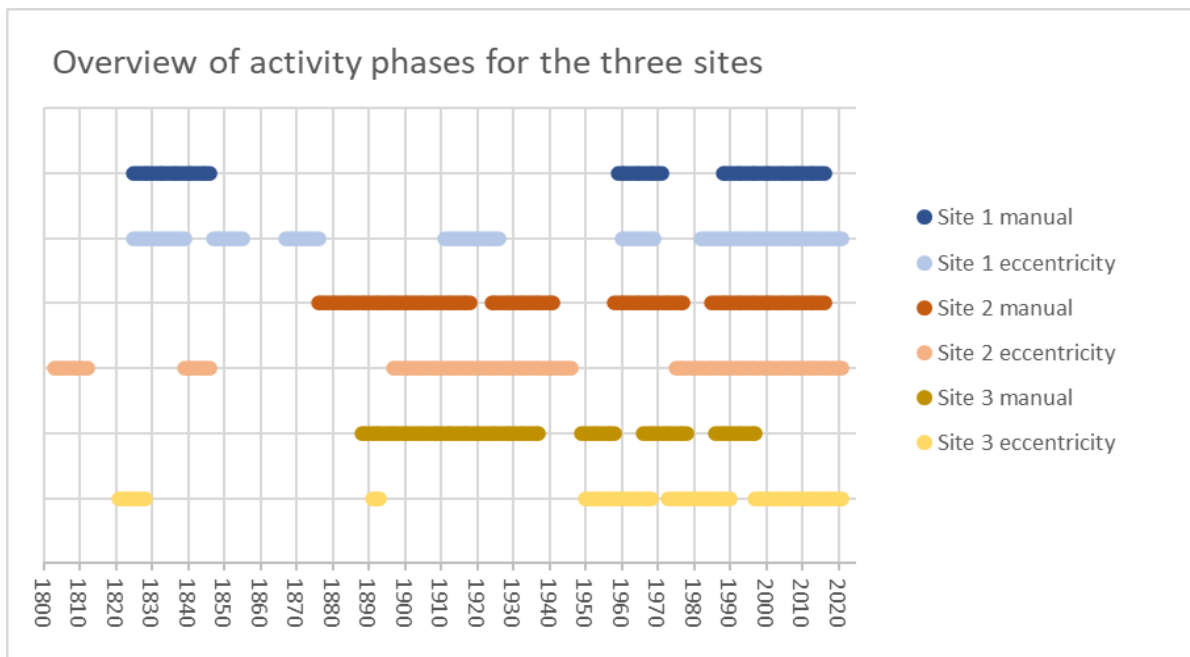


Figure 36: Visual comparison for the three sites of all event phases based on different approaches.

Figure 36 shows the summary of results for the three individual sites for both the manual approach and the eccentricity calculations with the artificial threshold (3). The approaches led to partly very different activity phases and event numbers.

Only site 1 shows in both approaches an active phase before 1850. Sites 2 and 3 only show short activity intermezzos for the eccentricity approach. The time period from 1875-1945 with two exceptions (site 1 manual approach and site 3 eccentricity approach (only very briefly)) has a clear activity phase. Site 3 shows for both approaches an active period around 1950. The manual approach started to detect events in 1949 and the eccentricity approach in 1950. For site 1 and 2 no phase with a higher event density around 1950 was detected. All sites and all approaches (except site 2 eccentricity) display an activity phase in the 1960s and early 1970s. And in the following decades all sites and approaches have activity phases. For the manual approach at site 3, this ends shortly before 2000, for all others it extends to the following two decades. It is clearly visible that the last phase for the eccentricity approaches continues until today, while the manual approaches end several years earlier.

6.6 Disturbance count in individual trees

Up to this point, the detected number of events has been presented in regard to the entire area or the three individual sites. This subchapter, however, will look at the individual trees. The following figures (Figure 37, Figure 38, Figure 39) show the distribution of the trees at their respective locations. The number of registered events is marked for each tree. Additionally, the cracks mapped during the fieldwork are also drawn in the figures. This should provide an insight into smaller-scale processes within the three study sites. Since no differences were found in the number of disturbances, where the species and not the location is a determining factor, the species will not be discussed further at this point.

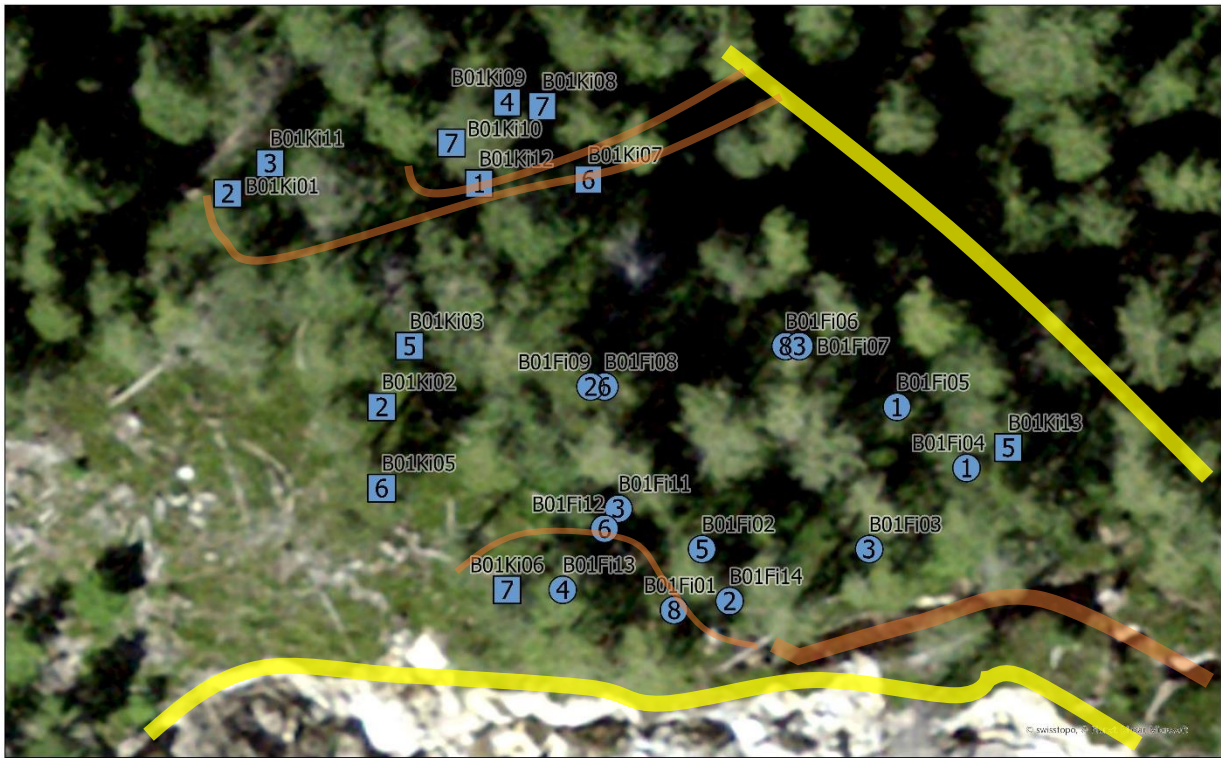


Figure 37: Location of individual trees at site 1. Light blue dots: Location of a tree and number of events detected for this tree. Circles represent spruces and squares represent pines. Orange line: Marking for gap opening in the ground (about 0.5 m to 2 m wide). Yellow line: Impassable terrain, in this case two break-off edges. The upper one separates site 1 from site 2 with a very large and deep gap. The lower one is the main breakaway edge. Map ©swisstopo



Figure 38: Location of individual trees at site 2. Blue dots: Location of a tree and number of events detected for this tree. Circles represent spruces and squares represent pines. Orange line: Marking for gap opening in the ground (about 0.5m to 2m wide). Dashed lines represent overgrown cracks. Yellow line: Impassable terrain. On the left side, the yellow line represents the break-off edge between sites 1 and 2. Site 1 is about 10m higher. On the right the transition between the active and inactive landslide, the active part has sunk about 15 m, the trench in between (in orange) is about 5 m deep. Map ©swisstopo

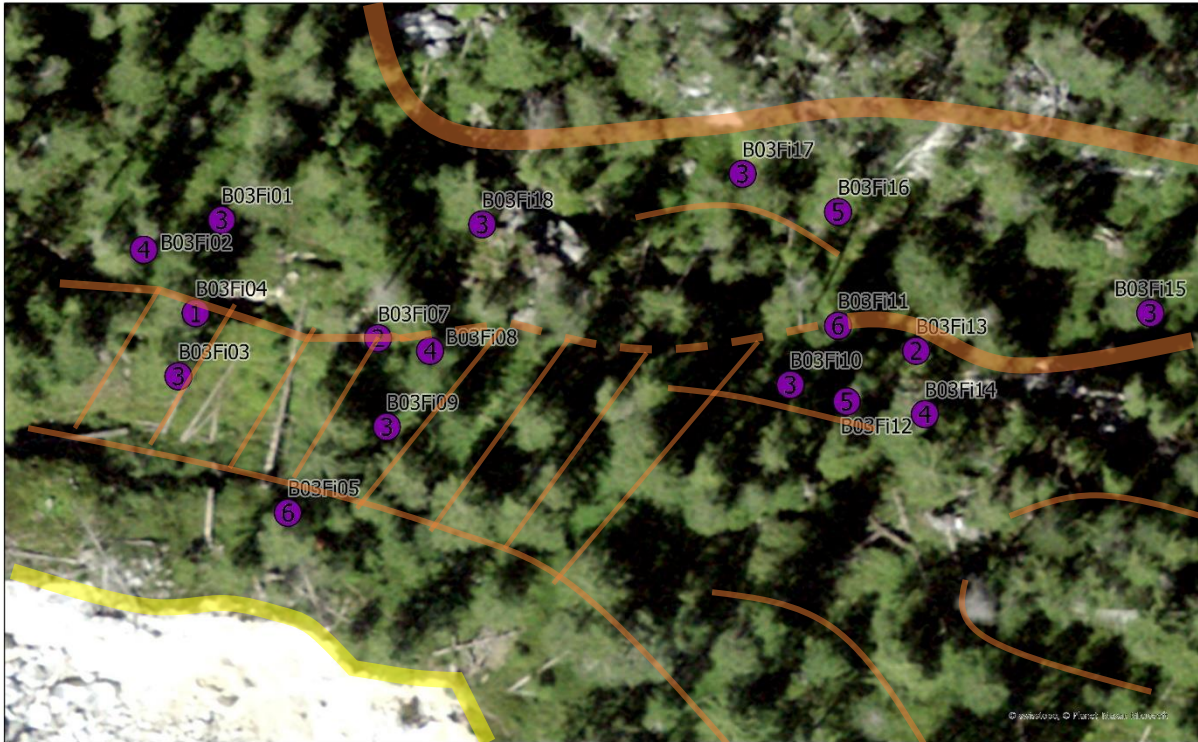


Figure 39: Location of individual trees at site 3. Violet dots: Location of a tree and number of events detected for this tree (only spruces at this site). Orange line: Marking for gap opening in the ground (ranges from 0.5 m to 10 m). Dashed lines represent overgrown cracks. Yellow line: Impassable terrain, in this case the main breakaway edge. Map ©swisstopo

In Figure 37 all 25 sampled trees from site 1 are displayed. The total event count per tree ranges from 1 to 8. For half of the trees five or more disturbances were detected. This site has fewer and smaller cracks in the soil compared to the other two sites. The site is very clearly bounded by the main break away edge and a very wide and deep rift opening. This large gap opening represents the boundary between site 1 and site 2. The two edges meet slightly outside the map, so the entire first site can be described as a peninsula.

In Figure 38 all 16 sampled trees from site 2 are displayed. The event count per tree ranges from 1 to 13. For the other sites, the maximum disturbance count is eight (site 1) and six (site 3). The area is not directly on the main breakaway edge, but it is below the landslide undisturbed area. Compared to the inactive area, it has slipped a few meters. The site is mainly characterized by the wide and deep fissure formed between disturbed and undisturbed areas. Along this rift run some smaller fissures. The other end of the site is bounded by the rift that separates this site from site 1. There are many small, jumbled cracks in this area. In addition, a long and about one meter wide fissure runs through the middle of the area.

Figure 39 shows all sampled spruces from site 3. The detected event count per tree ranges from one to six. Of the 17 trees sampled, one-third recorded three disturbances. The number of disturbances in the trees is more regular at this site compared to the other two sites. In addition, there is a very large, shallow fissure opening in this area (marked by orange cross lines), in which new cracks have again opened.

6.7 Comparison of precipitation data with the number of events

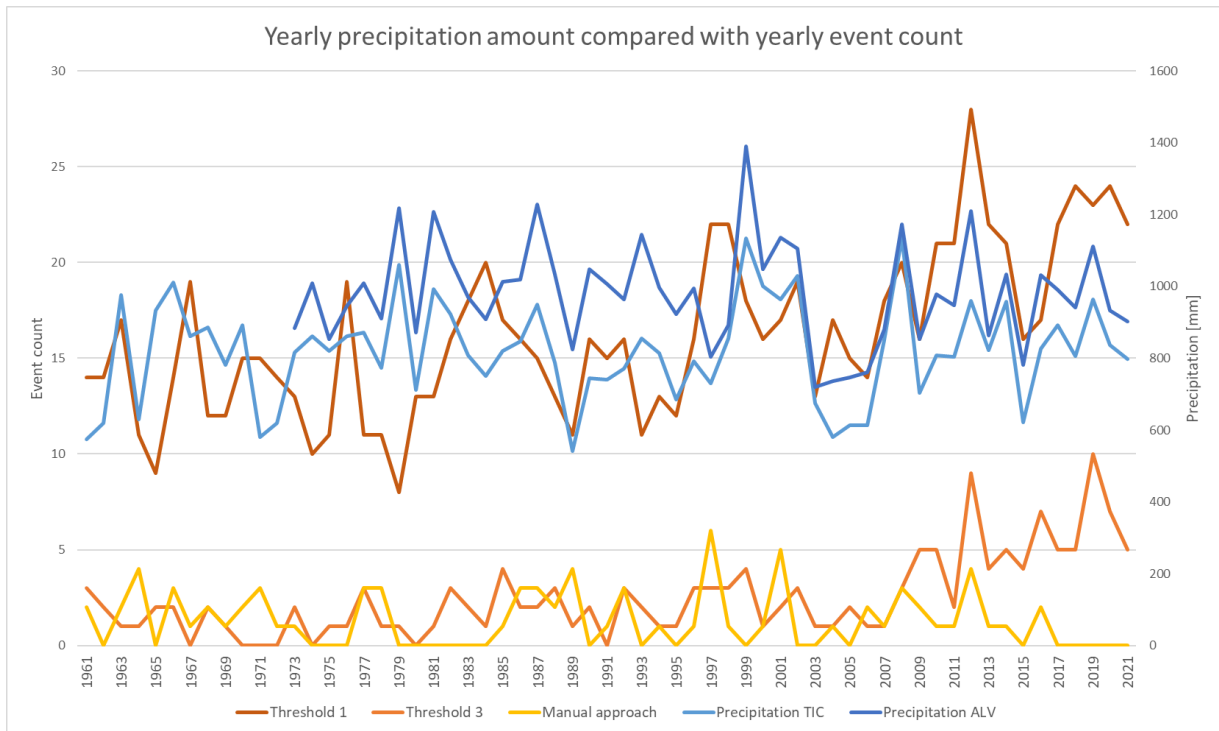


Figure 40: Precipitation data from nearby meteorological stations (TIC= Tiefencastel, ALV = Alvaneu) in blue hues compared to the number of events of all three sites together (assessed by different approaches) in red/yellow hues.

In Figure 40 the precipitation data of the two weather stations closest to the study area are shown. As expected for two stations so close to each other, the precipitation curves coincide. The curves for thresholds 1 and 3 often align as well. This is also not unexpected, as both use the same approach, only with different sensibilities. The longer precipitation measurement series lasts from 1961 until today. Therefore, only the tree ring data back to this year can be discussed here.

There are some years in which the amount of precipitation correlates with the event number. Most striking are the last 10 years. The strong precipitation peak in 2012 is reflected in all event counts regardless of the approach and also the precipitation low three years later correlates with an event low in the same year. In 2018, renewed low precipitation numbers also provide lower event numbers for threshold 3 and the manual approach, but not for threshold 1. The following year, the event peak of threshold 3, but not threshold 1 and manual approach, correlates with higher precipitation. In the last year of the data series, lower precipitation values again coincide with overall lower event numbers.

6.8 Measured soil movement near the investigated sites

CSD Engineers carry out regular movement measurements in different points in the study area. Figure 41 shows the handmade GPS measurements over the last 13 years for four points that are in vicinity to the three study sites (CSD Engineers 2022). These points are all within 40 m from a sampled tree. The exact distances can be seen in the appendix, Table 6. There are other measurement points for site 1 that are even closer. However, these are behind the breakaway edge and have therefore a different dynamic. Meaning that the measuring points in the loose scree have travelled up to 300 times longer distances than the ones shown here. They can be seen in the appendix Figure 47, where the movements of the other measuring points are shown.

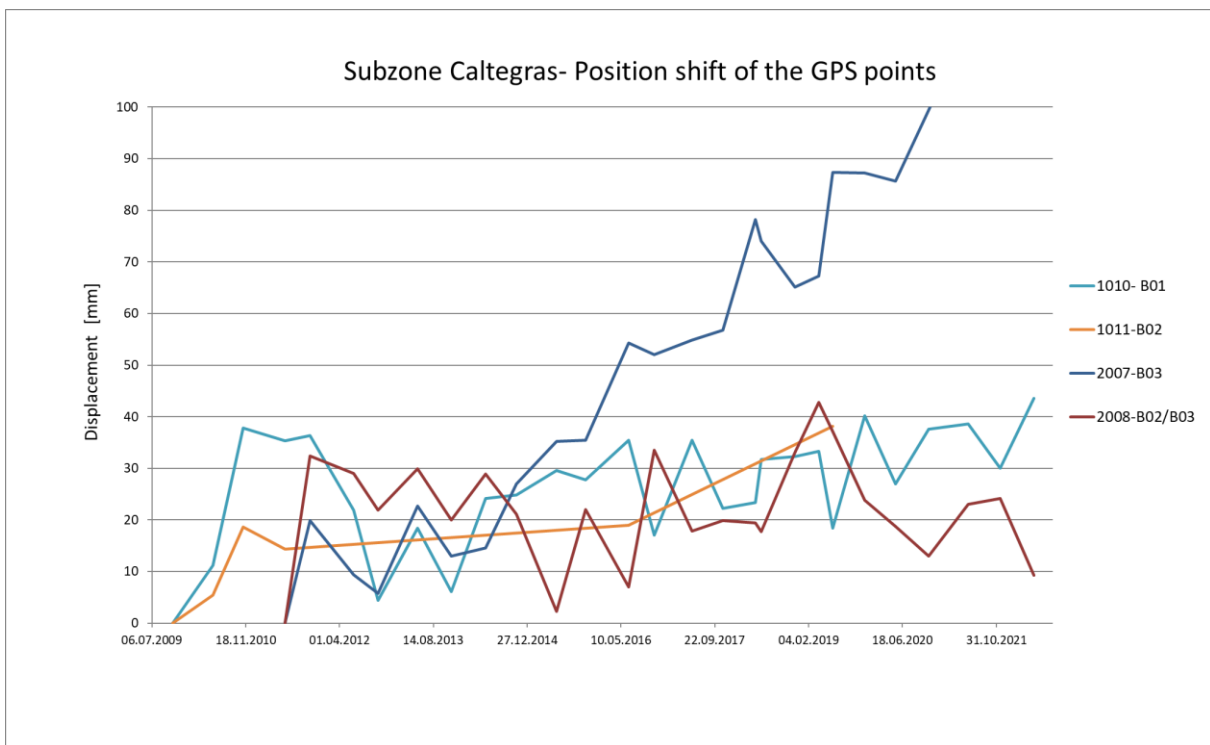


Figure 41: Motion data from four measurement points near the study sites. The legend also indicates which measurement point is closest to which site. All measurements were made by CSD Engineers (2022).

Figure 41 shows that three out of four measurement points tend to cover increasingly greater distances between measurement sections and the end of the respective measurement series. The only measuring point where this is not true, is the one between site 2 and 3 (point 2008). The figure also shows that the distances covered vary from year to year. So, although there is a tendency for movement to increase, it is not linear.

7. Discussion

7.1. Strengths and limitations of the different methods used in this study

One of the biggest challenges of this work was mapping the three study sites. The forest above was so heavily marked by cracks in the ground that it was very difficult to keep track of the geomorphologic features. For correct mapping, GPS coordinates were taken from all sampled trees. However, since many trees were in a very confined space, it was difficult to distinguish the exact locations by GPS measurements. For this very reason, it would have been useful to measure certain coordinates multiple times. Nevertheless, with the help of the GPS data and the handmade maps of the area, it was possible to reconstruct all the locations of the trees.

Another challenge was to set the core drill correctly. Many trees were not only tilted in one direction but several times in different directions. It was therefore not always clear on which side of the tree the compression wood was to be expected. This could also be a reason why compression wood was only found in one sample of the thin sections. A higher number of thin sections could also have provided information as to whether there was really no reaction wood or whether it was missed during drilling. In favour of the former is the fact that the cuts examined for compression wood were selected based on the eccentricity curves. According to the literature conifers can respond to an inclination with eccentric growth without the formation of compression wood Schweingruber (1996). And vice versa, the presence of reaction wood does not guarantee tree-ring eccentricity in the same year according to Šilhán & Stoffel (2015).

Different approaches were used to reconstruct active phases of the landslide in Brienz. A first impression of the activity phases was obtained by visual analysis of the different chronologies of the disturbed trees. In the next step, these chronologies were analysed individually for each tree, recording the years of disturbance. The disturbance years of all trees together were then also divided into individual activity phases. Finally, the disturbance number was calculated using the eccentricity index. These results were again used to determine activity phases. Although both approaches have their limitation.

When comparing the two cores per tree manually, it is important to set clear conditions for the classification as an event. These, however, are made on the basis of one's own assessment and not on the basis of generally valid guidelines. On the other hand, manual assessment allows to look at the individual years in the context of the previous years and the following years. Also one falsely classified event has no effect on the other results.

Calculating the eccentricity index to date landslides is widespread in the literature (Braam et al. 1987; Fabiánová et al. 2021; Malik & Wistuba 2012; Šilhán et al. 2013; Šilhán & Stoffel 2015; Šilhán 2019; Wistuba et al. 2013; Wistuba et al. 2019). It has the advantage that human errors in determining the events (e.g. a forgotten entry or the disregard of the set conditions) can be avoided. However, the results depend strongly on the selected threshold. The approach described in the literature for calculating a threshold was of limited use for this Master's thesis. The threshold (1) was much too sensitive and has detected countless events. This might be since the used threshold was calculated according to the default of Wistuba et al. (2019). They used the eccentricity of the trees to date individual completed landslides at different locations. In contrast, the sites studied in this Master's thesis are in constant motion, as they are not affected by one

single event but a landslide that has been ongoing for several centuries. Accordingly, the eccentricity of the trees could already be relatively high in principle and years are also counted as disturbance years that do not stand out in the manual analysis. In short, the threshold from the literature is too sensitive for this location. The same applies to the alternative threshold (2), which was calculated using the median of the relative variation from year to year instead of the mean. The third threshold shows another weakness of this method. This threshold leads to results that are most similar in terms of event number per year and total event count to those of the manual approach. But this threshold was determined artificially and not based on calculations from the literature. The threshold from the literature and the one defined in this study are thus far apart. This leads to the question how meaningful the eccentricity calculations really are if they are so strongly dependent on a possibly arbitrarily set threshold.

However, there are two points in favour of the eccentricity approach results: The results of this method show a strong increase in the number of events in the last 10 to 20 years. This fits the faster landslide movements since 2000. Furthermore, the event numbers of threshold 1 (average-based) match the precipitation data in many years. This is consistent with the findings of the literature, which sees strong precipitation as a major factor for triggering landslides (Chiarle et al. 2021; Corominas & Moya 1999; Lopez Saez et al. 2012; Shi et al. 2022; Šilhán et al. 2012; Stefanini 2004; Malik & Wistuba 2012).

Although several methods were used in this Master's thesis in order to generate reliable knowledge about past activities of the landslide in Brienz, the results were not always consistent. However, conclusions can also be drawn from results that are not in complete accordance with each other which is discussed in subchapter 7.2. This Master's thesis shows clearly how important it is to be aware of the partial reliability of such an analysis. As discussed above, a different sample group or a change in fieldwork methods could lead to different findings. But also, different approaches can lead to differing results. Šilhán (2019) came to a similar conclusion. He analysed three different approaches based on eccentricity, their limitations, and their advantages. He concluded that the choice of method influences the resulting disturbance chronologies but not the spatial distribution of the landslides. Šilhán & Stoffel (2015) compared the results of the eccentricity approaches with those of reaction wood and found that they also differed. Furthermore Fabiánová et al. (2021), Šilhán & Stoffel (2015) and Šilhán (2019) all point out that the age of the sampled trees influences the results as well. Younger trees tend to be more sensitive than old ones (Šilhán 2019). Thus, for a future study it would certainly be useful to pay attention to the spatial and age distribution of the sampled trees. Furthermore, it should be carefully considered which approach is most appropriate for answering the research question.

7.2. Determination of major event phases based on activity at three different sites

As it is shown in Figure 36 the event phases determined by the different methods often overlap but never completely coincide. However, all approaches clearly show that the forest in the investigated area is greatly influenced by continuous ground movements. Although the results for the manual and eccentricity approaches do not always align with each other certain conclusions on intervals with differing activity levels can still be drawn mainly based on time periods where no activity phases were detected, regardless of the approach or location. It must be stated that the

following discussion of periods is based on the division into activity phases and phases with no activity as shown Figure 35 and Figure 36. No activity does not implicate that there were no events at all detected during that time. It means that there were no or only very isolated events in this period and they were therefore counted as inactive periods. Similarly, there may be years with no detected events in an activity phase.

The period from 1850-1876 appears to be, with exception of the site 1 eccentricity approach, a quiet phase, as no disturbance phases were detected for all three sites (see Figure 36). A quiet period may also have occurred around 1980 as all three sites show an event-free phase around 1980 based on the manual approach for all three sites (see Figure 29, Figure 30 and Figure 31). Even though, based on the eccentricity approach 1980 is located in an active phase (see Figure 36). Neither with threshold 1 nor threshold 3 any event in 1980 were detected. Even two years before and after 1980, there were only isolated disturbances according to the eccentricity approach, and none at all with the manual approach.

Interestingly, the year ring chronologies for site 3 show an extreme growth increase in 1947 to 1949 (Figure 27), while the chronologies for the other two sites and the reference chronology only show a moderate increase. Additionally, the mean chronology for site 1 (Figure 25) and 2 (Figure 26) and the reference chronology all show a growth drop in the year 1947/48 while, site 3 does not. Thus, the growth rates at site 3 differ significantly from the other two sites and also from the reference. This extreme growth at site 3 cannot be explained by a very favourable climate during these years, because this would have been reflected in an increased growth in the reference and the other sites as well.

The nudation of the sampled trees due to the logging of other trees could have strongly favoured their growth and could thus be a possible explanation for this extreme growth release (Gärtner & Heinrich 2013). However, according to the local forester there is no record of logging for site 3 during this time period (Guetsg 2022). The assumption is therefore that a movement in the soil could have led to favourable growth in the trees and at the same time acted as a precursor for a strong disturbance phase (see the disturbance accumulation for the years 1950-1952 in Figure 31).

When comparing these results with the visual interpretation of the activity phases, there are both agreements and discrepancies detectable. First, the visual classification leads to three main phases (1828-1915, 1947-1970, 1977-2021). The first phase of the visual interpretation (1828-1915) does not align well with the results over all sites that are visible in Figure 35.

Nevertheless, site 1 (manual and eccentricity) and site 2 (manual) (see Figure 36) reflect the two later phases of the visual approach (1947-1970 & 1977-2021) quite well. Furthermore, the results of the eccentricity approach for sites 2 and 3 also cover approximately the third and last visual based phase (1977-2021). However, it is striking that the period from 1916 to 1946, which was not classified as an active phase in the first impression of the visual classification, was ultimately clearly marked as active at all sites. This could be due to the fact that in the visual overview of all chronologies, these are less dispersed this period. However, this impression is created especially in relation to the very scattered decades before and after. Thus, these years may have appeared less active in the initial visual view. At the same time, however, the manual and eccentricity approaches detected enough disturbances to classify them as event phases.

As it was mentioned in the previous subchapter, the eccentricity approaches all showed a strong increase in the number of events in recent decades. This increase can be explained by the greater activity of the landslide. With the increasing speed of the landslide, the trees are increasingly disturbed in their growth. This in turn promotes the eccentric growth leading to tree ring widths that exceed the threshold and are therefore held as an event year. It can therefore be concluded that the number and distribution of the disturbances allow conclusions to be drawn about past events (Šilhán et al. 2019; Stoffel & Bollschweiler 2009; Wistuba et al. 2013) and in this case about the development of the Brienz' landslide in this subzone.

7.3 Disturbance of individual trees in relation to their location

7.3.1 Influence of the location on the number of disturbances

At site 1 a handful trees were sampled that were standing in immediate vicinity of the breakaway edge. Three trees stood on their own small island, since they were separated from the rest of the study site by a crack (shown in Figure 37). Two of them, even though they have only a slight inclination, are with seven and eight events among the highest number of disturbances per tree in this area. This can probably be derived from the fact that this small island has started to detach from the rest of the ground. Directly on, the above mentioned, crack grows one additional tree. Although these this tree also has little inclination, the soil breaking apart must have a strong influence on it, since it also has a high event number with six disturbances.

Another cluster of trees with partly high number of disturbances, can be found near two crevices in the ground. Although these cracks are relatively small, they may also explain the disturbances. On the other hand, no obvious explanation can be found for the eight disturbances of tree B01Fi06. There is no crack opening nearby, the tree stands at a relatively large distance from the edges, and the nearest neighbouring tree (B01Fi07) shows a relatively low disturbance count of three.

Since site 2 is the only one located at some distance away from the main breakaway edge and thus the most active area (Schneider 2022), it was previously assumed that this area might be somewhat freer of new disturbances. Already the sampling of partly very strongly inclined trees contradicted this assumption. In addition, the four trees with the highest disturbance numbers (9, 9, 10, 13) are located at this site. All four of these trees are standing very close to either a crack or the gap between the active and inactive area (see Figure 38). Sample B02Fi08, the tree with 13 disturbances, had by far the thickest trunk. The assumption was that this is the oldest sampled tree. Unfortunately, it was rotten in the centre, so the rings could be only dated to the year 1804. The second highest disturbance number was found in tree B022Fi09 in vicinity. This tree did not show any visual hints for such a high number of disturbances, but during the sampling it became visible that the tree was undercut to a large extent. Since the terrain in this area also became steeper, this could have provided additional instability to the already disturbed ground and caused the high number of events.

The second tree showing nine disturbances is also growing in immediate vicinity of a crack. Likewise, very old and relatively recent disturbances were detected in both. So, if the disturbances originate from the opening of the crack and not from the general movements, these cracks must be already relatively old (first events dated in 1876 and 1877). Since the cores did not reach further

back, it cannot be said whether there were any disturbances previous to these years. It was a bit surprising that the trees closest to the gap (top left) did not show higher event numbers, since they were amongst the most inclined trees at all three sites. Two of the trees even lay on top of the edge of the inactive area.

Site 3 visually appeared to be the most disturbed, mainly due to the impressive cracks in the ground. From very narrow and deep, to large and shallow, countless cracks were present here. For example, the area marked with several crossbars (see Figure 39) was one big relatively shallow crack. Contrary to that impression, the least number of disturbances was noted here in the individual trees as well as overall. Of the two trees with the highest event count (6), one is growing on a crack and the other is close to the main breakaway edge.

7.3.2 Conclusion drawn from analysing the disturbance number of individual trees

It is interesting that all 58 sampled trees showed at least one disturbance that was defined as an event. And with the exception of five trees, all showed more than one disturbance. This by itself shows that the forest in general is very strongly affected by the landslide.

All sites including, it can be noted that often the trees with a higher event number were standing on or close to a crack in the ground, or one of the big breakaway edges. Even the presence of a number of high-disturbance trees far away from cracks does not have to contradict this finding. The study sites were sometimes confusing since cracks were often partly hidden or opening into two cracks. It was not possible to accurately map all cracks. For this reason the Figure 37, Figure 38 & Figure 39 only show the few main cracks in the study area. Unnoticed or underestimated cracks could still strongly influence these trees. Overall, the site conditions appear to be a good indicator for tree disturbances.

In contrast, the outer appearance of a tree is not necessarily a good indicator for its past disturbance experiences. Site 2 and site 3 had the appearance of a strongly disturbed forest. The trees were often heavily inclined, some trees were split by a crack opening in the ground, and some were even lifted out of the ground. Site 1, on the other hand, appeared relatively undisturbed. The trees were mostly growing straight, and only a few had any visual injuries due to the landslide. Nevertheless, site 1 showed higher disturbance numbers per tree than site 3. And about one and a half times as many events were detected at site 2 in comparison to site 3. The physical shape of the trees alone, therefore, is not always a sufficient indicator for a geomorphologically active area (Šilhán & Stoffel 2022).

Furthermore, the question arises, why significantly fewer events were detected at site 3. This very much contradicts the visual impression of site 3. Since all sites lie within 300 m to each other, they are exposed to the same climatic conditions. According to the geological profile they all have the same geological foundations. It is of course possible that a higher number or a different set of samples from this location could lead to a different result. But with the present data available, it appears that the landslide had a greater impact on the forest at the other two sites within the reconstructed time frame. It could be considered that the movements that lead to the sites today's appearance i.e., to the high number of cracks took place farther back than the age of the trees dated here. However, this does not seem very likely, since according to oral reports, the cracks

have, also at site 3, opened up considerably in recent years. Another argument against this is that the landslide was much slower 200 years ago (SRF Einstein 2019).

7.4 Climatic influence on the study site

The temporal distribution and strength of precipitation can have a strong influence on the development and the nature of landslides (Corominas & Moya 1999; Esposito 2023; Fentucci & McCord 1995; Shi et al. 2022; Šilhán et al. 2012; Stefanini 2004). While shallow landslides can be triggered by reasonably short and intense rainfall, continuous rainfall over longer time can result in deep-seated landslides (Stefanini 2004). The precipitation is also influencing the landslide in Brienz. According to the regular information events for the residents of Brienz, many velocity peaks or relaxations in the various subzones can be associated with the precipitation as well as the snow melt in spring (Schneider 2021; Schneider 2022). For this reason, the relation between the event data and the precipitation data provided by Meteo Schweiz (2022) will be addressed in the following paragraph.

Overall, event counts do not always correlate with the precipitation data which can have several reasons. For example, only the amount of precipitation is considered in this analysis without distinguishing between the different types of precipitation. This means that, for example, snowmelt in the spring is not included in the analysis. In addition, the yearly rainfall does not tell whether extreme phases of rain occurred within a year, which can also occur in years with low annual rainfall and booster events.

The years 1967, 1989 and 2000 are characterized by low precipitation values (see Figure 40). Fittingly two of three event counts were also low in these years. In 1979, on the other hand, many more events should have been registered with the high precipitation values. Also in 1999, despite high precipitation, only the approach with threshold 3 resulted in a peak.

The clearest correlation of event number and precipitation is found within the last ten years. The landslide velocity started to increase progressively since 2000. Accordingly, the fast movement of the terrain could have made the entire system even more susceptible to precipitation. In order to confirm or refute such an assumption, a longer series of measurements of the precipitation data and a larger sample depth of the trees would be necessary. Furthermore, dendrogeomorphology can only be used to determine the number of disturbances per year, but not the direct response of the landslide to a heavy rainfall. For this purpose, motion measurements from different locations, made on a regular basis, are more suitable since these have a much higher temporal resolution.

7.5 Movement data in comparison to the number of events

All presented measurement points except for point 2008 have an overall increase in movement (see Figure 41). This is in accordance with the expectations. Measurement point 2007 which shows the strongest acceleration is located directly at the tear-off edge at site 3. This is very close to spruce B03Fi5, which is also located at the tear-off edge and has the highest disturbance number at this site. Measurement point 1010 is located in the vicinity of the main breakaway edge as are the trees of site 1. Compared to measurement point 2007 the movement rate of point 1010 is only slightly increasing. Yet the measurements still clearly show that this area is moving as well. However, this slower movement could be a reason why the trees, despite many disturbances, are

nevertheless in general relatively vertical. Measurement point 1011 is located even farther away from the main tear-off edge than site 2. At this point measurements were taken less often and stopped in 2019, still the displacement increases between the measurements, showing that the forest is affected over a large area.

Measuring point 2008 is the only one showing a decrease in motion, and this despite being placed near a large crack. However, this does not necessarily contradict the findings of the other measurements. They already show that different movements are detected in a relatively small space. And additionally, in comparison to the much higher movement rates of the measuring points not discussed in detail here (see appendix Figure 47), it is clear that the landslide is not characterized by uniform movements but by many varying movements. Both the motion of the point measurements and the dendrogeomorphological data of the sites, therefore, confirm the strong and increasing activity of the area. Although, all the sampled trees recorded disturbances to different degrees, the measured velocity data still shows that the movements here are relatively subtle in comparison to other subzones of the landslide.

8. Conclusion

The ongoing landslide of Brienz and the danger of a big rockfall event are formative geomorphologic processes not only for the village but the whole valley. In this Master's thesis, the temporal and spatial evolution of a subarea of the landslide was investigated using dendrogeomorphological techniques.

The aim of this thesis was to evaluate dendrochronological techniques for their suitability to monitor the history of landslide movements at Brienz. The obtained and discussed results indicate, that by means of analysing the year ring patterns conclusion about past movement phases can be made. The results of all sites clearly showed that the investigated area is strongly affected by the landslide. However, the movements do not seem to have taken place continuously but in several phases. Yet, these phases not only differ between the chosen subsites but also showed some variation depending on the method used. Simplified it can be said that within the time periods 1850-1875, 1945-1955, and 1975-1985 a less active phase occurred for all sites.

Additionally, the disturbance data resulting from this study go several centuries further back than those of the current monitoring projects. This makes dendrogeomorphological techniques a valuable addition to the current investigation of the landslide.

A second aim of this study was to compare different methods of dendrogeomorphology to each other to assess the reliability of the methods and thus the results of such a study. For this purpose, in addition to an initial visual interpretation, in particular the manual classification of each event and the classification based on the eccentricity calculations were compared and discussed. This Master's thesis has shown that it is important to compare and question the methods, since they do not always show consistent results. Activity phases detected by only one method should be interpreted with more caution. For example, in the time period from 1820 to 1870 the eccentricity approach detects several short phases at all sites, while the manual approach only detects one activity phase at site 3 (1825-1850). In the 1990s, on the other hand, both approaches indicate a phase of activity at all sites. These activity phases that were detected by several methods in the same period have a greater legitimacy.

The direct comparison of the two approaches (manual and eccentricity) allowed to assess strengths and limitations of both methods. In contrast to the manual approach, it was possible to determine the expected increase in events in the last decades with the eccentricity approach. However, the eccentricity approach depends very much on the set threshold. If the threshold is set too low, too many events will be detected (noise), if it is set too high, events will be overlooked. The choice of the threshold always remains arbitrary to a certain degree. Although the manual approach is not exempt from possible human error (e.g. very weak disturbances may be overlooked) the detection of events is not dependent on a general threshold but on the estimation of each individual event by itself. A single misinterpreted year does not affect the entire classification, as is the case with an inappropriate threshold. Therefore, the manual approach overall may allow for more consistent results. Nevertheless, it is advantageous to use different methods, because on one hand they can strengthen the results and on the other hand point out their lackings.

Finally, the last question of this thesis was to elaborate whether location and visual damage of the tree are good indicators of the quantity of disturbance. In many cases, the location provided a good explanation for the disturbances in the trees. Often crack openings and/or the main break-away edge was in close vicinity to particularly affected trees. In contrast, the visual appearance of a tree was not always a correct indicator of the amount of disturbance in a tree. Some of the sampled trees were strongly inclined and accordingly many disturbances could be detected. But in other cases, for example at site 1, several trees without any visible inclination were sampled and they still recorded many disturbances. Based on the results of this Master's thesis, it can be concluded that while a visible inclination indicates that the tree has been disturbed, the absence of an inclination does not necessarily mean that the tree has not been disturbed. When selecting trees for sampling, it is therefore important to record not only their visual damage but also their environment.

8.1 Outlook

Although this study already allows some conclusions about the character of this landslide subzone, there are many more important questions to explore. The most obvious is to enlarge the study area in order to obtain more data. However, it would also be interesting to date individual cracks more precisely. For example, one could select trees specifically along cracks for a new project. In addition, it would also be instructive to take cores with increasing distance from the main edge, to map the extent of the slide by dendrogeomorphological techniques. Further it would be interesting to sample the trees at some faster moving locations. However, in many places this is not possible since the forest is already completely destroyed. And the areas with large movement rates where the trees are still standing are mostly single, detached islands in the landslide. Apart from expanding or adjusting the study area, a complementary approach would be to focus on the compression wood formation of the sampled trees. Cutting trunk disks instead of taking cores would ensure that existing compression wood was not missed, as it cannot be ruled out for the samples in this thesis. It would be interesting to see if the compression wood formation aligns with the disturbance years based on the manual approach and/or the eccentricity approach.

As is evident from the preceding paragraph, there are several more questions that need to be answered for the Brienz landslide in the future. What has been clearly shown in this work however, is that with the help of dendrogeomorphological methods, a lot can be learned about the character of a landslide. The strength of dendrogeomorphology clearly lies in its ability to look back several centuries into the past, which is not possible with other monitoring methods. It can be useful as a complement to existing monitoring techniques. For study sites where regular monitoring is not possible for various reasons, such as costs or the remoteness of the area, dendrogeomorphology provides an efficient stand-alone to study mass movements. The examination of other landslides by analysing the tree ring data is therefore recommendable.

9. Bibliography

- Alestalo, J. (1971): Dendrochronological interpretation of geomorphic processes. In: *Fennia-International Journal of Geography*, vol. 105:1, 140 p.
- Alexander, D. (2008): A brief survey of GIS in mass-movement studies, with reflections on theory and methods. In: *Geomorphology*, vol. 94, pp. 261–267.
- Bégin, Y. (2001): Tree-Ring Dating of Extreme Lake Levels at the Subarctic–Boreal Interface. In: *Quaternary Research*, vol. 55:2, pp. 133-139.
- Bodoque, J.M.; Díez-Herrero, A.; Martín-Duque, J.F.; Rubiales, J.M.; Godfrey, A.; Pedraza, J.; Carrasco, R.M. & Sanz, M.A. (2005): Sheet erosion rates determined by using dendrogeomorphological analysis of exposed tree roots: Two examples from Central Spain. In: *Catena*, vol. 64, pp. 81–102.
- Bovi, R.C.; Romanelli, J.P.; Ferraz Caneppele, B. & Cooper, M. (2022): Global trends in dendrogeomorphology: A bibliometric assessment of research outputs. In: *Catena*, vol. 210, pp. 1-12.
- Braam, R.R.; Weiss, E.E.J. & Burrough, P.A. (1987): Spatial and temporal analysis of mass movement using dendrochronology. In: *Catena*, vol. 14, pp. 573–584.
- Breitenmoser, T.; Thöny, R.; & Figi, D. (2021): Ein Blick in den Berg. In: *Bündner Wald*, vol. 71, pp. 30-35.
- Breitenmoser, T. (2022): Geologie. In: 11. Bevölkerungsinformation der Gemeinde Albula/Alvra zum Brienzner Rutsch. <https://www.youtube.com/watch?v=J5Vb-3vnHj4> [Status: 07.04.22, Access: 20.12.22].
- Bundesamt für Umwelt (BAFU) (2016): Schutz vor Massenbewegungsgefahren. In: *Vollzugshilfe für das Gefahrenmanagement von Rutschungen, Steinschlag und Hangmuren*. Bundesamt für Umwelt (ed.), Bern. Umwelt-Vollzug Nr. 1608, p. 98.
- Bundesamt für Umwelt (BAFU): Landslide Monitoring. <<https://www.bafu.admin.ch/bafu/en/home/topics/natural-hazards/state/natural-hazards--monitoring-programmes/landslide-monitoring.html>> [Status: 05.11.2018, Access: 06.01.202].
- Carrara, P.E. & O’Neill, J.M. (2003): Tree-ring dated landslide movements and their relationship to seismic events in southwestern Montana, USA. In: *Quaternary Research*, vol. 59:1, pp. 25-35.
- Chelli, A. & Stefanini, M.C. (1999): Geomorphological features and temporal distribution of the present-day landslides activity in the high Gordana basin (Zeri, Northern Apennines): a dendrogeomorphological analysis. In: *Geografia Fisica e Dinamica Quaternaria*, vol. 22:2, 105–114.
- Cherubini, P.; Gärtner, H.; Esper, J.; Dobbertin, M.K.; Kaiser, K.F.; Rigling, A.; Treydte, K.; Zimmermann, N.E. & Ulrich Bräker, O. (2004): Jahrringe als Archive für interdisziplinäre Umweltforschung. In: *Schweizerische Zeitung für Forstwesen*, vol. 6, pp. 162-168.
- Chiarle, M.; Geertsema, M.; Mortara, G. & Clague, J.J. (2021): Relations between climate change and mass movement: Perspectives from the Canadian Cordillera and the European Alps. In: *Global and Planetary Change*, vo. 202, pp. 1-25.

- Corominas, J. & Moya, J. (1999): Reconstructing recent landslide activity in relation to rainfall in the Llobregat River basin, Eastern Pyrenees, Spain. In: *Geomorphology*, vol. 30, pp. 79–93.
- Corominas, J. & Moya J. (2010): Contribution of dendrochronology to the determination of magnitude–frequency relationships for landslides. In: *Geomorphology*, vol. 124, pp. 137–149.
- Corona, C.; Georges, R.; Lopez Saez, J.; Stoffel, M. & Perfettini, P. (2010): Spatio-temporal reconstruction of snow avalanche activity using tree rings: Pierres Jean Jeanne avalanche talus, Massif de l'Oisans, France. In: *Catena*, vol. 83:2-3, pp. 107–118.
- CSD engineers (2022): Movement data for Caltegras subzone (Tachymeter & handheld GPS).
- Cybis Elektronik & Data AB: CooRecorder & CDendro program.
<<http://www.cybis.se/forfun/dendro/helpcoorecorder7/index.php>> [Status: 22.03.20, Access: via WSL].
- Douglass, A.E. (1935): Dating Pueblo Bonito and Other Ruins of the Southwest. In: National Geographic Society, Contributed Technical Paper, Pueblo Bonito Series, vol. 1, 74 pp.
- Ernst, C. (2022): Sondierstollen und Entwässerungstollen. In: 11. Bevölkerungsinformation der Gemeinde Albula/Alvra zum Brienzer Rutsch.
<<https://www.youtube.com/watch?v=J5Vb-3vnHj4>> [Status: 07.04.22, Access: 20.12.22].
- Esposito, G.; Salvati, P. & Bianchi, C. (2023): Insights gained into geo-hydrological disaster management 25 years after the catastrophic landslides of 1998 in southern Italy. In: *International Journal of Disaster Risk Reduction*, vol. 84, pp. 1–18.
- Fabiánová, A.; Chalupa, V. & Šilhán, K. (2021): Dendrogeomorphic dating vs. low-magnitude landsliding. In: *Quaternary Geochronology*, vol. 62, pp. 1–12.
- Ferguson, C.W. (1970): *Concepts and Techniques of Dendrochronology*. Tucson (AZ): University of Arizona, Laboratory of Tree-Ring Research.
- Funada, R.; Yamagishi, Y.; Begum, S.; Kudo, K.; Nabeshima, E.; Nugroho, W.D.; Hasnat, R.; Oribe, Y. & Nakaba, S. (2016): Chapter 2- Xylogenesis in Trees: From Cambial Cell Division to Cell Death. In: Kim, Y.S., Funada, R. & Singh, A. P. (eds.): *Secondary Xylem Biology. Origins, Functions and Applications*, Elsevier, pp. 25–43.
- Gartmann, C. (2021): Im Mittelpunkt stehen die Betroffenen. In: *Bündner Wald*, vol. 71, pp. 14–17.
- Gärtner, H. (2007): Tree roots—Methodological review and new development in dating and quantifying erosive processes. In: *Geomorphology*, vol. 86, pp. 243–251.
- Gärtner, H. & Nievergelt, D. (2009): The core-microtome: A new tool for surface preparation on cores and time series analysis of varying cell parameters. In: *Dendrochronologia*, vol. 28, pp.85–92.
- Gärtner, H. & Heinrich, I. (2013): Dendrogeomorphology. In: Elias, S.A. & Mock, C.J (eds.): *Encyclopedia of Quaternary Science*, vol.2, Amsterdam: Elsevier, pp.91–103.
- Gärtner, H. & Schweingruber, F. (2013): *Microscopic Preparation Techniques for Plant Stem Analysis*. Remagen- Oberwinter: Dr. Kessel.

- Gemeinde Albula (2019): Brienz/Brinzauls, Vazerol, Surava, Tiefencastel - Informationsbroschüre Evakuierungsablauf. Available at: Info Briener Rutsch. <<http://www.albula-alvra.ch/Aktuelles/Evakuierungsablauf%20-%20Brosch%C3%BCren/default.htm>> [Status: unknown, Access: 27.12.22]
- Gischig, V.; Schneider, S.; Largiadèr, A.; Huwiler, A. & Nänni, C. (2021): Bergsturzscenarien bei der Rutschung Brienz/Brinzauls (GR)- Probabilistische Ansätze zur Abschätzung der Prozessräume, in: FAN-Fachleute Naturgefahren Schweiz (Ed.): Agenda 2021, pp. 18-25.
- Guetg, C. (2022): District Forester, information on logging records in the study area. [carlo.guetg\(at\)forstalbula.ch](mailto:carlo.guetg(at)forstalbula.ch)
- Häne, K. (2007): Die Waldföhre (*Pinus sylvestris*). <<https://www.waldwissen.net/de/lebensraum-wald/baeume-und-waldpflanzen/nadelbaeume/die-waldfoehre-pinus-sylvestris>> [Status: 04.05.2007, Access 22.12.22].
- Häne, K. (2017): Die Fichte (*Picea abies*). <<https://www.waldwissen.net/de/lebensraum-wald/baeume-und-waldpflanzen/nadelbaeume/die-fichte-picea-abies>> [Status: 30.10.2017, Access 22.12.22].
- Häusler, M.; Gischig, V.; Thöny, R.; Glueer, F. & Fäh, D. (2021): Monitoring the changing seismic site response of a fast-moving rockslide (Brienz/Brinzauls, Switzerland). In: Geophysical Journal International, vol. 229, pp. 299-310.
- Hebertson, E.G. & Jenkins, M.J. (2003): Historic climate factors associated with major avalanche years on the Wasatch Plateau, Utah. In: Cold Regions Science and Technology, vol. 37:3, pp. 315-332.
- Heinrich, I.; Gärtner, H. & Monbaron, M. (2007): Tension wood formed in *fagus sylvatica* and *alnus glutinosa* after simulated mass movement events. In: IAWA Journal, vol.28, pp.39-48.
- Huwiler, A. & Larigiader, A. (2021): Die Rutschung Brienz- ein Blick zurück. In: Bündner Wald, vol. 71, pp. 8-13.
- Info flora: *Pinus sylvestris*. <<https://www.infoflora.ch/de/flora/pinus-sylvestris.html>> [Status: 03.01.2023, Access 22.12.22]
- Info flora: *Picea abies*. <<https://www.infoflora.ch/de/flora/picea-abies.html>> [Status: 22.12.2022, Access 03.01.23]
- IPCC, 2022: Climate Change 2022: Impacts, Adaptation and Vulnerability. In: H.-O. Pörtner, D.C. Roberts, M. Tignor, E.S. Poloczanska, K. Mintenbeck, A. Alegría, M. Craig, S. Langsdorf, S. Löschke, V. Möller, A. Okem, B. Rama (eds.): Contribution of Working Group II to the Sixth Assessment Report of the Intergovernmental Panel on Climate Change, Cambridge University Press. Cambridge University Press, Cambridge, UK and New York, NY, USA, 3056 pp.
- Kaennel, M. & Schweingruber, F.H. (1995): Multilingual Glossary of Dendrochronology: Terms and Definitions in English, German, French, Spanish, Italian, Portuguese and Russian. Bern: Paul Haupt Publishers.

- Kashiwaya, K.; Okimura, T. & Kawatani, T. (1989): Tree ring information and rainfall characteristic for landslide in the Kobe District, Japan. In: Earth Surface Processes and Landforms, vol. 14:1, pp.63-71.
- Kurath, J. (2021): Projekt Sondierstollen. In: 10. Bevölkerungsinformation der Gemeinde Albula/Alvra zum Brienzer Rutsch. <https://www.youtube.com/watch?v=eKC9y5cNmnc> [Status: 25.08.2021, Access: 20.12.22].
- Lopez Saez, J.; Corona, C.; Stoffel, M.; Schoeneich, P. & Berger, F. (2012): Probability maps of landslide reactivation derived from tree-ring records: Pra Bellon landslide, southern French Alps. In: Geomorphology, vol. 138, pp. 189-202.
- Lopez Saez, J.; Corona, C.; Stoffel, M. & Berger, F. (2013): High-resolution fingerprints of past landsliding and spatially explicit, probabilistic assessment of future reactivations: Aiguettes landslide, Southeastern French Alps. In: Tectonophysics, vol. 602, pp.355-369.
- Malik, I. & Wistuba, M. (2012): Dendrochronological methods for reconstructing mass movements- an example of landslide activity analysis using tree-ring eccentricity. In: Geochronometria, vol. 39:3, pp. 180-196.
- MeteoSchweiz: Das Klima der Schweiz. <https://www.meteoschweiz.admin.ch/klima/klima-der-schweiz.html> [Status: unknown, Access: 20.12.22].
- Perret, S.; Stoffel, M. & Kienholz, H. (2006): Spatial and temporal rockfall activity in a forest stand in the Swiss Prealps—A dendrogeomorphological case study. In: Geomorphology, vol. 76:1-4, pp. 219-231.
- Petrascheck, A. & Kienholz, H. (2003): Hazard assessment and mapping of mountain risks in Switzerland. In: Rickenmann, D. & Chen, C.L. (eds.): Debris Flow Hazards Mitigation: Mechanics, Prediction and, Assessment. Rotterdam: Millpress, pp. 25–38.
- Přecechtělová, H. & Šilhán, K. (2019): Tree ring-based estimation of landslide block displacement: Evaluation of a new experimental approach. In: Geomorphology, vol. 339, pp.104-113.
- Rathgeber, C.B.K.; Cuny, H.E. & Fonti, P. (2016): Biological Basis of Tree-Ring Formation: A Crash Course. In: Frontiers in Plant Science, pp. 1-7.
- Rinntech: TSAP-Win™- Time series analysis software. <https://rinntech.info/products/tsap-win/> [Status. Unknown, Access: 19.01.23] (access to program via WSL key).
- Sartorius, O. & Schneider, S. (2021): Frühwarndienst und aktuelle Lage Rutschung Brienzen/Brinzauls GR. In: Bündner Wald, vol. 71, pp. 36-41.
- Sartorius, O.; Schneider, S. & Wurster, D. (2022): Frühwarndienst und Beurteilung der aktuellen Lage. In: Schweizerische Zeitschrift für Forstwesen, vol. 173:3, pp.144-146.
- Schneider, S. (2021): Aktuelle Lager Rutschungen. In: 10. Bevölkerungsinformation der Gemeinde Albula/Alvra zum Brienzer Rutsch. <https://www.youtube.com/watch?v=eKC9y5cNmnc> [Status: 25.08.2021, Access: 20.12.22].
- Schneider, S. (2022): Aktuelle Lage Rutschungen & Szenarien in Bezug auf die Gefahrenlage. In: 11. Bevölkerungsinformation der Gemeinde Albula/Alvra zum Brienzer Rutsch. <https://www.youtube.com/watch?v=J5Vb-3vnHj4> [Status: 07.04.22, Access: 20.12.22].

- Schneuwly, D.; Stoffel, M. & Bollschweiler, M. (2009): Formation and spread of callus tissue and tangential rows of resin ducts in *Larix decidua* and *Picea abies* following rockfall impacts. In: *Tree Physiology*, vol.29, pp. 281-289.
- Schweingruber, F.H. (2007): *Wood Structure and Environment*. Springer Series in Wood Science. Heidelberg: Springer.
- Shi, X.; Wang, J.; Jiang, M.; Zhang, S.; Wu, Y. & Zhong, Y. (2022): Extreme rainfall-related accelerations in landslides in Danba County, Sichuan Province, as detected by InSAR. In: *International Journal of Applied Earth Observations and Geoinformation*, vol. 155, pp. 1-13.
- Shroder J.F. (1980): Dendrogeomorphology: review and new techniques of tree ring dating. In: *Progress in Physical Geography*, vol. 4, pp. 161-188.
- Šilhán, K.; Pánek, T.; Dušek, R.; Turský, O.; Brázdil, R.; Klimeš, J. & Kašičková, L. (2012): Spatio-temporal patterns of recurrent slope instabilities affecting undercut slopes in flysch: A dendrogeomorphic approach using broad-leaved trees. In: *Geomorphology*, vol. 213, pp. 240-254.
- Šilhán, K.; Pánek, T.; Dušek, R.; Havlů, D.; Brázdil, R.; Kašičková, L. & Hradecký, J. (2013): The dating of bedrock landslide reactivations using dendrogeomorphic techniques: The Mazák landslide, Outer Western Carpathians (Czech Republic). In: *Catena*, vol. 104, pp. 1-13.
- Šilhán, K. & Stoffel, M. (2015): Impacts of age-dependent tree sensitivity and dating approaches on dendrogeomorphic time series of landslides. In: *Geomorphology*, vol. 236, pp. 34-43.
- Šilhán, K.; Tichavský, R.; Fabiánová, A.; Chalupa, V.; Chalupová, O.; Škarpich, V. & Tolasz, R. (2019): Understanding complex slope deformation through tree-ring analyses. In: *Science of the Total Environment*, vol. 665, pp. 1083-1094.
- Šilhán, K. & Stoffel, M. (2022): Landslide-induced changes in tree-ring anatomy: A new dendrogeomorphic avenue? In: *Catena*, vol.213, pp. 1-10.
- Smith, D. & Lewis, D. (2007): Dendrochronology. In: Elias, S.A. (ed.): *Encyclopedia of Quaternary Science*, pp. 459-465.
- Smith, K.T. (2008): An organismal view of dendrochronology, In: *Dendrochronologia*, vol. 26.3, pp.185–193.
- Speer, J.H. (2011): *Fundamentals of tree-ring research*. Tucson: The University of Arizona Press.
- SRF Einstein (2019): Brienztal – ein Bergdorf am Abgrund.
<https://www.srf.ch/play/tv/einstein/video/brienztal---ein-dorf-am-abgrund?urn=urn:srf:video:09dd6d5b-4941-421b-81b8-e438023987b1> [Status: 19.09.19, Access: 20.12.22].
- SRF Einstein (2023): Brienztal rutscht – Gelingt die Rettung?
<https://www.srf.ch/play/tv/einstein/video/brienztal-rutscht---gelingt-die-rettung?urn=urn:srf:video:5139b08e-01ae-4861-b309-99ceb10b96d5> [Status: 12.01.23, Access: 15.01.23].
- Stefanini, M.C. (2004): Spatio-temporal analysis of a complex landslide in the Northern Apennines (Italy) by means of dendrochronology. In: *Geomorphology*, vol. 63, pp. 191-202.

- Stoffel, M.; Schneuwly, D.; Bollschweiler, M.; Lièvre, I.; Delaloye, R.; Myint, M. & Monbaron, M. (2005): Analyzing rockfall activity (1600–2002) in a protection forest—a case study using dendrogeomorphology. In: *Geomorphology*, vol. 68, pp. 224-241.
- Stoffel, M. & Perret, S. (2006): Reconstructing past rockfall activity with tree rings: Some methodological considerations. In: *Dendrochronologia*, vol. 24, pp. 1-15.
- Stoffel, M. & Bollschweiler, M. (2008): Tree-ring analysis in natural hazards research – an overview. In: *Natural Hazards and Earth System Sciences*, vol. 8, pp.187-202.
- Stoffel, M. & Bollschweiler, M. (2009): What Tree Rings Can Tell About Earth-Surface Processes: Teaching the Principles of Dendrogeomorphology. In: *Geography Compass*, vol. 3, pp. 1013-2037.
- Stoffel, M. (2010): Magnitude–frequency relationships of debris flows — A case study based on field surveys and tree-ring records. In: *Geomorphology*, vol. 116, pp. 67-76.
- Swisstopo 2022: Bundesamt für Landestopografie, Seftigenstrasse 264, 3084 Wabern.
- Wanner, H.; Rickli, R.; Salvisberg, E.; Schmutz, C. & Schuepp, M. (1997): Global climate change and variability and its influence on Alpine climate—concepts and observations. In: *Theoretical and Applied Climatology*, vol. 58, pp. 221–243.
- Wistuba, M.; Malik, I.; Gärtner, H.; Kojš, P. & Owczarek, P. (2013): Application of eccentric growth of trees as a tool for landslide analyses: The example of *Picea abies* Karst. in the Carpathian and Sudeten Mountains (Central Europe). In: *Catena*, vol. 111, pp. 41-55.
- Wistuba, M.; Malik, I. & Badura, J. (2019): Tree rings as an early warning against catastrophic landslides: Assessing the potential of dendrochronology for determining slope stability. In: *Dendrochronologia*, vol. 53, pp. 82-94.
- Worbes, M. (2004): MENSURATION, Tree-Ring Analysis. In: Burley, J. (ed.): *Encyclopedia of Forest Sciences*, pp.586-599.
- WSL (2022): Skippy- The new high-resolution image capturing system for tree rings developed at WSL. <https://www.wsl.ch/en/services-and-products/research-instruments/skipky.html> [Status: unknown, Access: 03.01.22].
- Zink-Sharp, A. (2004): Wood formation and properties. Formation and Structure of Wood. In: Burley, J.(ed.): *Encyclopedia of Forest Sciences*, pp. 1806-1815.

10. Appendix

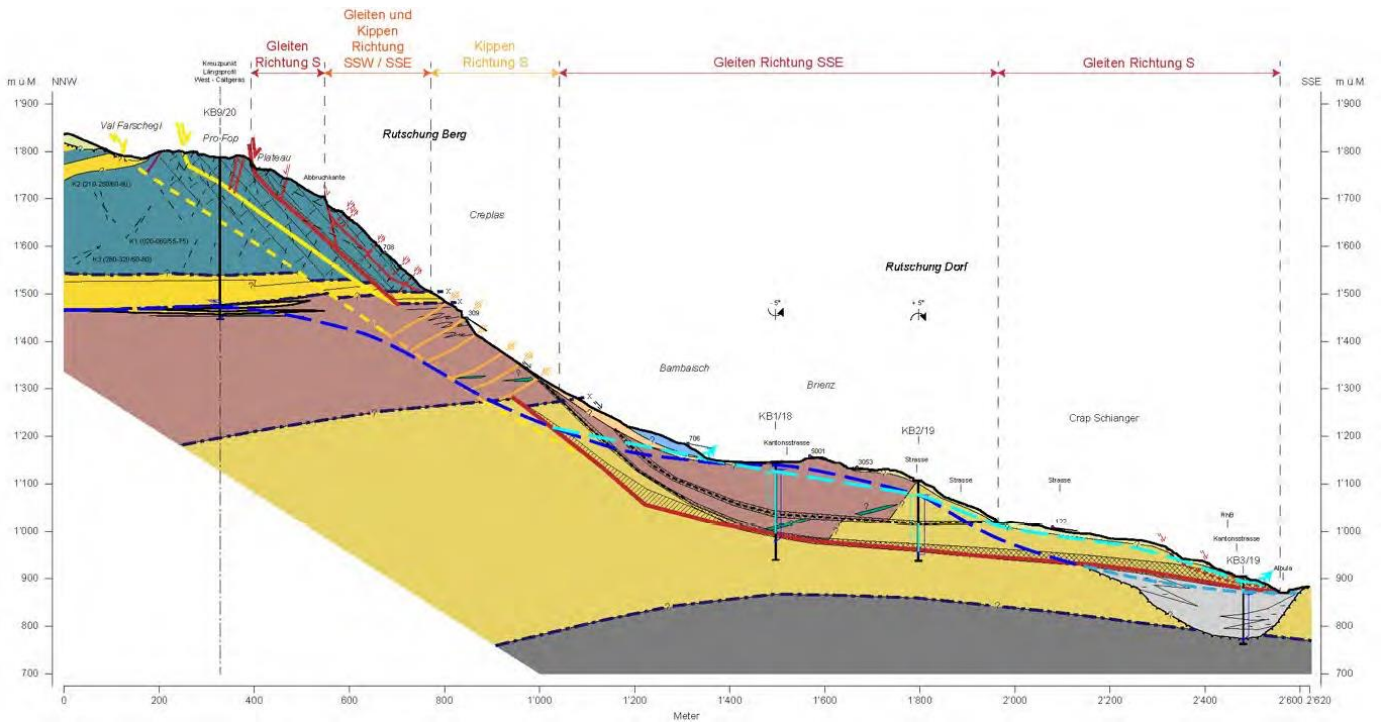


Figure 42: Geological profile of the landslide with the following components: Vallatscha formation (blue), Raibler formation (bright yellow), Allgäu formation (brown), Flysch (dull yellow), Nivaigl-Serie (grey) and Alluvions (light grey). The landslide horizon is marked in red and tilts (rockfall) in orange. In light blue is the water level of the sliding mass drawn and in dark blue potential water level of the water fraction in the mountain (=mountain water level). However, this water is blocked by the impermeable sliding horizon (red line). This means that there is both a water pressure from above (landslide mass) and one from below (rock mass) acting on the landslide horizon (Breitenmoser 2022, p. 21).

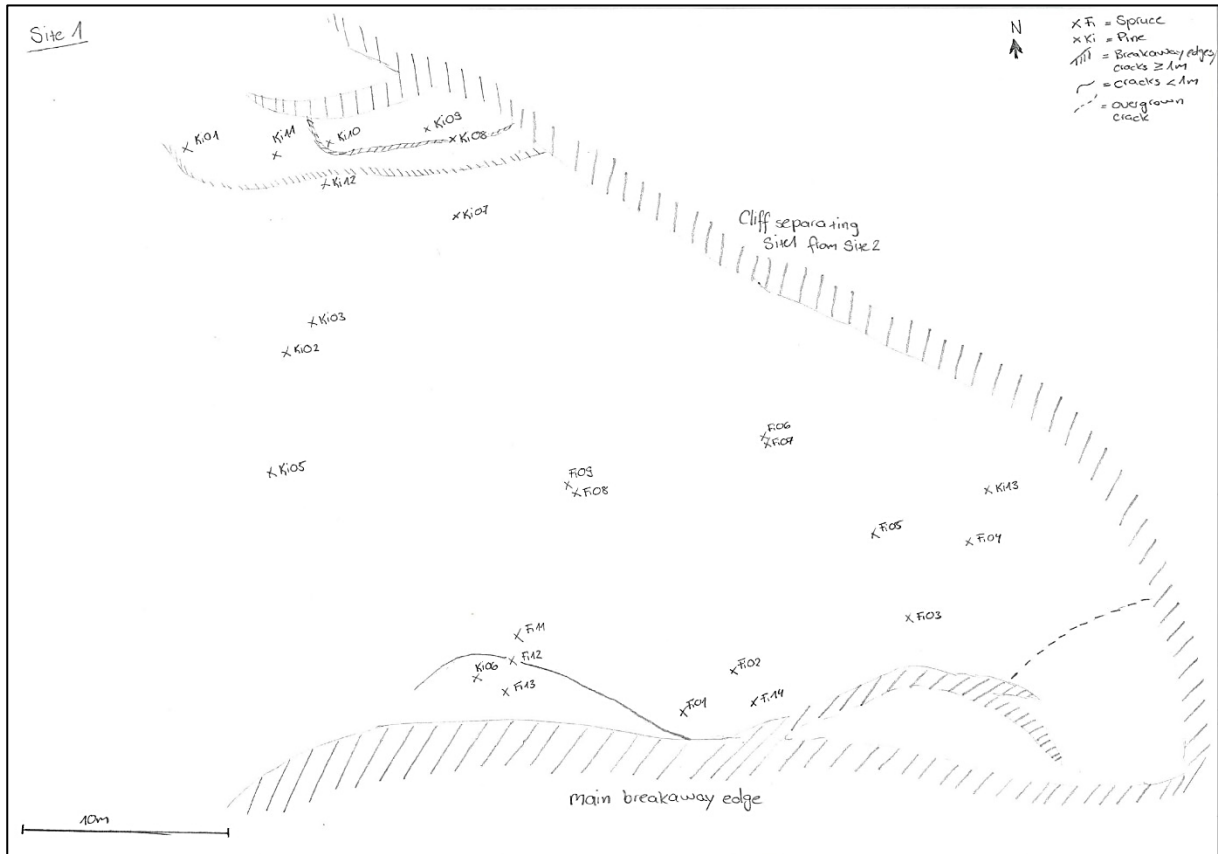


Figure 43: Geomorphic sketch of site 1.

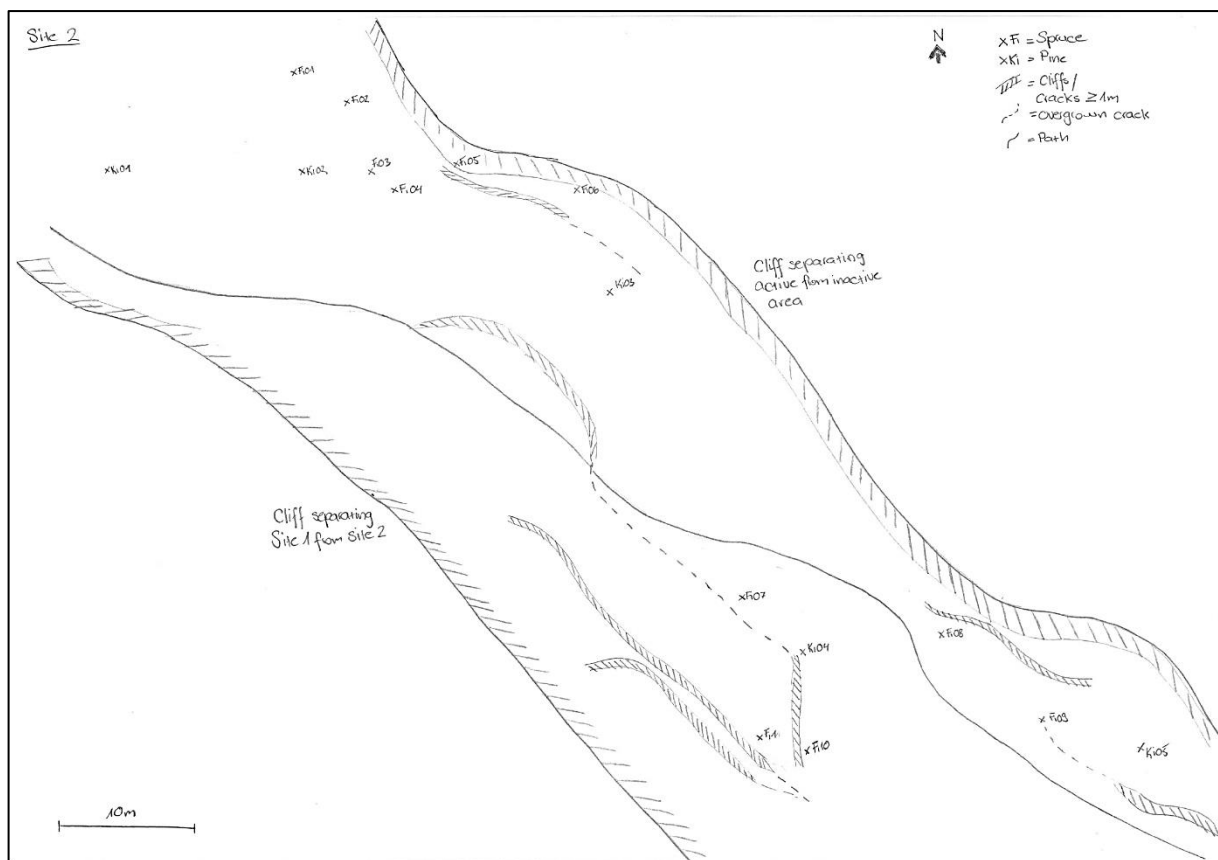


Figure 44: Geomorphic sketch of site 2.

Table 5: Overview of the detected phases based on the different approaches. This overview is based on the analysis of all events from all sites together.

Method	No. phases	Duration of phases
Visual analysis of chronologies	3	1828-1915, 1947-1970, 1977-2021
Manual event count	5	1825-1841, 1850-1882, 1885-1952, 1957-1973, 1985-2016
Eccentricity calculated threshold (1)	1	1800-2021
Eccentricity chosen threshold (3)	3	1800-1855, 1867-1926, 1942-2021
	6	1821-1855, 1867-1883, 1891-1899, 1906-1926, 1942-1970, 1973-2021

Table 6: Distance of the four measuring points to the study areas.

GPS-Point	Time	Closest Tree	Distance [m]
1010	2009-2022	B01Fi14	17
1011	2009-2019	B02Fi01	31
2007	2011-2022	B03Fi03	17
2008	2011-2022	B02Ki05	40
		B03Fi02	43

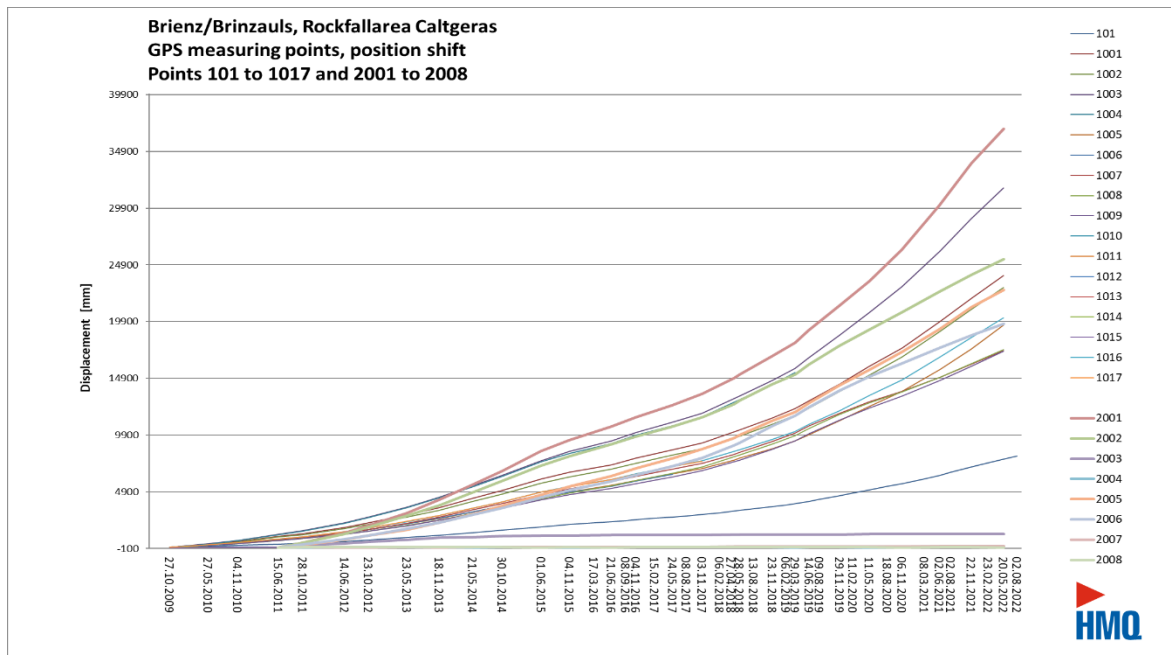
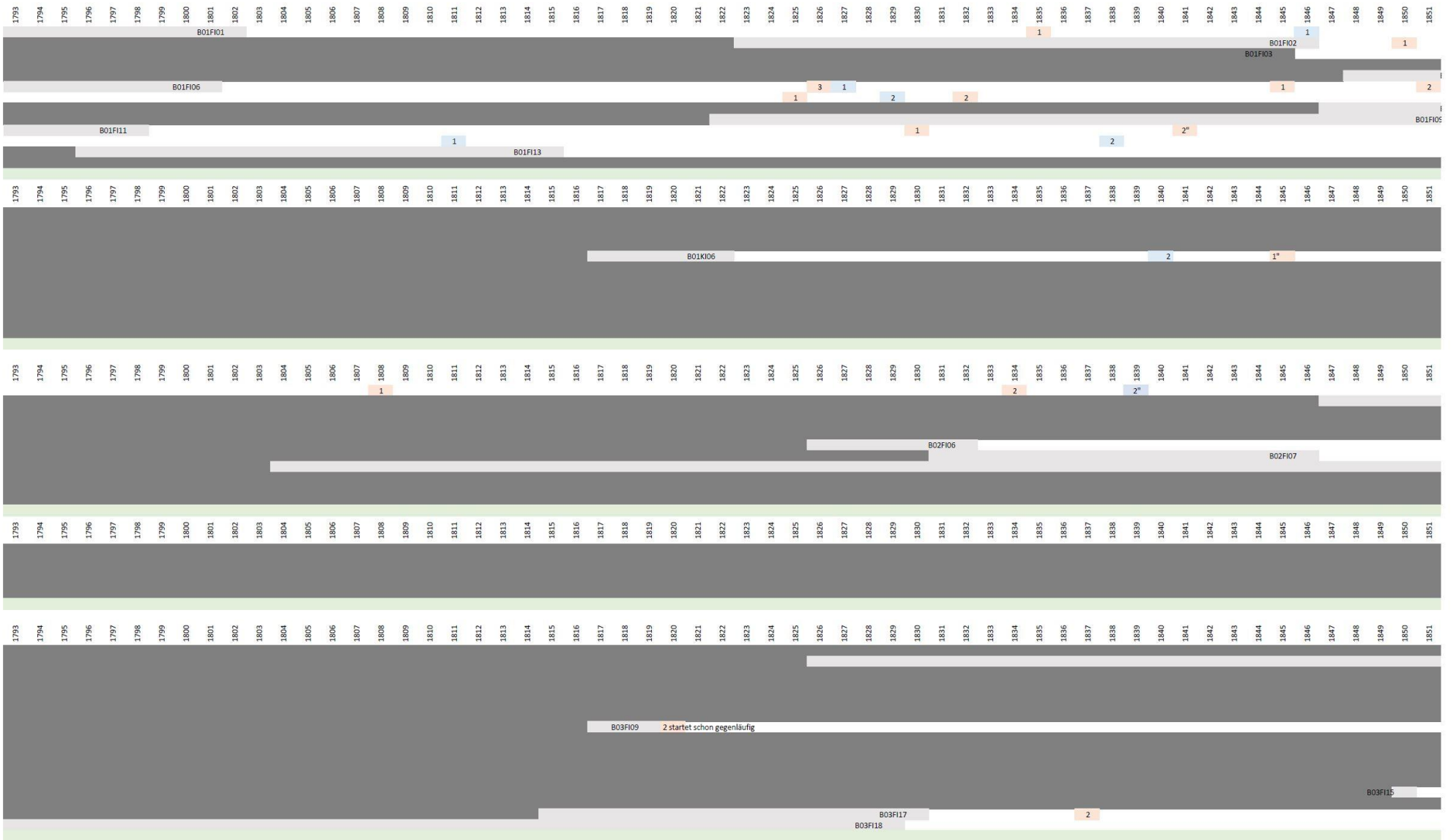
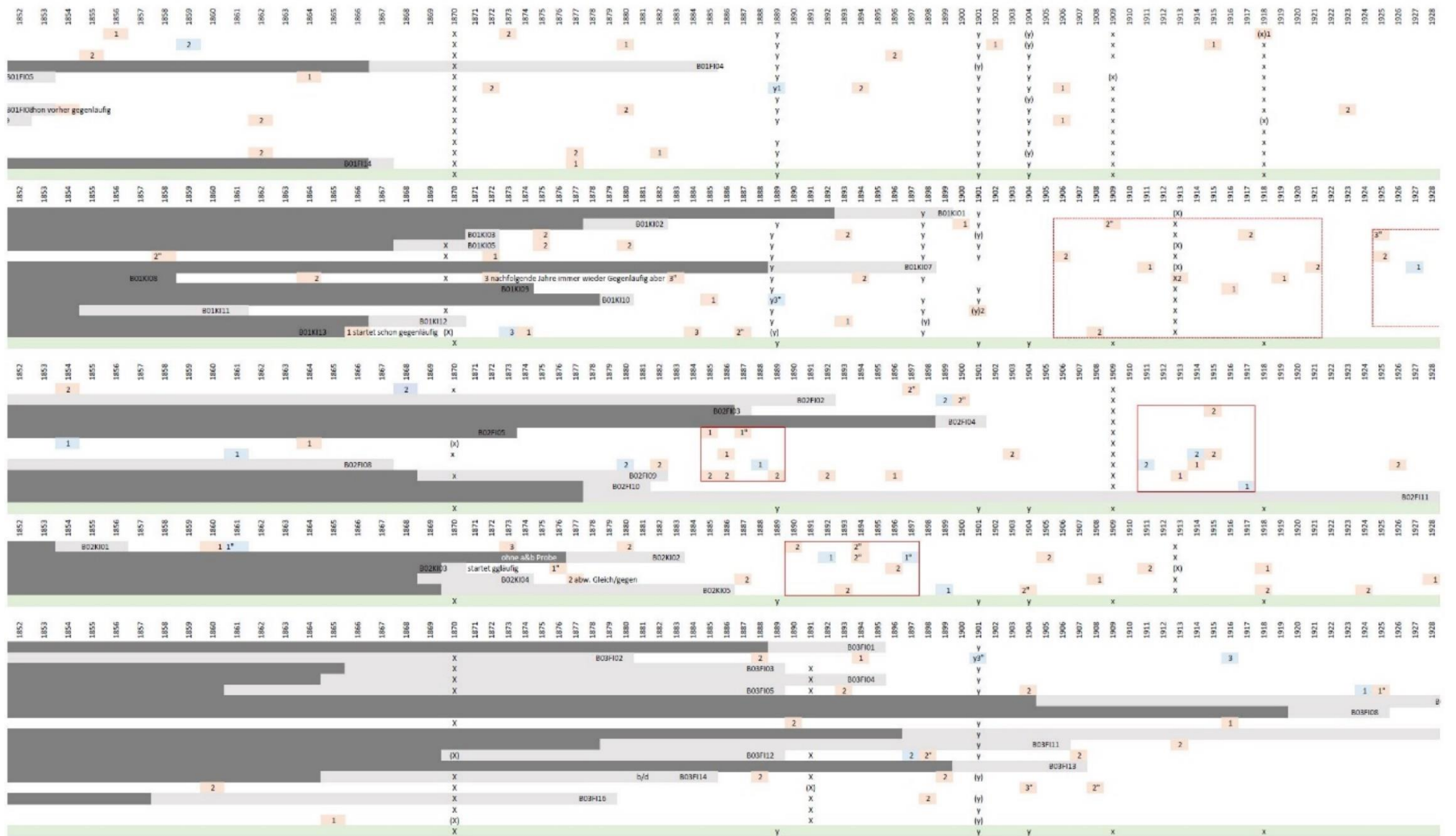


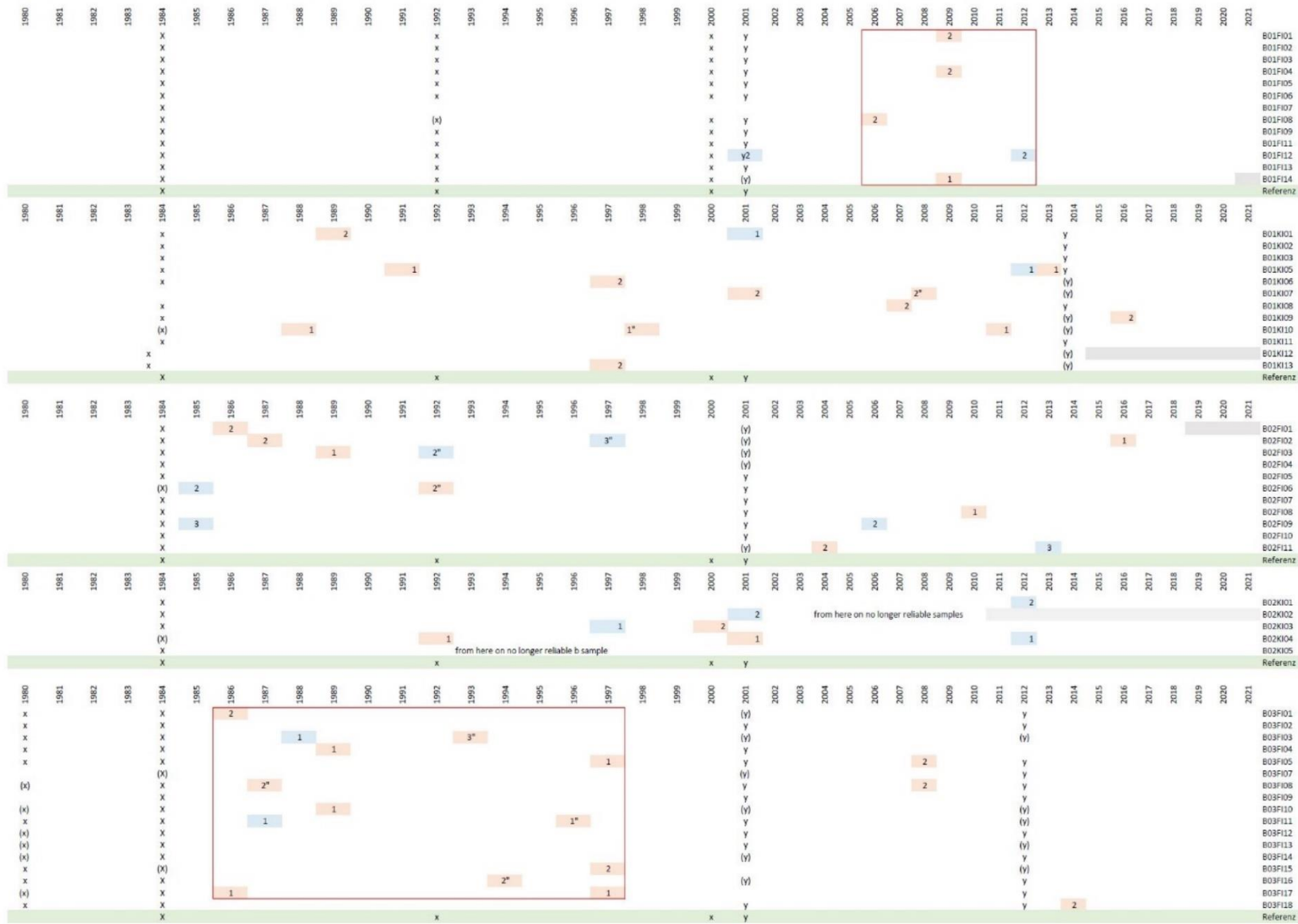
Figure 47: GPS Measurements by CSD engineers (2022) Shown are all Points in the Caltgeras area.

Table 7: Complete excel file that shows all results based on the manual approach.









11. Acknowledgements

This Master's thesis would not be existing without the help of a few others. First, I would like to thank Dr. Holger Gärtner for the helpful discussions, the regular email replies, and the constructive feedback on work excerpts - in short, for the patient guidance and support during my Master's thesis.

During the field work, I received support from several people. Many thanks to Anita Bruppacher, Dânia Faria Pinto, Gregi Wiech, Oliver Thalmann, Ivan Tijan, Madeleine Bühler and Jost Bielitzer! Without you, the fieldwork would have been only half as successful, entertaining, and adventurous.

I also had a lot of support with the lab work. Many thanks to Anne Verstege and Loïc Schneider for explaining the various devices and the procedure for sample preparation! But even at WSL you can't work all the time, fortunately there were always good conversations during many lunches and coffee aka bread breaks.

Of course, I would also like to thank all those who had the nerve to proofread my thesis and give their feedback. Thank you, Monika Maurhofer aka Mami, Anita Bruppacher & Marçal Argelich Ninot!

And last but not least thanks to all the other master students and my boyfriend Ivan Tijan for keeping my spirits up during writing.

12. Personal Declaration

Personal declaration: I hereby declare that the submitted Thesis is the result of my own, independent work. All external sources are explicitly acknowledged in the Thesis.

Location, Date:

Signature:

Zürich, 29.01.23

A. Bingoff